

RHODES UNIVERSITY
Where leaders learn

**Genetic analysis and field application of a
UV-tolerant strain of CrleGV for
improved control of *Thaumatotibia
leucotreta***

A thesis submitted in fulfilment of the requirements

for the degree of

MASTER OF SCIENCE

At

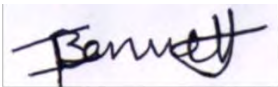
RHODES UNIVERSITY

By

Tahnee Tashia Bennett

Declaration

I, Tahnee Tashia Bennett (16B4622) hereby declare that the thesis submitted is my own work. It is being submitted for the degree of Master of Science at Rhodes University. It has not been previously submitted for assessment of any degree at any other university or other body, organisation outside of the university.



Author's Signature

24 February 2022

Date

Abstract

Thaumatotibia leucotreta (Meyrick) (Lepidoptera: Tortricidae), also known as false codling moth (FCM), is indigenous to sub-Saharan Africa. *Thaumatotibia leucotreta* has been controlled through an integrated pest management (IPM) programme, which includes chemical control, sterile insect technique (SIT), cultural and biological control. As part of the biological control, a key component is the use of *Cryptophlebia leucotreta* granulovirus (CrleGV-SA). Currently, Cryptogran™, a commercial formulation of CrleGV, is the preferred product to use in South Africa for the control of *T. leucotreta*. The registration of the biopesticide Cryptogran (River bioscience, South Africa) was established after conducting extensive field trials with CrleGV-SA. One of the major factors affecting the baculovirus efficacy in the field is UV irradiation. A UV-tolerant *Cryptophlebia leucotreta* granulovirus (CrleGV-SA-C5) isolate was isolated after consecutive cycles of UV exposure. This UV-tolerant isolate is genetically distinct from the CrleGV-SA isolate. The CrleGV-SA-C5 isolate has the potential as a biological control agent. The control of *T. leucotreta* in South Africa could be improved by the development of novel isolates into new biopesticide formulations. To date, there has not been any field trials conducted on the CrleGV-SA-C5 isolate. Therefore, it is important to determine the biological and genetic stability of this isolate and to conduct field trials with CrleGV-SA-C5 to test the efficacy of the isolate before possible production into a biopesticide.

A *de novo* assembly was conducted to reassemble the genome of CrleGV-SA-C5 which was followed by a sequence comparison with the CrleGV-SA genome. The identification of SNPs, led to the design of oligonucleotides flanking the regions where the SNPs were detected. Polymerase chain reaction amplification of the target regions was conducted using the oligonucleotides. After sequence comparison, seven SNPs were detected and PCR amplification was successful using the three oligonucleotides, *Pif-2*, *HypoP* and *Lef-8/HP*. To differentiate between CrleGV-SA-C5 and CrleGV-SA genomes and confirm the presence of the SNPs, two methods of screening were conducted. The first was the construction of six plasmids, the plasmids contained the targeted *pif-2*, *HypoP*, and the *Lef-8/HP* insert regions from both the CrleGV-SA-C5 and CrleGV-SA genome region where the SNPs were identified, followed by sequencing. The Five recombinant plasmids, pC5_Pif-2, pSA_Pif-2, pC5_HypoP, pSA_HypoP, and pC5_Lef-8/HP were successfully sequenced. No amplicon was obtained for one of the plasmids used as template (pSA_Lef-8/HP) and therefore the PCR product used for cloning was sequenced instead. Sequence alignment confirmed the presence of four of the five

targeted SNPs in the genome of the CrleGV-SA-C5 isolate. However, of these only one SNP (UV_7) rendered a suitable marker for the differentiation between the CrleGV-SA-C5 and CrleGV-SA isolates as the SNPs, UV_2, UV_3 and UV_5, were also present in the CrleGV-SA sequences. The second screening method was a quantitative polymerase chain reaction (qPCR) melt curve analysis to differentiate between the CrleGV-SA-C5 and CrleGV-SA isolates. qPCR melt curve analysis was done using the CrleGV-SA-C5 and CrleGV-SA HypoP PCR products. This technique was unable to differentiate between the CrleGV-SA-C5 and CrleGV-SA isolates. However, this may be as a result of sequence data confirming that SNP UV_5 originally identified in the CrleGV-SA-C5 HypoP region was identical to the SNP at the same position in the CrleGV-SA HypoP region.

Following the differentiation of the CrleGV-SA-C5 and CrleGV-SA isolates through two screening methods, the genetic integrity of the CrleGV-SA-C5 isolate after two virus bulk-ups was determined by PCR amplification of the target regions in the bulk-up virus followed by sequencing. Prior to virus bulk-up, surface dose bioassays were conducted on 4th instar larvae and LC₅₀ and LC₉₀ values of 4.01×10^6 OBs/ml and 8.75×10^9 OBs/ml respectively were obtained. The CrleGV-SA-C5 isolate was then bulked up in fourth instar *T. leucotreta* larvae using the LC₉₀ value that was determined. Sequencing of the target regions from the CrleGV-SA-C5_BU2 (bulk-up 2) was conducted. Sequencing results confirmed the presence of the target SNPs in the CrleGV-SA-C5_BU2 genome.

The UV-tolerance of the CrleGV-SA-C5 isolate in comparison to the CrleGV-SA isolate was evaluated by detached fruit bioassays under natural UV irradiation. Two detached fruit bioassays were set-up, a UV exposure and a non-UV exposure bioassay set-up. Three treatments were used for each bioassay set-up which were the viruses CrleGV-SA-C5 and CrleGV-SA and a ddH₂O control. Statistical analysis indicated that there was no significant difference between the virus treatments in both the UV exposed detached fruit bioassay and the non-UV exposed detached fruit bioassay.

This study is the second study to report on the *de novo* assembly of the CrleGV-SA-C5 and sequence comparison with the CrleGV-SA genome, and the first to report on the UV-tolerance of the CrleGV-SA-C5 isolate by detached fruit bioassays. Future work could involve further evaluation of intraspecific genetic variability in the CrleGV-SA-C5 isolate and to identify any additional SNPs present within the genome that can be used as suitable markers for differentiation between the CrleGV-SA-C5 and CrleGV-SA isolates. It was recognised that it

is required to conduct further detached fruit bioassays and field trials, but with improved protocols, for the efficacy and UV-tolerance of the CrleGV-SA-C5 isolate to be conclusively determined.

Table of Contents

Declaration	ii
Abstract	iii
Table of Contents	vi
List of Figures	ix
List of Tables	xiii
List of Equations	xv
List of Abbreviations	xvi
Acknowledgements.....	xx
Chapter 1	1
1.1 THE SOUTH AFRICAN CITRUS FRUIT INDUSTRY	1
1.2 THAUMATOTIBIA LEUCOTRETA	2
1.2.1 Taxonomy & distribution of <i>T. leucotreta</i>	2
1.2.2 Host Range of <i>T. leucotreta</i>	2
1.2.3 <i>T. leucotreta</i> lifecycle	3
1.2.4 Control of <i>T. leucotreta</i>	5
1.3 BACULOVIRUSES	8
1.3.1 Taxonomy	8
1.3.2 Characteristics of baculoviruses	8
1.3.3 Baculovirus lifecycle & infection process	10
1.3.4 Baculovirus genomes	13
1.3.5 Baculoviruses as biopesticides	13
1.3.6 Cryptophlebia leucotreta granulovirus	14
1.3.7 Factors that influence the use of baculoviruses as biopesticides	15
1.4 THE EFFECT OF UV ON BACULOVIRUSES	16
1.4.1 Improving baculovirus UV-tolerance	17
1.4.2 Selection of UV-tolerant baculoviruses	19
1.5 MOTIVATION	20
1.6 AIMS AND OBJECTIVES	20
Chapter 2	22
2.1 INTRODUCTION	22
2.2 METHODOLOGY	24
2.2.1 <i>De novo</i> assembly and genome alignment	24

2.2.2	Oligonucleotide design targeting variable regions.....	24
2.2.3	Virus samples, occlusion body purification and TEM	25
2.2.4	Genomic DNA extraction	25
2.2.5	PCR amplification of targeted genome regions.....	26
2.3	RESULTS.....	27
2.3.1	<i>De novo</i> assembly and genome alignment.....	27
2.3.2	Transmission electron microscopy	29
2.3.3	Genomic DNA extraction	29
2.3.4	Oligonucleotide design and PCR amplification of genomic regions	30
2.4	DISCUSSION	34
Chapter 3	39
3.1	INTRODUCTION.....	39
3.2	METHODS	41
3.2.1	Recombinant plasmids	41
3.2.2	Ligation of amplicons into pJET1.2/blunt and transformation into <i>E. coli</i>	42
3.2.3	Colony PCR.....	42
3.2.4	Plasmid extraction	43
3.2.5	Restriction enzyme digestion	43
3.2.6	Plasmid sequencing and sequence alignment.....	44
3.2.7	Melt curve analysis	44
3.3	RESULTS.....	45
3.3.1	Cloning of PCR amplicons into pJET1.2/blunt plasmid vector and colony PCR	45
3.3.2	Plasmid extraction and restriction digestion.....	48
3.3.3	Sequencing of recombinant plasmids	50
3.3.4	SYBR melt curve analysis.....	56
3.4	DISCUSSION	57
Chapter 4	60
4.1	INTRODUCTION.....	60
4.2	METHODS	61
4.2.1	Occlusion body enumeration	62
4.2.2	<i>Thaumatotibia leucotreta</i> diet preparation	63
4.2.3	Rearing of <i>Thaumatotibia leucotreta</i> larvae.....	63
4.2.4	Surface dose-response bioassays to determine the lethal concentration estimates	64
4.2.5	CrleGV-SA-C5 bulk-up in fourth instar <i>T. leucotreta</i>	65

4.2.6 Crude purification of occlusion bodies	65
4.2.7 Genomic DNA extraction	66
4.2.8 Polymerase chain reaction of target regions	66
4.2.9 Sanger sequencing of polymerase chain reaction amplicons.....	66
4.3 RESULTS.....	67
4.3.1 Occlusion body enumeration	67
4.3.2 Surface dose-response bioassays to determine the lethal concentration estimates	67
4.3.3 CrleGV-SA-C5 bulk-up 1 and bulk-up 2	69
4.3.4 Genomic DNA extraction	70
4.3.5 Polymerase chain reaction of target regions	71
4.3.6 Sanger sequencing of polymerase chain reaction amplicons.....	72
4.4 DISCUSSION	77
Chapter 5	80
5.1 INTRODUCTION.....	80
5.2 METHODS	82
5.2.1 Collection and preparation of oranges and virus treatment preparation	82
5.2.2 Detached fruit bioassay	83
5.3 RESULTS.....	86
5.3.1 Detached fruit bioassay	86
5.4 DISCUSSION	89
Chapter 6	94
6.1 Thesis Overview.....	94
6.2 CrleGV-SA-C5 Genomic Analysis and SNP Screening.....	94
6.3 CrleGV-SA-C5 Virus Propagation and UV tolerance comparison.....	97
6.3.1 Propagation of CrleGV-SA-C5 in <i>T. leucotreta</i> larvae and genome analysis...97	
6.3.2 Comparing the UV-tolerance of the CrleGV-SA-C5 isolate.....	98
6.4 Conclusion and Future Work.....	100
REFERENCES.....	103

List of Figures

Chapter 1

Figure 1.1: The life cycle of *Thaumatotibia leucotreta* at 25 °C showing the duration of each developmental stage adapted from (Daiber, 1979a, 1979b, 1979c, 1980).4

Figure 1.2: Citrus fruit damage as a result of infestation by *T. leucotreta* larvae. A: Visible damage of larval infestation on the orange rind and B: Larval damage inside the orange.....5

Figure 1.3: Baculovirus occlusion bodies, virions and nucleocapsids. Top left: The structures of occlusion bodies from baculoviruses in the genera Alphabaculovirus (nucleopolyhedrovirus, NPV) and Betabaculovirus (granulovirus, GV) are illustrated. Virions embedded in nucleopolyhedrovirus occlusion bodies may contain multiple nucleocapsids (MNPV) or single nucleocapsids (SNPV). Top right: The two baculovirus virion phenotypes are illustrated as diagrams with shared and phenotype-specific components (from Blissard, 1996). (Bottom) Transmission electron micrographs of occlusion bodies (MNPV, SNPV and GV). Nucleopolyhedrovirus occlusion bodies of the MNPV (*Autographa californica* MNPV, bottom left) and SNPV (*Trichoplusia ni* SNPV, bottom middle) types are compared to granulovirus occlusion bodies (*Estigmene acrea* GV, bottom right) (Herniou et al., 2011). 10

Figure 1.4: A life cycle of a baculovirus causing systemic infection. Occlusion bodies ingested by an insect dissolve in the midgut and ODV are released which then infect midgut epithelial cells (A). The virion buds out of the cell in a basal direction and initiates a systemic infection (B). Early in the systemic infection, more BV are produced, which spread the infection throughout the insect (C). Late in infection occluded virions are produced, and the cell then dies releasing the occlusion bodies (D) (Rohrmann, 2019). 12

Figure 1.5: Aims of the study to determine the biological and genetic stability of the UV-tolerant strain of CrleGV-SA21

Chapter 2

Figure 2.1: Transmission Electron Micrograph of A: CrleGV-SA-C5 and B: CrleGV-SA. The red arrow is indicating the nucleocapsid within the OB (CrleGV-SA TEM images courtesy of Thuthula Mela).....29

Figure 2.2: Agarose gel electrophoresis of extracted genomic DNA. A: CrleGV-SA-C5. B: CrleGV-SA.30

Figure 2.3: In silico test conducted on the CrleGV-SA using the three sets of oligonucleotides designed targeting five different SNPs identified. The binding sites are shown in green, with the various SNPs indicated in yellow. The CrleGV-SA genes are shown in purple.31

Figure 2.4: Schematic diagram indicating where the oligonucleotides bind to the target regions relative to the identified SNPs32

Figure 2.5: AGE with ethidium bromide staining of PCR amplicons, using three different oligonucleotide sets at three different annealing temperatures. A) Pif-2 PCR amplicons of 348 bp in size. B) HypoP PCR amplicons of 302 bp in size. C) Lef-8/HP PCR amplicons of 311 bp in size.33

Figure 2.6: AGE with ethidium bromide staining of PCR amplicons resulting from gDNA extracted from A: CrleGV-SA and B: CrleGV-SA-C5. The Pif-2 amplicon size is 348bp, the HypoP amplicon size is 302bp and the Lef-8/HP amplicon size is 311bp.34

Chapter 3

Figure 3.1: A generalised plasmid map of the recombinant vectors that were created using Pif-2, the insert (Orange) represents the target gene that was ligated into the pJET1.2/blunt cloning vector. Annotations: The disrupted lethal gene (Eco47I/T7) in maroon, the Ampicillin resistance gene (AmpR) in green, and the multiple cloning site (MCS) in blue. Oligonucleotide and restriction enzyme binding sites are labelled in purple and black text respectively.46

Figure 3.2: A 1% agarose gel with ethidium bromide staining of the colony PCR amplification of the cloned CrleGV-SA and CrleGV-SA-C5 PCR amplicons.....47

Figure 3.3: Agarose gel electrophoresis (1 %) with ethidium bromide staining showing the results with undigested and digested plasmids. A) pC5_Pif-2 and pSA_Pif-2. B) pC5_HypoP and pSA_HypoP. C) pC5_Lef-8/HP and pSA_Lef-8/HPs.49

Figure 3.4: Multiple sequence alignment of the CrleGV-SA-C5 and CrleGV-SA Pif-2 regions against the plasmid sequence of pC5_Pif-2 and pSA_Pif-2. The targeted SNPs, UV_2 and UV_3, are highlighted by the black box.51

Figure 3.5: Multiple sequence alignment of the CrleGV-SA-C5 and CrleGV-SA HypoP region against the plasmid sequence of pC5_HypoP and pSA_HypoP. The targeted SNP, UV_5 is highlighted by the black box.53

Figure 3.6: Multiple sequence alignment of the CrleGV-SA-C5 and CrleGV-SA Lef-8/HP region against the plasmid sequence of pC5_Lef-8/HP and the sequence of the CrleGV-SA Lef-8/HP PCR amplicons. The targeted SNPs, UV_6 and UV_7, are highlighted in with the black box.....55

Figure 3.7: Melt Curve generated using the CrleGV-SA-C5 HypoP PCR product and the CrleGV-SA HypoP PCR Product. The blue curves represent the CrleGV-SA-C5 HypoP PCR products, the red curves represent the CrleGV-SA HypoP PCR products, and the green line the NTC reaction.....56

Chapter 4

Figure 4.1: Schematic diagram describing the various steps of the study62

Figure 4.2: Rearing of *T. leucotreta* larvae in artificial diet in baking trays, incubated at 25 °C with 16 h:8 h (L:D) photoperiod.....64

Figure 4.3: Dilution series of CrleGV-SA-C5 for surface dose-response bioassays against *T. leucotreta* fourth instars to determine LC₉₀.65

Figure 4.4: Analysis of the first two bioassay replicates. A: The larval survival rate against concentration rate of UV-tolerant C5 CrleGV OBs (OBs/ml). B: Probit analysis of the percentage mortality against the concentration rate of UV-tolerant C5 CrleGV OBs (OBs/ml), with the response curve (—) and 95 % confidence intervals (---) shown.69

Figure 4.5: Images from the virus bulk-up of A & B: 24-well plates and C & D: Infected *T. leucotreta* larvae that were collected.70

Figure 4.6: AGE with ethidium bromide staining of genomic DNA extractions from CrleGV-SA-C5_BU2 OBs.....71

Figure 4.7: AGE with ethidium bromide staining of PCR amplicons resulting from gDNA extracted from CrleGV-SA-C5_BU2. A) Pif-2 oligonucleotide set, B) HypoP oligonucleotide set and C) Lef-8/HP oligonucleotide set. The Pif-2 amplicon size is 348bp, the HypoP amplicon size is 302bp and the Lef-8/HP amplicon size is 311bp.72

Figure 4.8: Pairwise sequence alignment of the consensus sequences generated of the CrleGV-SA-C5_BU2 Pif-2 PCR amplicons against the CrleGV-SA-C5 Pif-2 gene. The targeted SNPs, UV_2 and UV_3, are highlighted within the black boxes.74

Figure 4.9: Pairwise sequence alignment of the CrleGV-SA-C5_BU2 HypoP consensus sequence, aligned against the CrleGV-SA-C5 HypoP gene. The targeted SNP, UV_5, is highlighted within the black box.....75

Figure 4.10: Pairwise sequence alignment of the CrleGV-SA-C5_BU2 Lef-8/HP consensus sequence aligned against the CrleGV-SA-C5 Lef-8/HP genes. The black boxes highlight the targeted SNPs UV_6 and UV_7.76

Chapter 5

Figure 5.1: A schematic flow diagram of the UV exposure and Non-UV Exposure detached fruit bioassay setup.85

Figure 5.2: Oranges infested with *T. leucotreta* larvae. A: Orange from UV_DFB replicate 2 CrleGV-SA-C5 treatment and B: Non-UV_DFB replicate 3 control treatment.....86

Figure 5.3: Mean (\pm SE) temperature recorded for the UV exposure period per day for each UV exposure detached fruit bioassay replicate set-up. Weather data from A: bioassay replicate 1, B: bioassay replicate 2 and C: bioassay replicate 3.87

Figure 5.4: Average (\pm SE) UV Index recorded per day for each UV exposure detached fruit bioassay replicate set-up. A: UV Index data from bioassay replicate 1, B: UV Index data from bioassay replicate 2 and C: UV Index data from bioassay replicate 3.....88

Figure 5.5: Analysis of the infested oranges from all three bioassay replicates from both UV_DFB and Non-UV_DFB. The oranges that were not infested by *T. leucotreta* larvae from both UV_DFB and Non-UV_DFB were also recorded (data not shown). There was no significant difference between the UV_DFB and Non-UV_DFB Control treatments ($p > 0.9999$).....89

List of Tables

Chapter 1

Table 1.1: *Thaumatotibia leucotreta* taxonomic classification.....2

Table 1.2: Examples of Commercially formulated baculovirus products for controlling lepidopteran pests.....14

Chapter 2

Table 2.1: Oligonucleotides targeting variable regions identified in CrleGV-SA-C5.....24

Table 2.2: PCR reaction set-up for each PCR run27

Table 2.3: Single polymorphisms identified in the genome sequence of CrleGV-SA-C528

Chapter 3

Table 3.1: Details of the recombinant pJET1.2/blunt plasmids following ligation of the Pif-2, HypoP and Lef-8/HP inserts, indicating the insert size, SNPs encompassed and the resulting size of each recombinant plasmid.41

Table 3.2: Reaction set-up for colony PCR of recombinant plasmids in transformed TOP10 E. coli cells.43

Table 3.3: Reaction setup for restriction digestion of recombinant plasmid DNA44

Table 3.4: SYBR Melt Curve reaction setup45

Table 3.5: Expected sizes of the colony PCR amplicons.....47

Chapter 4

Table 4.1: *Thaumatotibia leucotreta* larval mortality in surface dose-response bioassay after 7 days for the first two bioassay replicates67

Table 4.2: *Thaumatotibia leucotreta* larval mortality in surface dose-response bioassay after 7 days for all three bioassay replicates68

Table 4.3: The LC₅₀ and LC₉₀ for the CrleGV-SA-C5 bioassay against fourth instar *T. leucotreta* larvae.....69

Table 4.4: CrleGV-SA-C5 bulk-up results showing the amount of tissue from which the OBs were extracted from, the concentration of the OBs and the final volume obtained.....70

Chapter 5

Table 5.1: Treatments applied to oranges for each UV_DFB and Non-UV_DFB set-up to determine the UV tolerance of the CrleGV-SA-C5 isolate in comparison to the CrleGV-SA isolate.....83

List of Equations

Equation 4.1: Equation to determine the concentration of the virus sample using a counting chamber.....63

List of Abbreviations

Units

Bp	Base Pair
°C	Degrees Celsius
ddH₂O	Double distilled water
G	Grams
g/L	Grams per litre
H	Hour
Kb/kpb	Kilobase pairs
µg.ml⁻¹	Micrograms per millilitre
µl	Microliter
µM	Micrometre
U/µl	Unit per microlitre
mg.ml	Milligrams per millilitre
ml	Millilitre
Mm	Millimetre
mM	Millimolar
Min	Minutes
M	Molar
Ng	Nanogram
ng/µl	Nanogram per microliter
Nm	Nanometre
N	Number
%	Percentage
pH	Potential of hydrogen
Rpm	Revolutions per minute
S	Seconds
×g	Times gravity
V	Volts
v/v	Volume per volume
w/v	Weight per volume

Abbreviations

AGE	Agarose gel electrophoresis
AmpR	Ampicillin resistance gene
BV	Budded virus
CBC	Centre for Biological Control
CRI	Citrus research international
CTAB	Cetyltrimethylammonium bromide
DNA	Deoxyribonucleic acid
dsDNA	Double stranded deoxyribonucleic acid
EPF	Entomopathogenic fungi
EPN	Entomopathogenic nematodes
EPV	Entomopathogenic viruses
ELVA	Envelope-labelled virus assay
EDTA	Ethylenediaminetetraacetic acid
FCM	False codling moth
gDNA	Genomic deoxyribonucleic acid
HRM	High-resolution melting
HP	Hypothetical Protein CDS
IPM	Integrated Pest Management
<i>lef-8</i>	Late expression factor-8
LC	Lethal concentration
LC₅₀	Lethal concentration (50 %)
LC₉₀	Lethal concentration (90 %)
LD₅₀	Lethal dose (50 %)
LET₅₀	Lethal exposure time (50 %)
Ltd	Limited
LA	Luria agar
LB	Luria broth
MCS	Multiple cloning site
Na₂CO₃	Sodium carbonate
NaCl	Sodium chloride
NGS	Next generation sequencing
NTC	No template controls

OAR	Original activity remaining
OBs	Occlusion bodies
OBs/ml	Occlusion bodies per millilitre
OBs/mm²	Occlusion bodies per square millimetre
ODV	Occlusion derived virion
ORF	Open reading frame
<i>pif-2</i>	Per os infectivity factor-2
PCR	Polymerase chain reaction
PIB	Polyhedral inclusion body
PIB.ml⁻¹	Polyhedral inclusion body per millilitre
Pty	Propriety
qPCR	Quantitative polymerase chain reaction
R	Rand
REN	Restriction endonuclease
RFU	Relative fluorescence units
SIT	Sterile insect technique
SDS	Sodium dodecyl sulphate
SA	South African
SNPs	Single nucleotide polymorphisms
SE	Standard error
TEM	Transmission electron microscope
TAE	Tris base, acetic acid and EDTA
UV	Ultraviolet
USA	United States of America
<u>Viruses</u>	
AdorGV	Adoxophyes orana granulovirus
AgMNPV	Anticarsia gemmatalis multiple nucleopolyhedrovirus
AcMNPV	Autographa californica multiple nucleopolyhedrovirus
BmNPV	Bombyx mori nucleopolyhedrovirus
CrleGV	Cryptophlebia leucotreta granulovirus
CrleGV-SA	Cryptophlebia leucotreta granulovirus, South Africa
CrleGV-SA-C5	Cryptophlebia leucotreta granulovirus, UV-tolerant isolate
CrleGV-CV3	Cryptophlebia leucotreta granulovirus, Cape Verde 3

CpGV	Cydia pomonella granulovirus
GmNPV	Galleria mellonella nucleopolyhedrovirus
GV	Granulovirus
HomaGV	Homona magnanima granulovirus
LdMNPV	Lymantria dispar multiple nucleopolyhedrovirus
MNPV	Multiple nucleopolyhedrovirus
PbGV	Pieris brassicae granulovirus
PlxyGV	Plutella xylostella granulovirus
SNPV	Single nucleopolyhedrovirus
SeMNPV	Spodoptera exigua multiple nucleopolyhedrovirus

Acknowledgements

Finishing my Master's thesis has been a long but rewarding and exciting journey. I want to express my appreciation to the following people who have helped me vastly towards the completion of my thesis:

- First and foremost, I would like to thank my supervisor Prof, Martin Hill and co-supervisors Dr Sean Moore, Dr Michael Jukes and Prof. Caroline Knox for all your time, endless support, guidance and for giving me valuable feedback throughout my Master's journey. This thesis would not have been possible without all of you, much appreciated.
- Sincere thanks to Citrus research international (CRI) and Rhodes University for providing me with financial support during my Master's degree.
- Dr Candice Coombes for her assistance with *T. leucotreta* host rearing and providing with host larvae.
- Marcel van der Merwe for his assistance with virus OB enumeration and help with fruit collection
- David Kinsler for his assistance with obtaining weather data from Rhodes University Geography department weather station.
- Mellissa Peyper for her help with getting *T. leucotreta* insect eggs
- Marvin Randall for his assistance with electron microscopy and the light microscope for OB enumeration.
- Thuthula Mela for her support, and assistance in the laboratory and thank you to my friends for your support, laughter, conversations, and very special memories.
- Finally, I would like to thank my parents, Mark and Virginia Bennett and twin sisters Chloe and Cleo, for your unconditional love, support and endless encouragement. Thank you for offering your help and guidance. You have kept me motivated and focused from the start until the end.

Chapter 1

Introduction & Literature Review

1.1 THE SOUTH AFRICAN CITRUS FRUIT INDUSTRY

The citrus fruit industry plays an integral part in the economy of South Africa (Sinngu & Antwi, 2014). With South Africa being the second biggest citrus exporter in the world. In the 2019 season almost 1.02 billion cartons of citrus were exported (CGA, 2020). According to DALRRD (2020), this industry impacts an estimation of over a million households, as many people are employed in the various sectors of the supply chain of services, for example, in port handling or transport. The industry is a fundamental source of job creation and foreign exchange income in South Africa (CGA, 2017; Moore, 2001). Citrus is cultivated in the Eastern Cape, KwaZulu-Natal, Free State, Limpopo, Northern Cape, Western Cape, North West, and Mpumalanga (CGA, 2019). Grapefruit and Valencia oranges are cultivated in Limpopo, Mpumalanga and KwaZulu-Natal (warmer citrus growing areas). Lemons, Navel oranges and soft citrus fruits are grown in the Eastern Cape and Western Cape provinces (colder citrus growing areas) (Sinngu & Antwi, 2014). Around 70 % of South Africa's fresh citrus is exported to foreign markets (CGA, 2013). Within South Africa's horticulture industry, the top three sectors that contribute the most with regards to the gross value are citrus fruits, vegetables and deciduous fruits (Sinngu & Antwi, 2014). With an overall 42% of the fruit production being exported. The amount that the citrus fruit industry contributed during the 2017/18 production season to the total gross value of South African agricultural production was over R19 billion (6.9 %) (DALRRD, 2020). Even though this industry is a highly profitable sector in agriculture, it is threatened by the phytosanitary pest *Thaumatotibia leucotreta* which causes damage to the fruit thereby affecting citrus exports and the economy of South Africa. *Thaumatotibia leucotreta* prefers citrus as host species, and the most vulnerable to damage caused by *T. leucotreta* are Navel oranges (Moore, 2012; Newton, 1998). The marketability of the citrus fruit is reduced due to the feeding lesions caused by *T. leucotreta* as the larvae burrow into the fruit (Malan et al., 2018). Thus, this pest must be controlled as it is endemic to Africa (Moore, 2002).

1.2 THAUMATOTIBIA LEUCOTRETA

1.2.1 Taxonomy & distribution of *T. leucotreta*

Thaumatotibia leucotreta (Meyrick) (Lepidoptera: Tortricidae), commonly known as false codling moth (FCM), is indigenous to sub-Saharan Africa (Catling & Aschenborn, 1974; Maniania et al., 2017). Komai (1999) proposed the name *Cryptophlebia leucotreta* to change to what it is now known as *T. leucotreta*. (Table 1.1). This pest has been found on the Reunion Island, Cape Verde Islands, St Helena and Mauritius Islands (Grout & Moore, 2015; Wysoki, 1986). *Thaumatotibia leucotreta* also occurs on nearby Atlantic and Indian Ocean Islands, south of Sahara (Newton, 1998) and in Israel (Wysoki, 1986). In 1899, *T. leucotreta* was first documented in what is now KwaZulu-Natal, South Africa as a pest in citrus (Bloem et al., 2007).

Table 1.1: *Thaumatotibia leucotreta* taxonomic classification

Taxa	Scientific Classification
Kingdom	Animalia
Phylum	Arthropoda
Class	Insecta
Order	Lepidoptera
Family	Tortricidae
Genus	<i>Thaumatotibia</i>
Species	<i>Thaumatotibia leucotreta</i>

1.2.2 Host Range of *T. leucotreta*

Thaumatotibia leucotreta has a wide host range and is a polyphagous pest (Newton, 1998; Timm et al., 2010). *Thaumatotibia leucotreta* is a key pest of citrus (Newton, 1998), avocados (Erichsen & Schoeman, 1992), stone fruit (Daiber, 1978), cotton (W. Reed, 1974), macadamias (La Croix & Thindwa, 1986) as well as numerous other crops. Additionally, this pest has been found on about 50 wild plant species and approximately 24 cultivated plant species (Kirkman, 2007c), of which some are incorrect, and others forced laboratory associations (Kirkman & Moore, 2007). Various non-commercial and natural hosts and subsistence and large-scale commercial environments are threatened by *T. leucotreta* in Southern Africa (de Villiers et al., 2015; Prinsloo & Uys, 2015). In South Africa *T. leucotreta* is a vital pest, infesting numerous

fruit crops (Malan et al., 2018). Many cultivated South African crops, such as citrus, table grapes, vegetable crops, and stone fruit, are affected by *T. leucotreta* (Blomefield, 1989; Prinsloo & Uys, 2015). The pre-harvest damage that results when the larvae feed on the fruit, and the interception of infested fruit post-harvest, make *T. leucotreta* an essential economic pest of various types of citrus (Moore, 2012; Newton, 1998). Grapefruit and Valencia oranges are less susceptible to the damage caused by *T. leucotreta*, with Mandarins and Navel oranges being more susceptible (Love et al., 2014). However, *T. leucotreta* is not a pest of limes and lemons (Grout & Moore, 2015; Moore & Hattingh, 2012). Macadamia's, avocados and litchis are also affected by *T. leucotreta* (Prinsloo & Uys, 2015). There are also several natural hosts of *T. leucotreta*, these include, marula (*Sclerocarya birrea caffra* (Sonder)), Port Jackson galls buffalo-thorn (*Ziziphus mucronata* (Willdenow)) and acorns (*Quercus robur* (Lam.)) (Stotter, 2009). Depending on host availability, *T. leucotreta* may move among its' different hosts (Timm et al., 2010). *Thaumatotibia leucotreta* causes different levels of pest pressure in South Africa, as this pest is not able to proliferate in the varying climates where citrus is grown (Malan et al., 2018).

1.2.3 *T. leucotreta* lifecycle

The *T. leucotreta* larvae are responsible for the damage caused by the insect. The complete life cycle is about 42-46 days at a temperature of 25°C, with multiple generations yearly (Opoku-Debrah et al., 2014). The adult *T. leucotreta* lays the eggs individually on the outside of the fruit, on fallen fruit or on the foliage with the eggs maturing in ~5 days (Daiber, 1979a; de Jager, 2013; Opoku-Debrah et al., 2014) (Figure 1.1). The eggs have three morphologically distinct stages of maturity, which are (i) Newly laid (transparent), (ii) Red-eye (on the inside of the egg there is red colouring) and (iii) Black head, this is when the first instar larva's head capsule is visible (Steyn, 2019). A pile of frass is left on the fruits' rind after the first instar larvae bore into the fruit (Daiber, 1979b). Development continues within the fruit as the first instar feeds and moults several times (Daiber, 1979b). According to EFSA PLH Panel et al. (2021), there are between 1-3 *T. leucotreta* larvae found per citrus fruit. A pinkish-red coloured fifth instar larva emerges from the fruit after development is complete and is ready for pupating (Daiber, 1979b). The larva pupates once it drops to the soil and burrows less than 5 mm down (Love et al., 2019). The larvae also move under the bark to spin cocoons (Stofberg, 1954). The colour of the pupae is dark brown (Newton, 1998). The pupa takes 14-21 days to mature, and then the adult moth emerges (Daiber, 1979c) (Figure 1.1). Prior to transformation into a pupa, the larvae go through a prepupal stage (Daiber, 1979c). Male and female pupae have different

developmental periods, males develop over a longer period than females (Daiber, 1979c). The overwintering population of *T. leucotreta* is mainly the pupae. During winter months, the development of *T. leucotreta* is long resulting in fewer generations as compared to that throughout the summer and spring months (Daiber, 1980; Gunn, 1921).

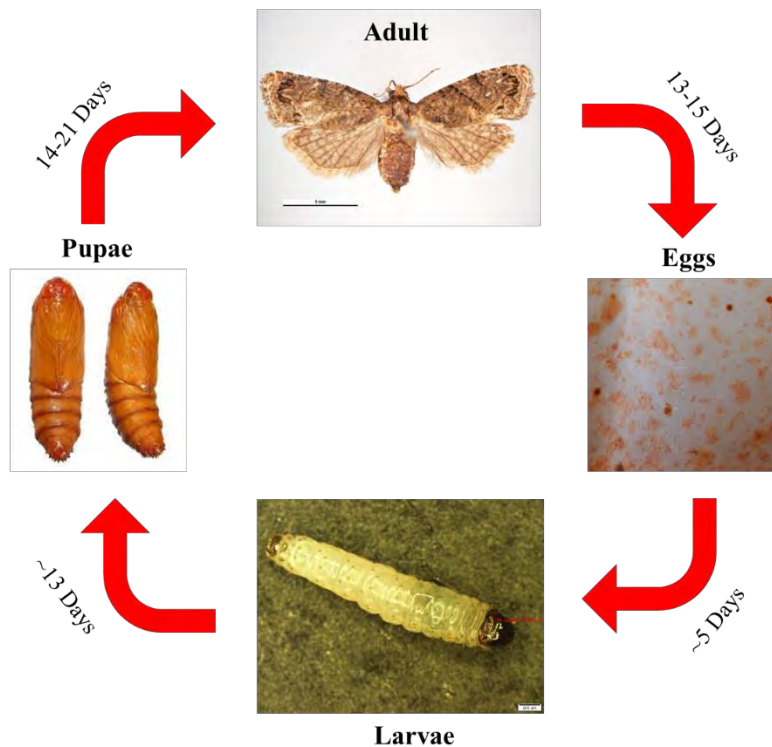


Figure 1.1: The life cycle of *Thaumatotibia leucotreta* at 25 °C showing the duration of each developmental stage adapted from (Daiber, 1979a, 1979b, 1979c, 1980).

Thaumatotibia leucotreta results in both indirect and direct damage to the fruit. The primary damage caused by *T. leucotreta* is through the feeding of the larvae in the fruit (Figure 1.2), which induces premature ripening, phytosanitary problems and the fruit dropping (Kirkman & Moore, 2007). The secondary damage caused by *T. leucotreta* is by increasing the susceptibility of the fruit to bacterial and fungal infections by the entry wounds caused by the larvae on the fruit. These infections cause post-harvest decay (Erichsen & Schoeman, 1994; Fullard & Hill, 2013). Nearly 80 % of the citrus fruit drop is a result of infection by *T. leucotreta* (Hofmeyr & Pringle, 1998).

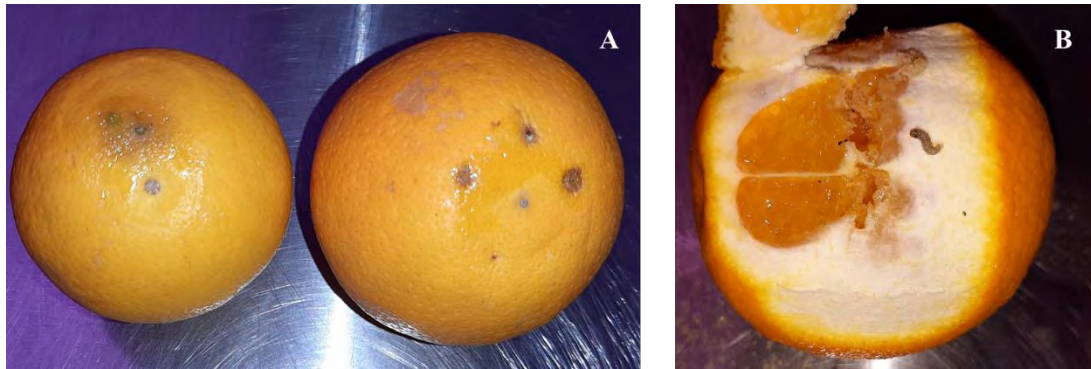


Figure 1.2: Citrus fruit damage as a result of infestation by *T. leucotreta* larvae. A: Visible damage of larval infestation on the orange rind and B: Larval damage inside the orange.

1.2.4 Control of *T. leucotreta*

Thaumatotibia leucotreta is an economically important pest that threatens the citrus industry and as a result there is a rigorous programme to control the pest. For many decades, research has been conducted on *T. leucotreta* and the control of it in citrus (Catling & Aschenborn, 1974; Grout & Moore, 2015; Hofmeyr et al., 1991). *Thaumatotibia leucotreta* is currently most effectively controlled through an integrated pest management (IPM) programme (Moore, 2021). The aim of the IPM programme is for integrating all the control measures available for the control of this pest into a single strategic arsenal, in conjunction with the problems of chemical pesticide dependency being counteracted (Moore & Hattingh, 2012). An IPM programme includes the use of chemical pesticides, mating disruption, sterile insect technique (SIT), cultural control (orchard sanitation) and biological control (parasitoids, entomopathogenic fungi, baculoviruses) (Hatting et al., 2019; Hofmeyr et al., 2016; Moore, 2021). It is important that a multidisciplinary-based approach is used for the control of *T. leucotreta* as the stand alone treatments is not effective enough (Moore, 2019). For effective management of a pest, monitoring is the first step. The indicators that determine how efficient the control options put in place are the size of the population of the pest and the degree of damage incurred (de Villiers & Pringle, 2007). An important source that provides crucial information is the larval infestation of the fruit.

1.2.4.1 Chemical Pesticides

Chemical insecticides are used as part of the control strategies against *T. leucotreta*. The following chemical pesticides, a spinosad (Delegate™), insect growth regulators (Nomolt®, Alsyntin® and Runner™) and a diamide (Coragen®) have been registered in South Africa for the control of *T. leucotreta* (Moore, 2021; Moore & Hattingh, 2012). There are many problems

associated with the use of chemicals to control *T. leucotreta* including unacceptable residue levels to markets and insect resistance developing to chemical insecticides (Malan et al., 2018; Moore et al., 2011). Additionally, the human, animal and ecological health risks that emerge as a result of chemical residue exposure has raised serious concerns for the use of chemical insecticides (Malan et al., 2018; Moore, 2002). Chemical pest control products negatively affect pathogens, natural enemies and target organisms (Catling & Aschenborn, 1974; Moore, 2002). According to Chandler et al. (2011), the adverse effects caused by various chemical pest control products can result in the ecosystem health being compromised and in turn repercussions for ecosystem service delivery. As a result, foreign markets have imposed for stricter chemical residue restrictions (Malan et al., 2018). There is an urge to reduce the number of chemicals used in the agricultural environment and to use products that are more environmentally friendly. As a result of the damaging and long-lasting effects of broad-spectrum chemicals, cases of resistance, and stricter regulations (Guedes et al., 2016). Numerous *T. leucotreta* management programmes still have chemical insecticides as a fundamental part of these programmes (Malan et al., 2018). *Thaumatotibia leucotreta* can be controlled effectively by newer chemical products that consist of IPM-compatible ingredients (Hill & Fullard, 2013; Moore et al., 2015a; Moore & Hattingh, 2012).

1.2.4.2 Mating disruption

Controlling insect pest behaviour is the basis of mating disruption. The *T. leucotreta* males are disorientated by synthesised female pheromones as a result they cannot find mates (Malan et al., 2018). Synthetic pheromone's have a temporary effect on male *T. leucotreta*, and large quantities of the synthetic pheromone's is required for the control. Mating disruption programmes result in the number of viable eggs oviposited being reduced as a result of preventing *T. leucotreta* from copulating (Foster & Harris, 1997). Examples of products registered in South Africa are, Isomate FCM and X-Mate FCM (Moore & Hattingh, 2012; Moore, 2021).

1.2.4.3 Sterile insect technique

Understanding the pest's biology and the life cycle is vital for an effective and target specific IPM programme (Bottrell & Smith, 1982). The IPM is an area-wide pest management approach (Dyck et al., 2021). This is the most effective technique available for area-wide population suppression (Moore, 2019). The mass reared male moths are sterilised by gamma radiation and thereafter the males are released into the orchard to colonise the environment (Malan et al.,

2018). The population growth is suppressed as a result of infertile eggs produced by the females when female moths mate with sterile males (Bloem et al., 2003). In citrus, the SIT has been used to control *T. leucotreta*. The commercial facility, XSIT (Pty) Ltd, Citrusdal, South Africa, has been utilizing this technique since 2007 (Barnes et al., 2015).

1.2.4.4 Cultural Control

Another vital strategy for controlling *T. leucotreta* is the cultural control method in the form of orchard sanitation (Bedford et al., 1998). The aim of this control method is for any hanging and fallen fruit that are suspected to be infested with *T. leucotreta* to be regularly removed and destroyed (Moore & Kirkman, 2009). There are three major benefits of orchard sanitation, these are: the control of fruit flies, the control of *T. leucotreta* and fungal spore removal from orchards (du Toit, 1998). An average of 75 % of fruit infested by *T. leucotreta* larvae gets removed by weekly sanitation between December to June (Moore & Kirkman, 2009). A component of the foundation of a control plan for the pest in an orchard is weekly orchard sanitation (Hofmeyr, 2003; Moore & Kirkman, 2009).

1.2.4.5 Biological Control

One of the key components to the IPM programme is biological control. Biological control consists of the use of entomopathogenic nematodes (EPN), entomopathogenic fungi (EPF) and parasitoids (Hatting et al., 2019; Malan et al., 2018). The aim of biological control is for the use of chemical pesticides to be reduced (Haase et al., 2015). Entomopathogenic nematodes and EPF are aimed at controlling the life stages of *T. leucotreta* that are soil-dwelling (Malan et al., 2018). Indigenous EPNs were first investigated by Malan et al. (2011) for *T. leucotreta* control. Six naturally occurring isolates of EPN that are virulent to the pupae and larvae of *T. leucotreta* have been identified by Malan et al. (2011). The only EPN commercially available product that targets the soil-dwelling stage of *T. leucotreta* is CryptoneemTM (River Bioscience, South Africa), consisting of *Heterorhabditis bacteriophora* Poinar as an active ingredient. This species is indigenous to South Africa (Malan et al., 2006). In terms of EPF, the environmental conditions that are beneficial to the different life stages of the insect host and the life cycle of the EPF are usually in synchrony with one another. Above 80 % of infestation of *T. leucotreta* was decreased from one spring application of *Metarhizium anisopliae* (Metonikoff) Sorokin (Hypocreales: Cordycipitaceae) and *Beauveria bassiana* (Balsamo) Vuillemin (Hypocreales: Clavicipitaceae) (Coombes et al., 2016; Moore et al., 2013).

Additionally, entomopathogenic viruses (EPV) such as baculoviruses are currently used as microbial insecticides (Grzywacz, 2017). Baculoviruses are environmentally friendly, they species-specific, leave no residues on the fruit and they have a narrow host range, these factors make them perfect biological control agents (Moore et al., 2004). The following chapters will discuss baculoviruses in more detail.

1.3 BACULOVIRUSES

1.3.1 Taxonomy

The first formal description of the silkworm's "wilting disease" in the sixteenth century is traced to be where the interest in insect disease originated (Benz, 1986). In the early eighteenth century, the wilting disease was said to be caused by a virus infection, and it was reported in 1947 that the virus had characteristics of microorganisms in the Baculoviridae family, with rod-shaped virions (Miller, 1996). The Baculoviridae is a large family of viruses that are arthropod-specific, with over 600 host species recorded worldwide (Rohrmann, 2019). Baculoviridae family is divided into four genera, namely the *Gammabaculovirus*, *Betabaculovirus*, *Deltabaculovirus* and *Alphabaculovirus* (Jehle et al., 2006). *Betabaculoviruses* are lepidopteran specific granuloviruses (GVs) and *Alphabaculoviruses* are nucleopolyhedroviruses (NPVs) that infect Lepidoptera. The genera *Deltabaculovirus* infect dipteran hosts and *Gammabaculovirus* infect hymenopteran hosts and both genera are NPVs (Herniou et al., 2003; Rohrmann, 2019). Granuloviruses are Lepidopteran viruses; alternatively, NPVs have been isolated from non-Lepidopteran hosts as well (Cory & Myers, 2003; Herniou et al., 2003). Baculovirus also infect Crustaceans in the order Decapoda (Herniou et al., 2003) and have also been isolated from the invertebrate orders Coleoptera, Trichoptera, Neuroptera, and Thysanura (Nishi & Nonaka, 1996; Popham et al., 2001). Baculoviruses are named according to the host from which they were isolated from (Harrison & Bonning, 1999). In baculovirus taxonomy, the highly conserved genes encoding polyhedron/granulin proteins are used as a molecular criterion (Jehle et al., 2006).

1.3.2 Characteristics of baculoviruses

The morphological characteristics of baculovirus occlusion bodies (OBs) namely, capsules or granules for GV and polyhedral for NPV are basis on which members of the baculoviridae family are classified (Rohrmann, 2019). These viruses are highly resilient in the environment due to the protein matrix made of either granulin or polyhedron that surrounds the enveloped nucleocapsid, forming OB (Herniou & Jehle, 2007). Granules are oval-shaped with

a diameter of about 0.2-0.4 μM and polyhedra have a diameter of about 0.6-2 μM (Ackermann & Smirnov, 1983). The OB is the infectious unit of baculoviruses (Figure 1.3) (Herniou et al., 2003). Polyhedral OBs contain multiple virions within a protein matrix. Multiple NPVs (MNPV) have several nucleocapsids within each virion, and single NPVs (SNPV) only have a single nucleocapsid within each virion (Cory & Myers, 2003; Herniou et al., 2003). Granuloviruses produce ovoid OBs, and these contain a single virion surrounding one nucleocapsid within each OB (Figure 1.3). Phylogenetically there is a subdivision of NPVs into group I and group II. Group I NPVs have Budded Viruses (BVs) which consist of GP64, which is essential for virus entry and transmission from cell-to-cell, and this is a low-pH-dependent membrane fusion protein (Blissard, 1996; Hefferon et al., 1999; Kingsley et al., 1999). Granuloviruses and group II NPVs, on the other hand, do not have a homolog of GP64 but a F protein which triggers the fusion of the membrane when the virus enters the host (IJkel et al., 2000; Pearson et al., 2000).

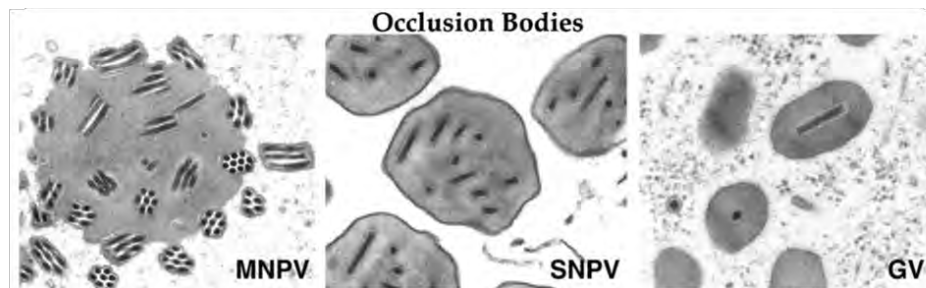
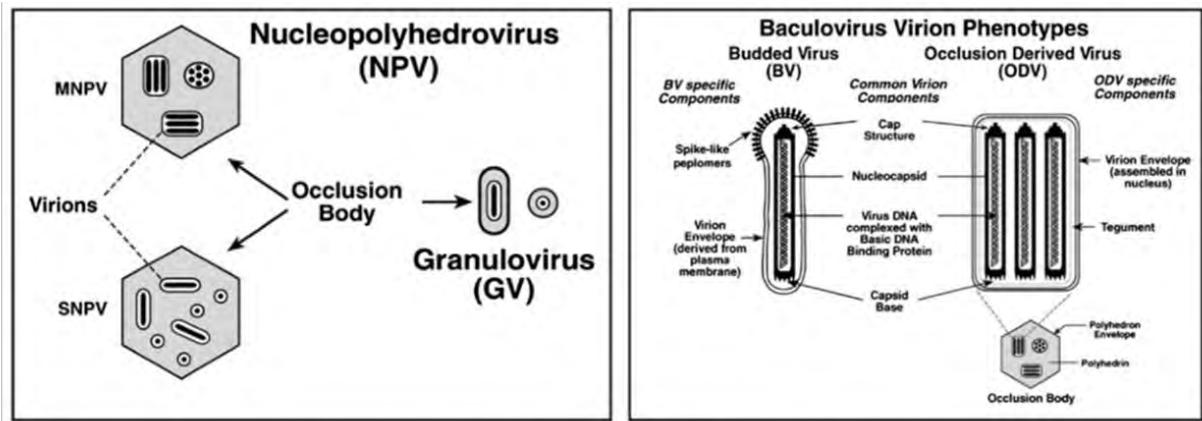


Figure 1.3: Baculovirus occlusion bodies, virions and nucleocapsids. Top left: The structures of occlusion bodies from baculoviruses in the genera Alphabaculovirus (nucleopolyhedrovirus, NPV) and Betabaculovirus (granulovirus, GV) are illustrated. Virions embedded in nucleopolyhedrovirus occlusion bodies may contain multiple nucleocapsids (MNPV) or single nucleocapsids (SNPV). Top right: The two baculovirus virion phenotypes are illustrated as diagrams with shared and phenotype-specific components (from Blissard, 1996). (Bottom) Transmission electron micrographs of occlusion bodies (MNPV, SNPV and GV). Nucleopolyhedrovirus occlusion bodies of the MNPV (*Autographa californica* MNPV, bottom left) and SNPV (*Trichoplusia ni* SNPV, bottom middle) types are compared to granulovirus occlusion bodies (*Estigmene acrea* GV, bottom right) (Herniou et al., 2011).

1.3.3 Baculovirus lifecycle & infection process

Baculoviruses have a biphasic replication cycle, with transmission from one host to the next through OB and from tissue-to-tissue through non-occluded budded virus (Cory & Myers, 2003). The OB is vital for the infection to proliferate between hosts (Popham et al., 2001). The larval feeding stages are the only stages infected by baculoviruses (Cory & Myers, 2003). Baculoviruses have two virion (virus particle) phenotypes produced in the lifecycle (Jehle et al., 2006; Rohrmann, 2019). Budded viruses transmit the infection from cell-to-cell. After the initial infection BVs are produced and bud from the plasma membrane of infected cells, the infection is spread throughout the tissues of the susceptible insect host through the haemolymph

(Blissard & Rohrmann, 1990; Rohrmann, 2019). Occluded-derived virions (ODV), which transmit the baculovirus infection through insect-to-insect transmission, which contain either a single or multiple nucleocapsids within an envelope. Occluded-derived virions are encased within the OB, which is a crystalline protein matrix (Blissard & Rohrmann, 1990; Jehle et al., 2006; Rohrmann, 2019).

The larvae feed on fruit containing the OB contaminants, which enter the midgut of the larvae. Once the OBs are ingested, the virions are released into the insect midgut enabling the infection of the midgut epithelial cells (Blissard & Rohrmann, 1990; Rohrmann, 2019). The alkaline gut pH and proteases of the midgut aid in the rapid release of the virions, which then move through the peritrophic membrane lined gut (Cory & Myers, 2003). The virions then fuse with the midgut columnar cells' plasma membranes, and the infection is initiated once the DNA-containing nucleocapsids move to the nucleus (Cory & Myers, 2003). Replication of GVs occurs in the nucleo-cytoplasmic stroma after the nuclear membrane has disintegrated, and NPV replication occurs in the nucleus (Jehle et al., 2006). The infection process of baculoviruses is enhanced by various proteins that baculoviruses encode (Popham et al., 2001). The plasma membrane of the host provides an envelope which encases a single nucleocapsid (Jehle et al., 2006). More OBs are produced by the infected tissues, and at the end of the infection cycle, the OBs are released into the environment once the caterpillar cadaver disintegrates (Blissard & Rohrmann, 1990) (Figure 1.4). The virions are protected in the environment from degradation by the occlusion bodies (Herniou et al., 2003). The persistence of OBs in the environment occurs over an extensive period and even more so, if they are protected from being degraded by UV-irradiation (Carruthers et al., 1988; Thompson et al., 1981). Disease transmission of baculoviruses is dependent upon whether a susceptible larva comes in contact and ingests the virus, which is typically from the death of an infected larva, and as a result, and therefore dependent upon how the susceptible and infected larvae behave (Cory & Myers, 2003).

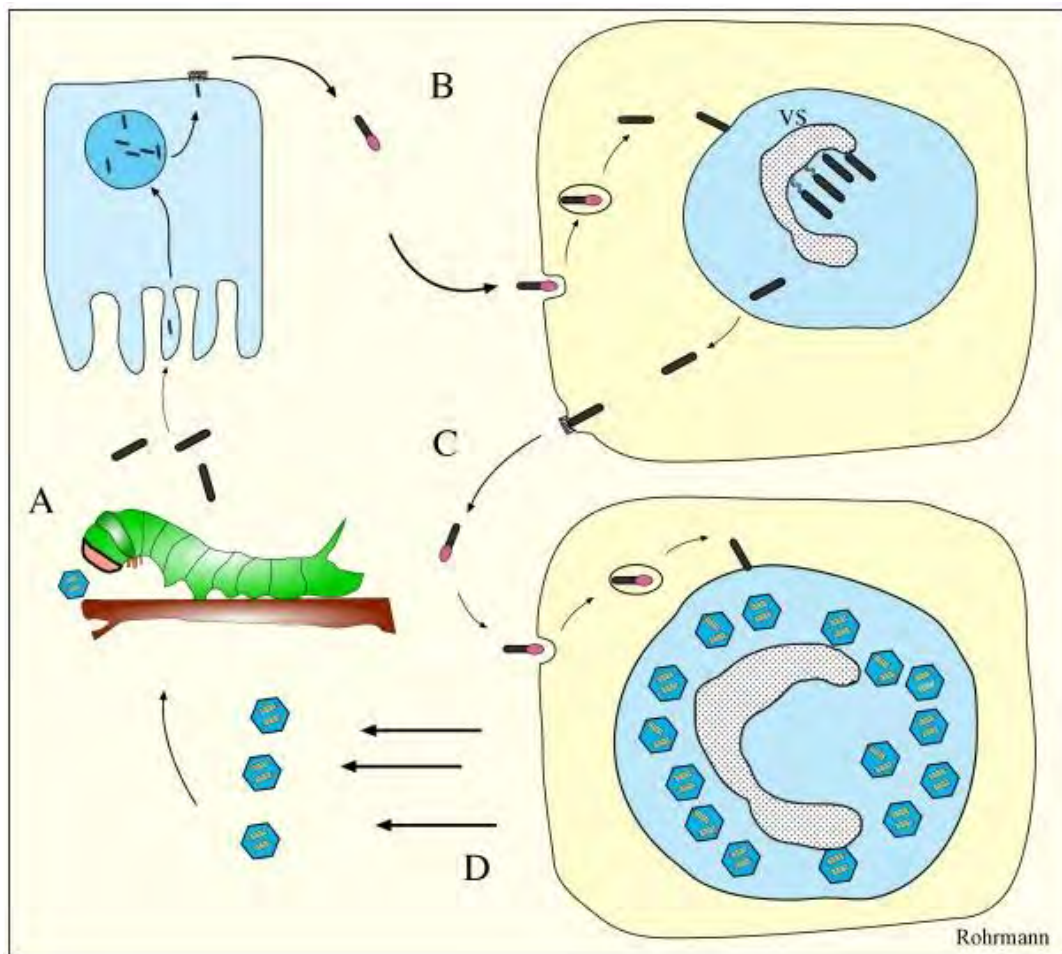


Figure 1.4: A life cycle of a baculovirus causing systemic infection. Occlusion bodies ingested by an insect dissolve in the midgut and ODV are released which then infect midgut epithelial cells (A). The virion buds out of the cell in a basal direction and initiates a systemic infection (B). Early in the systemic infection, more BV are produced, which spread the infection throughout the insect (C). Late in infection occluded virions are produced, and the cell then dies releasing the occlusion bodies (D) (Rohrmann, 2019).

When the host larvae are infected, they are weakened, resulting in a reduction in feeding, mobility, development and increasing predator exposure (Young & Kring, 1991). Infected larvae die 5-8 days after climbing to the upper parts of the plant (Fuxa, 1987). A decrease in reproductive longevity and capacity and lower adult and pupal weights are some of the post-larval effects from infection (Rothman & Myers, 1996). In Sawflies, infection occurs in the midgut and OBs are released with the faeces (frass) (Cory & Myers, 2003).

1.3.4 Baculovirus genomes

Baculoviruses are one of the largest groups of dsDNA viruses (Harrison et al., 2018). The size of baculovirus genomes is 80 to 180 kbp long and 100 to 200 open reading frames are encoded (Harrison et al., 2018; Herniou et al., 2003). There are three phases for baculovirus gene expression, namely: early, late and very late gene expression. Various baculovirus genes are either only present within a small group of baculoviruses or conserved within large groups or genera of related baculoviruses or are unique to a single baculovirus genome (Harrison & Hoover, 2012). Baculoviruses have been shown to be genetically variable, and this is evident in the restriction endonuclease (REN) profiles of the DNA of baculoviruses (Cory & Myers, 2003).

1.3.5 Baculoviruses as biopesticides

Baculoviruses have been used as biopesticides for many years because of the nature of their lifecycle. The first attempt for using a virus for controlling insects was a NPV against the pest *Lymantria monacha* found in pine forests, conducted in Germany in 1892 (Moscardi, 1999). Thézé et al. (2018) stated that there have been more than 165 identified baculovirus species and each year novel species are discovered, evaluated and characterised. According to Cunningham (1995), most baculoviruses have been used for the control of Lepidoptera, however, they have been successfully used for control of Hymenoptera Symphyta (Sawflies) found in forests. Since the 1900s, agriculture and forestry pests have been biologically controlled by baculoviruses (Beas-Catena et al., 2014a).

Various factors that make baculovirus favourable to use as biological pesticides include, the basic knowledge of baculovirus biology, taxonomy and pathogenicity is available; the commercially viable mass production systems for many baculoviruses are well advanced making them feasible; they are safe and environmentally acceptable; they have a detailed and long history of research; and they are highly efficacious pathogens to some of the most vital crop pests (Wilson et al., 2020). Additionally, baculoviruses have a narrow specificity, they are not harmful to wildlife and people, and are pathogens found naturally in pest populations providing an environmentally friendly approach (Beas-Catena et al., 2014a; Szewczyk et al., 2006). In a similar process to chemical pesticides, baculoviruses can be mass-produced, formulated, packaged, stored, and marketed (Beas-Catena et al., 2014a). Examples of baculovirus biopesticides are highlighted in Table 1.2 (Moore & Jukes, 2020). Baculovirus biopesticide must, however, be applied correctly in terms of the correct timing of application

during the day to reduce ultraviolet (UV) degradation, targeted against susceptible host life stages, ensuring suitable adjuvants are added, and the provision of adequate coverage (Moore et al., 2004; Moore & Hattingh, 2012). In the South Africa the CrleGV virus is one of the major components in the IPM programme.

Table 1.2: Examples of commercially formulated baculovirus products for controlling lepidopteran pests

Baculovirus	Abbreviation	Host insect	Product examples
Adoxophyes orana NPV	AdorNPV	<i>Adoxophyes orana</i>	Capex, Capex 2
Cydia pomonella GV	CpGV	<i>Cydia pomonella</i>	Carpovirusine, Cyd-X, Madex, VirosoftCP4
Cryptophlebia leucotreta GV	CrleGV	<i>Thaumatotibia leucotreta</i>	Cryptogran, Cryptex
Helicoverpa zea NPV	HzNPV	<i>Helicoverpa zea</i>	Gemstar
Lymantria dispar NPV	LdNPV	<i>Lymantria dispar</i>	Gypcheck
Neodiprion abietis NPV	NeabNPV	<i>Neodiprion abietis</i>	Abietiv
Phthorimaea operculella GV	PhopGV	<i>Phthorimaea operculella</i>	Matapol, PTM Baculovirus, Tutavir
Spodoptera littoralis NPV	SpliNPV	<i>Spodoptera littoralis</i>	Littovir

1.3.6 *Cryptophlebia leucotreta* granulovirus

Cryptophlebia leucotreta granulovirus (CrleGV) was described first by Angélini et al. (1965). The CrleGV isolate was isolated from *T. leucotreta* larvae that were infected in Ivory Coast. An additional strain was obtained from diseased larvae collected from the Cape Verde Islands (Mück, 1985). The Hoechst Corporation in Germany had a laboratory colony, established from samples collected from the field in South Africa, and this was where the third isolate was obtained (Jehle et al., 1992). Citrus Research International (CRI) in Port Elizabeth held a laboratory colony of *T. leucotreta*, and a novel isolate was obtained from a larva collected from this colony that was diseased (Singh et al., 2003). This isolate was contrasted with the Cape Verde isolate, CrleGV-CV3, by restriction endonuclease analysis of viral DNA, which indicated that the South African isolate was distinct and thus named CrleGV-SA (Jehle et al., 1992; Lange & Jehle, 2003; Singh et al., 2003). *Cryptophlebia leucotreta* GV has been

formulated into three biopesticides in South Africa to control *T. leucotreta*, these are, Cryptogran™ (River Bioscience (Pty) Ltd, South Africa), Gratham® (Andermatt Biocontrol, Switzerland) and Cryptex® (Andermatt Biocontrol, Switzerland) (Hatting et al., 2019; Moore & Jukes, 2020). Cryptogran® has been successfully utilised for nearly twenty years in the field (Moore et al., 2015b). A study by van der Merwe et al. (2017) showed that over many years the CrleGV-SA genome has remained stable.

1.3.7 Factors that influence the use of baculoviruses as biopesticides

According to Moscardi (1999), there is an increase in the interest of the industry for the use of baculoviruses. Despite their widespread use, various factors affect how well baculoviruses persist in the field. These factors include, temperature, speed of kill, host range, commercial production and UV irradiation.

1.3.7.1 Temperature

Temperature affects the efficiency of baculoviruses in the field; high and low temperatures can inhibit the infection (Moscardi, 1999). It can also affect how successful the virus is in regions that have low mean temperatures by having the lethal time of the virus increased (Moscardi, 1999). It was also stated that a rapid inactivation of baculoviruses occurs when temperatures exceed 50 °C (Ignoffo, 1992).

1.3.7.2 Speed of kill

Another limiting factor to the baculoviruses as biopesticides is the slow speed of kill of baculoviruses (Szewczyk et al., 2011). It was shown that the *egt* gene present in baculoviruses enables the replication of the virus by prolonging the host larval stage (Maeda, 1989). As a result, this may influence the speed of kill of baculoviruses. The rate of kill of chemical pesticides is hours as opposed to baculoviruses ranging from five days up to more than two weeks (Beas-Catena et al., 2014a). Baculovirus speed of kill can be increased through genetic modification of the baculovirus (O'Reilly & Miller, 1991). Alternatively, the hormones of the insect larvae can be targeted. In comparison to the wild type virus, the speed of kill of *Bombyx mori* NPV (BmNPV) to *Bombyx mori* larvae was increased by 20% when diuretic hormones were introduced to BmNPV (Maeda, 1989).

1.3.7.3 Host range

The host range of baculoviruses is typically narrow and is confined to a few species within a family or few insect families (Moore & Jukes, 2020). This is in comparison to the broader host

range of chemical insecticides. The range of hosts which baculoviruses are able to infect, has an effect on their role in IPM programmes. In order to establish the same level of control as what would be achieved with the application of a single or few chemical insecticides, multiple control options need to be included in an IPM programme and this is because of the narrow host range of baculoviruses (Moore & Jukes, 2020). A few baculoviruses do however have a host range that is relatively broader. For example, more than one species within a genus or family can be infected by NPVs. *Autographa californica* NPV is an example of a baculovirus with broader host range (Hitchman et al., 2007).

1.3.7.4 Commercial production

The production of baculoviruses at a large-scale is also a limiting factor for the industry. This large-scale production is usually done *in vivo*, where insects are reared on diets that are artificial (Moscardi, 1999), and also under conditions that are similar to that in the field (Moscardi & Sosa-Gómez, 1992, 1996). An alternative to this is cell-culture based mass production (Lacey et al., 2015; Moscardi et al., 2011). However, there are difficulties associated with this, as well (Claus et al., 2012) such as variable OB quality and low OB/cell yield associated with the production of baculoviruses *in vitro* (Nguyen et al., 2011). In comparison to chemical pesticide production, baculovirus production *in vivo* costs are relatively high (Lacey et al., 2015). Additionally, the main limiting factors associated with scaling up functional OBs from small scale to industrial production is that the virulence and yield are decreased (Grzywacz & Moore, 2017). A virus yield of 150 OBs per cell and at least 10000 litre culture is required for commercial production of baculoviruses (Greenfield et al., 1999). In order to obtain a 10000 litre scale of virus product it requires 11 passages. However, when serial passaging baculoviruses in cell culture they are not stable, and they spontaneously form defective interfering particle mutants and few polyhedral mutants (Lui & Reid, 2005).

1.3.7.5 UV irradiation

One of the major factors that affect how well baculoviruses persist in the field is solar radiation (Jacques, 1985; Shapiro, 1995; Szewczyk et al., 2006). The effects of UV irradiation will be discussed further in the next section.

1.4 THE EFFECT OF UV ON BACULOVIRUSES

The use of baculovirus biopesticides is largely affected by UV irradiation (Shapiro, 1995). Ultraviolet radiation in region A (UV-A) (320-400 nm) may have a negative effect on baculovirus deactivation, whereas UV-B (280-310 nm) will cause baculoviruses to be

inactivated (Shapiro, 1995). UVC (100-280) is reflected by the clouds and ozone layer prior to reaching the surface of the earth, and is, therefore, less severe compared to UVA and UVB (Robberecht, 1989). Photosensitisation of DNA is promoted by UVA, and in photosensitisation type I it is triggered by electron abstraction, and in photosensitisation type II it is triggered by single oxygen radicals (Girard et al., 2011). UVA is not readily absorbed by DNA, and as a result pyrimidine (6-4) pyrimidine photoproducts, cyclobutane pyrimidine dimers and their Dewar valence isomers are also not caused by UVA (Girard et al., 2011; Ridley et al., 2009).

The way UV affects baculoviruses is that adjacent pyrimidine residues are cross-linked, resulting in pyrimidine dimers. This may cause lethal mutations because of incorporating incorrect nucleotides, or there is no copying of the DNA after the site that is damaged, or the interaction of the proteins that play a role in gene regulation may be hindered (Rohrmann, 2013; Tyrrell et al., 1974). Baculovirus degradation may also occur due to the highly active radicals, singlet oxygen, peroxides, and hydroxyls, which are produced by sunlight (Ignoffo & Garcia, 1994). More intense sunlight exposure of baculoviruses on branch tips increases inactivation of the virus (Cory & Myers, 2003). For the UV impact on baculoviruses to be reduced in the field, the majority of the spraying occurs in the evenings. Different species of baculovirus have different degrees of inactivation as a result of UV exposure. There is a mutualistic relationship between time of exposure and UV inactivation and an indirectly proportional relationship between the concentration of the virus present and UV inactivation (Shapiro et al., 2002). Ignoffo et al. (1977) tested the susceptibility of microbial control agents to UV and found that the most susceptible to UV was GVs, and the least susceptible was *Bacillus thuringiensis*.

A study by Mwanza (2015), showed that more rapid damage was caused to CrleGV-SA by UVB compared to UVA. The study by Mwanza (2015) also showed that 21 days after the initial spraying of the virus in the field, there was higher insecticidal activity on the Southern side (shaded side) of the citrus trees in comparison to the northern side (sun facing). There was a clear dose-response on the southern side of the trees 28 days after spraying in comparison to the northern side of the trees virulence which was indeterminable because it was very low.

1.4.1 Improving baculovirus UV-tolerance

There have been tests done on various substances which could act as sun screening agents to aid in prolonging the activity of baculoviruses used in the field (Shapiro, 1995). According to Lacey et al. (2015), the natural appearance of the fruit or plants should not be altered by UV-protectants, factors such as blockage of spray filters and high viscosity should not change the

concentration of the UV-protectants required, the UV-protectants should be low cost and the conditions required for the UV-protectants storage must be compatible with the virus. Sunscreen products and cosmetic foundation powders consist of iron oxide as a sunscreen component. This sunscreen component was tested to determine the effect it had on HamakiTendeki (Arysta LifeScience Co.), a commercial product which consists of two species of GV, *Adoxophyes orana* granulovirus (AdorGV) and *Homona magnanima* granulovirus (HomaGV) (Asano, 2005). The effects of the addition of iron oxide compared to using the biopesticide product without the iron oxide was that UV inactivation was decreased by between one-eighteenth and one-sixth (Asano, 2005). Another study tested substances as possible sun screening agents and showed that folic acid, 2-hydroxy-4-methoxy-benzophenone, Tinopal DCS, p-aminobenzoic acid, uric acid, and 2-phenylbenzimidazole-5-sulfonic acid were the best at protecting against UV (Shapiro, 1995).

Additionally, according to Behle & Birthisel (2014), dyes can absorb at the wavelength region of 280-400 nm. Out of 79 dyes tested, those that were effective at providing protection against UV are acidine yellow, mercuriocrome, brilliant yellow, lissamine green and alkali blue. The NPV of *Lymantria dispar* was fully protected from UV by the dye Congo Red (Shapiro, 1995). The dyes that were more effective were able to absorb UV-A (Shapiro, 1995). The fluorescent brighteners of the stilbene group are able to absorb both UV-B and UV-A, and this makes them effective to use for baculovirus protection against solar radiation (Shapiro, 1995). It was shown through laboratory test that baculoviruses are protected from UV by several tea extracts (Shapiro et al., 2008). Several plant-derived extracts were tested as potential UV-protectants for *Spodoptera exigua* multiple nucleopolyhedrovirus (SeMNPV) (Shapiro et al., 2009). After 30 minutes' exposure to UVB irradiation, it was found that out of 67 extracts tested that 15 provided adequate UV protection and after 300 minutes of UVB exposure four out of the fifteen provided excellent protection with an OAR of over 90% (Shapiro et al., 2009). Additionally, a study by El-Salamouny et al. (2009) showed that a good UV protectant that could protect SeMNPV from UV by nearly 100% is black tea. Spreaders/wetting agents, anti-evaporants or metallic oxides are used to protect the virus from UV irradiation and are, therefore, added to the virus formulations (Mishra, 1998). For baculovirus formulations it is desirable for baculoviruses to have the field activity extended, however, if increased protection will result in added costs when producing the final product, then there might not be substantial returns (on the product) (Fuxa, 1991). According to Arthurs et al. (2008), many published studies on UV-protection have analysed the potential of lignin and its derivative as successful UV-protectants.

A study showed that the residual activity of CpGV was considerably improved when used as a spray dried lignin formulation containing CpGV in comparison to using CpGV formulation alone (Arthurs et al., 2008). When lignin derivative as a natural UV protectant was used as an additive it demonstrated a high protecting effect (El-Salamouny et al., 2002).

1.4.2 Selection of UV-tolerant baculoviruses

Tests have also been conducted for the selection of UV-tolerant baculoviruses to protect the virus from UV irradiation. The effect of UV irradiation on *Galleria mellonella* nuclear polyhedrosis virus (GmNPV) was tested by Witt & Stairs (1975). It was observed that, in the virus population, there was a part of the virus susceptible to high UV dosage and others susceptible to low UV dosage. Witt & Stairs (1975) suggested that genetic variability could be the cause of the heterogeneity in UV-response. A strain of AcMNPV that was close to UV-tolerant was successfully isolated by Witt & Hink (1979) after five selection cycles. It was observed that the strain had a loss in virulence which was thought to be due to independent events or linked to the selection of UV-tolerance. A study by Shapiro & Bell (1984) used the *Lymantria dispar* multiple nucleopolyhedrovirus (LdMNPV), the gypsy moth NPV, and performed six cycles of UV-exposure and propagation. This study found that virus persistence increased by 2.5-fold.

Similarly, Mwanza (2019) and Mwanza et al. (2022) isolated a UV-tolerant CrleGV by repeated UV exposure of a laboratory colony of CrleGV-SA. The study sequenced the UV-tolerant CrleGV-SA and conducted a sequence comparison between the unexposed CrleGV-SA isolate and the UV-tolerant CrleGV-SA and determined the differences in the structure between the non-UV-irradiated virus, UV irradiated virus and the selected UV-tolerant virus. Sequencing and sequence comparison showed that in cycle one, there were seven Single Nucleotide Polymorphisms (SNPs), and in cycle five, there were an additional seven SNPs (14 SNPs). Transmission electron microscopy data revealed that UV irradiation caused damage to the virion and the crystalline structure of the OB. The UV exposed OBs from cycle one was found to be notably smaller in comparison to those from cycle 5. The study also found that, after five exposure cycles of UV irradiation in a Q-Sun Xe-3 HC test chamber (Q-lab, USA), it was found that samples in cycle 1-4 had higher LC₅₀ values in comparison to samples in cycle 5 with LC₅₀ values that were lower. After 24 h UV-exposure there was a decline in LC₅₀ values from 2.89 x 10⁸ OBs/ml (cycle 1) to 2.16 x 10⁵ OBs/ml (cycle 5), and after 72 h UV-exposure from 2.11 x 10⁹ OBs/ml (cycle 1) to 1.73 x 10⁶ OBs/ml (cycle 5). The LC₅₀ values of

the virus showed an improvement in the virulence of more than 1000-fold (Mwanza, 2019; Mwanza et al., 2022).

1.5 MOTIVATION

Thaumatotibia leucotreta is a serious pest of citrus and has been controlled through several control strategies within an IPM programme. One of the components in the IPM programme is the use of *Cryptophlebia leucotreta* granulovirus (CrleGV-SA). It has been formulated as Cryptogran[®] (River Bioscience (Pty) Ltd, South Africa) and has been used in the field successfully for many years to control *T. leucotreta*. One of the main factors influencing baculovirus insecticides such as Cryptogran[®] and its application in the field is UV irradiation. The DNA of the virus is damaged by exposure to UV light, and this decreases the efficiency of the biopesticide. Thus, there is a need to improve the resistance of the OBs to UV. In a recent study, a UV-tolerant virus strain of CrleGV-SA which differed genetically and biologically from the wildtype virus was selected after repeated exposure of viral OBs to UV irradiation (Mwanza, 2019; Mwanza et al., 2022). This UV-tolerant strain has potential as a biocontrol agent for improving the control of *T. leucotreta* in the field. Whether the genetic and biological stability of this strain is maintained when passaged repeatedly through the host for commercial purposes is not known.

1.6 AIMS AND OBJECTIVES

This study aims to determine the biological and genetic stability of the UV-tolerant strain of CrleGV-SA, which can potentially improve *T. leucotreta* control (Figure 1.5). The aim will be investigated through the following objectives:

- A To identify and compare variations between the CrleGV-SA-C5 and the CrleGV-SA genome sequences.
- B To develop screening methods to distinguish between CrleGV-SA-C5 and CrleGV-SA isolate regions.
- C To determine whether the genetic stability of the CrleGV-SA-C5 isolate is retained when bulked up *in vivo*.
- D To compare the UV-tolerance of the CrleGV-SA-C5 and CrleGV-SA isolates under natural UV irradiation via detached fruit bioassays.

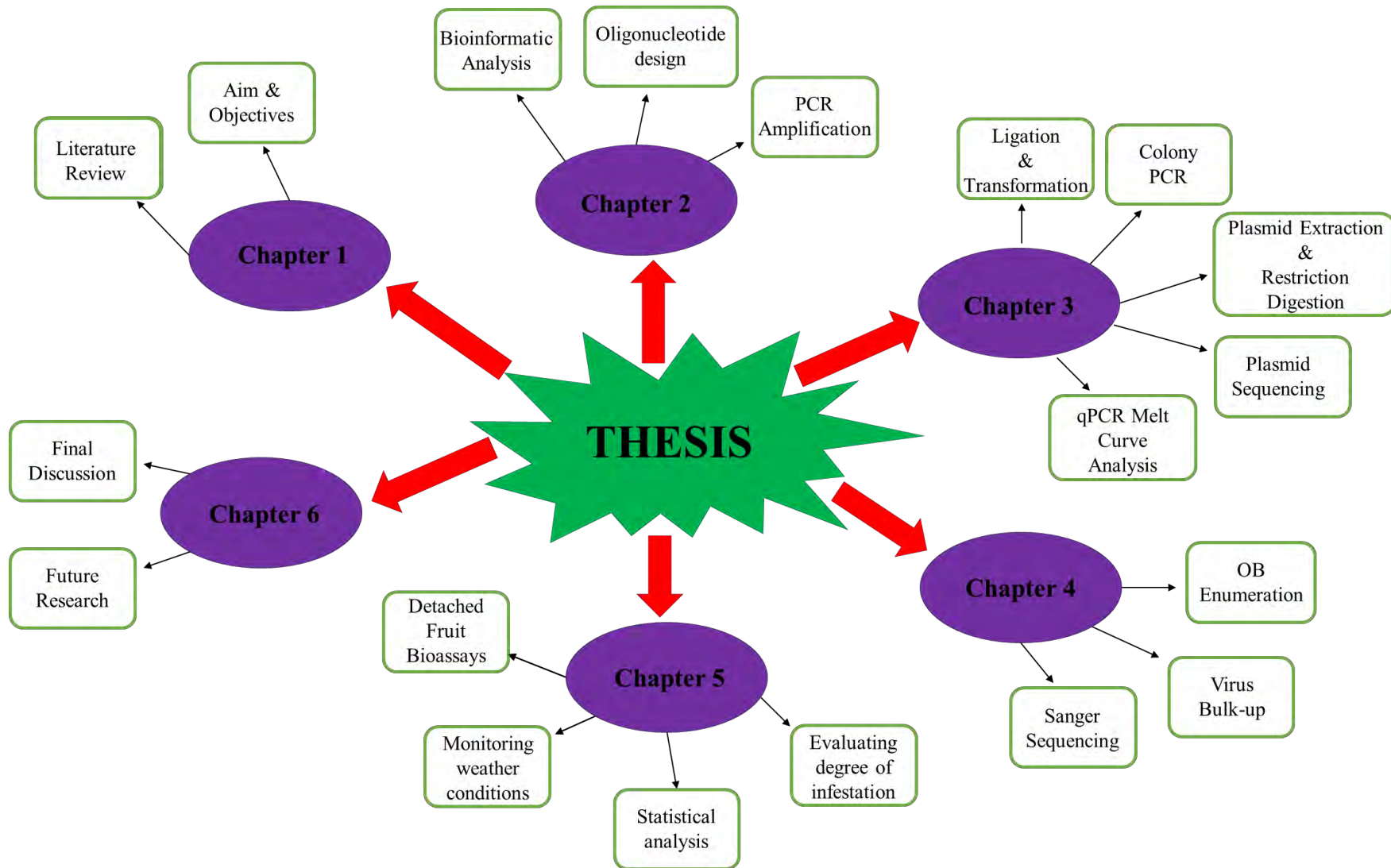


Figure 1.5: Aims of the study to determine the biological and genetic stability of the UV-tolerant strain of CrleGV-SA

Chapter 2

Genomic analysis of UV-tolerant CrleGV-SA & Oligonucleotide Design

2.1 INTRODUCTION

In a previous study conducted by Mwanza (2019) and Mwanza et al. (2022), a UV-tolerant *Cryptophlebia leucotreta* granulovirus (CrleGV) isolate (referred to CrleGV-SA-C5) was isolated following successive cycles of UV exposure. In the same study, next generation sequencing (NGS) was carried out using genomic DNA extracted from occlusion bodies (OBs) obtained from CrleGV samples before and after UV exposure. Pairwise alignments using the consensus sequence generated and mapped against the published CrleGV-SA genome (GenBank accession number: MF984563; (van der Merwe et al., 2017)) revealed the presence of 14 non-synonymous SNPs in the CrleGV-SA-C5 genome. In order to corroborate the data obtained by Mwanza (2019) and Mwanza et al. (2022), *de novo* assembly of the CrleGV-SA-C5 genome was repeated using the same NGS data and analysed for the presence of SNPs. According to Sohn & Nam (2018), *de novo* assembly is described as a massive multiple pieced jigsaw puzzle. It is not possible to read a whole genome sequence within one glance. Therefore, regions of reads up to the chromosomal level that are shared need to be detected and assembled into numerous fragmented sequences (Miller et al., 2010). There are three steps within the basic strategy for the *de novo* assembly of short NGS reads, namely: contig assembly, scaffolding and gap filling. During the contig assembly, long consensus sequences (contigs) without gaps are assembled from the generated reads. Large-insert reads connect the contigs together during the scaffolding step. During the gap filling step, other independent reads are used to fill the gaps for the assembly to be completed. The gaps are the spaces that remain between the contigs after the contigs are scaffolded (Sohn & Nam, 2018). A new consensus sequence is then generated. Conducting an additional *de novo* assembly may result in a different consensus sequence being generated and therefore different SNPs may be identified to those identified by Mwanza (2019) and Mwanza et al. (2022).

Once a consensus sequence is constructed, the next step is to conduct a sequence alignment. Alignments of related protein or DNA sequences are an appropriate way for sequence

comparison (Altschul & Pop, 2017). Nucleotide mismatches, deletions and insertions can be identified by conducting an alignment (Madigan et al., 2012). The first complete genome sequence for the South African CrleGV-SA isolate was described by van der Merwe et al. (2017). Prior to this, the Cape Verde 3 (CrleGV-CV3) isolate's complete genome sequence was the only sequence available as a reference sequence. The CrleGV-SA genome length is 111334 bp, and a 96.6 % pairwise identity was achieved when the genome of CrleGV-SA was compared to the CrleGV-CV3 genome (van der Merwe et al., 2017). The CrleGV-SA genome was used as a reference sequence in the current study and used during sequence alignment.

Polymerase chain reaction (PCR) is the replication of DNA *in vitro*. During the amplification process oligonucleotides initiate the synthesis of DNA and up to a billion-fold of copies of a specific gene or segment of DNA is copied (Madigan et al., 2012). Oligonucleotide design is an important aspect of PCR amplification (Madigan et al., 2012). The length of DNA oligonucleotides is generally between 18 and 30 nucleotides long (Saiki et al., 1985). Oligonucleotides are used to amplify selected regions in a targeted genome (Vincent et al., 1994). The PCR amplification starts with denaturing the template DNA, oligonucleotides then anneal to the template DNA strands, thereafter DNA polymerase synthesizes the new DNA strands. Each strand is then used to create two new copies and the process is repeated (Madigan et al., 2012). Therefore, oligonucleotides were designed to amplify target regions identified in the CrleGV-SA-C5 genome where SNPs have been detected and these target regions were amplified through PCR amplification.

The overall aim of the study reported in this chapter was to identify and compare variations between the CrleGV-SA-C5 and the CrleGV-SA genome sequences. The first objective of the study was to conduct a *de novo* assembly alignment. The second objective was identification of any SNPs, followed by the third objective which was oligonucleotide design, covering the regions where the SNPs were detected. The fourth objective was virus sample preparation and transmission electron microscopy (TEM) to visualise the virus samples. The fifth objective was genomic DNA (gDNA) extraction of the purified virus OBs and PCR amplification of the target regions.

2.2 METHODOLOGY

2.2.1 *De novo* assembly and genome alignment

The Illumina sequence data obtained from the CrleGV-SA-C5 isolate sequence was provided by Mwanza (2019). Duplicates within the sequence reads were removed using the Duplicate Read Remover function, and the reads were error corrected using Geneious R11 (v11.1.5) (Biomatters, New Zealand). The complete CrleGV-SA genome sequenced by van der Merwe et al. (2017) was used as the reference sequence for mapping the CrleGV-SA-C5 *de novo* assembly against it. In Geneious R11 (v11.1.5), a *de novo* assembly was run using the contigs and the *de novo* assembly function, with the assembler set to Geneious and the sensitivity set to medium sensitivity/fast and a single consensus sequence was generated. A pairwise alignment was performed on the consensus sequence and the reference CrleGV-SA sequence using the ClustalW method. The find SNPs/Variants tool in Geneious R11 was used to search for SNPs between the CrleGV-SA and the CrleGV-SA-C5.

2.2.2 Oligonucleotide design targeting variable regions

After a pairwise alignment between the CrleGV-SA reference sequence (van der Merwe et al., 2017) and the CrleGV-SA-C5 was performed, three sets of oligonucleotides were designed to bind to target regions of the genome where SNPs were identified. Primer3 v0.4.0 (Untergasser et al., 2012) was used to design the oligonucleotide sets. An *in silico* test was conducted in Geneious R11 to determine if the sets of oligonucleotides bind to the target regions correctly. The sets of oligonucleotides were synthesized by Inqaba Biotechnical Industries (Pty) Ltd (South Africa) (Table 2.1).

Table 2.1: Oligonucleotides targeting variable regions identified in CrleGV-SA-C5

Gene	Oligonucleotide Name	Sequence 5'-3'	Position	Tm (°C)	% GC	Product size (bp)
<i>pif-2</i>	Pif-2 F	GACGATACGCTCCATTGCAT	38101→38120	58.5	50.0	348
	Pif-2 R	TCAAGTTACCTTCTCCCGCA	38448→38429	58.7	50.0	
HP	HypoP F	CATATGTAGGGTTCGCGTCAG	79632→79652	58.6	52.4	302
	HypoP R	AAACGACACCTATTACACTTTGC	79933→79911	57.6	39.1	
<i>lef-8</i>	Lef-8/HP F	CCAACCAAGTACCAATAACGAC	104295→104316	57.3	45.5	311
HP	Lef-8/HP R	TTCGACGGATAGCATGTTTCG	104605→104586	58.2	50.0	

Pif-2: Per os infectivity factor-2, HP: Hypothetical Protein CDS, lef-8: Late expression factor-8

2.2.3 Virus samples, occlusion body purification and TEM

Purified CrleGV-SA-C5 OBs were provided by Nelson Mandela University, South Africa. CrleGV-SA OBs were purified from infected larval cadavers following the protocol described in Jukes (2015), originally adapted from Hunter-Fujita et al. (1998) and Moore (2002). Briefly, 6 ml of 0.1 % SDS (sodium dodecyl sulphate) was used to homogenise 0.75 g of the cadavers using a mortar and pestle. The homogenate was filtered into a beaker using cheese cloth and then equally divided into two JA-20 centrifuge tubes. The tubes were filled with ddH₂O and centrifuged at 7840 ×g for 30 min at 4 °C in a Beckman Coulter Avanti® J-E centrifuge. The supernatant was discarded with the pellet resuspended using ddH₂O and centrifuged again at 7840 ×g for 30 min at 4 °C. The supernatant was again discarded, and the pellet was resuspended with 1.5 ml ddH₂O. Continuous 30-80 % (v/v) glycerol gradients were prepared in two ultracentrifuge tubes using 0.1 % SDS. 1.5 ml of the substrate was pipetted on top of the glycerol gradient, and this was centrifuged at 27783 ×g (15000 rpm) for 15 min in a Beckman Coulter Optima™ L-90K Ultracentrifuge. The whitish brown OB forming bands were collected and pipetted into two new clean JA-20 tubes, ddH₂O was used to fill each tube to the top and this was centrifuged at 7840 ×g for 30 min at 4 °C. The supernatant was discarded and ddH₂O was used to resuspend the pellets. The centrifugation step at 7840 ×g for 30 min at 4 °C was repeated. Thereafter, the supernatant was discarded, the pellets were combined into one JA-20 tube, resuspended with ddH₂O, and centrifuged for a final time at 7840 ×g for 30 min at 4 °C. The pellet was resuspended in 750 µl ddH₂O and transferred into a 1.5 ml microcentrifuge tube. The purified OBs were used for subsequent experiments.

Purified CrleGV-SA and CrleGV-SA-C5 OBs were used for TEM. The preparation of transmission electron microscope grids was done following the method described by Opoku-Debrah et al. (2013). 5 µl of the purified OBs was pipetted onto a carbon formvar grid and left for 60 s. The excess liquid was removed using filter paper, followed by 5 µl 1 % uranyl acetate (w/v) pipetted onto the grid for 60 s to stain the grid. Filter paper was used to remove the excess uranyl acetate and the grid was left at room temperature to dry overnight. A Libra 120 (Zeiss, Germany) TEM was used to view the grid and OB images were captured. The size of 30 OBs was measured and the average OB size was calculated in Microsoft Excel® 2016.

2.2.4 Genomic DNA extraction

Genomic DNA was extracted from both purified CrleGV-SA OBs and purified CrleGV-SA-C5 OBs following the cetyltrimethylammonium bromide (CTAB) method described by

Opoku-Debrah et al. (2013). 200 μ l of purified OB sample was added to 90 μ l Na_2CO_3 (1M) in a 1.5 ml Eppendorf tube and incubated for 30 min at 37 $^\circ\text{C}$. After incubation, 120 μ l Tris-HCl (1M, pH 6.8) was added to neutralise the suspension, followed by the addition of 20 μ l Proteinase K (25 mg/ml), and 90 μ l SDS (10 % w/v) to the tube and incubation at 37 $^\circ\text{C}$ for an additional 30 min. A further 10 μ l RNase A (10 mg/ml) was added to the sample and then incubated at 37 $^\circ\text{C}$ for 30 min. Using a MiniSpin table top centrifuge (Eppendorf, Germany), the sample was centrifuged for 3 min at 12,100 $\times g$. The supernatant was placed in a new tube followed by the addition of 400 μ l of pre-warmed (70 $^\circ\text{C}$) CTAB buffer (54 mM CTAB, 20 mM Na_2EDTA , 0.1 M Tris-HCl, 1.4 M NaCl). The sample was then incubated for 45 min at a temperature of 70 $^\circ\text{C}$. Into the CTAB mixture, 400 μ l of pre-cooled (to 4 $^\circ\text{C}$) chloroform was added. The tube containing the sample was inverted a few times before centrifugation for 10 min at 6700 $\times g$. Into a new 2 ml tube, the upper aqueous phase of the sample was collected, and to this 400 μ l isopropanol (ice-cold, -20 $^\circ\text{C}$) was added. The sample was incubated overnight in a -20 $^\circ\text{C}$ freezer for the DNA to precipitate.

The sample was then centrifuged for 20 min at 12100 $\times g$, followed by discarding the supernatant. To the pellet, 1 ml of ice-cold (-20 $^\circ\text{C}$) 70 % ethanol (v/v) was added. The sample was centrifuged for the last time for 5 min at 12100 $\times g$. The pellet was left to air dry after discarding the supernatant; this is in order for the ethanol to be completely evaporated. 20 μ l ddH₂O was added to resuspend the pellet and stored at -20 $^\circ\text{C}$ until needed.

2.2.5 PCR amplification of targeted genome regions

Each 25 μ l PCR reaction was set up according to Table 2.2. No template controls (NTC) were used for each PCR, replacing the template gDNA with ddH₂O. The oligonucleotide sets were first optimised by PCR amplification at three different annealing temperatures, 50 $^\circ\text{C}$, 53 $^\circ\text{C}$ and 55 $^\circ\text{C}$, thereafter the annealing temperature of 55 $^\circ\text{C}$ was used. The PCR cycling parameters consist of an initial denaturation period of 1 min at 95 $^\circ\text{C}$, followed by 30 cycles at 95 $^\circ\text{C}$ for 30 s, 55 $^\circ\text{C}$ for 30 s, 72 $^\circ\text{C}$ for 30 s and final elongation at 72 $^\circ\text{C}$ for 3 min.

Table 2.2: PCR reaction set-up for each PCR run

Reagents	Sample	No Template Control
2× Amplicon Taq	12.5 µl	12.5 µl
Forward primer (10 µM)	2 µl	2 µl
Reverse primer (10 µM)	2 µl	2 µl
Template	4 µl	—
ddH₂O	4.5 µl	8.5 µl
Total	25 µl	25 µl

The PCR products were analysed by 1% agarose gel electrophoresis (AGE) with ethidium bromide staining in 1 × TAE buffer (1 mM EDTA, 20 mM acetic acid, 40 mM Tris-acetate) for 30 min at 80 V. The GeneRuler™ 1 kb DNA ladder (Thermo Fisher, USA) was used to estimate amplicon size. A ChemiDoc™ XRS+ System with Image Lab™ Software (Bio-Rad Laboratories, USA) was used to visualise the agarose gel.

2.3 RESULTS

2.3.1 *De novo* assembly and genome alignment

The genome sequence of the CrleGV-SA-C5 was assembled *de novo* from previously generated NGS data and aligned against the full-length genome of CrleGV-SA. The length of the generated CrleGV-SA-C5 sequence was determined to be 111334 bp. A percentage identity of 99.99 was shown after a pairwise alignment between the CrleGV-SA-C5 with the reference genome for CrleGV-SA. Following alignment, seven SNPs were identified between the CrleGV-SA and the CrleGV-SA-C5 (Table 2.3).

Table 2.3: Single polymorphisms identified in the genome sequence of CrleGV-SA-C5

Name	Nucleotide Position	Change	Codon Change	Amino Acid Change	Protein	Protein Effect	Polymorphism Type	ORF numbers
UV_1	21222	G → C					SNP (Transversion)	
*UV_2	38194	T → C	ATT→ACT	I → T	Pif-2	Substitution	SNP (Transition)	ORF 45
UV_3	38366	G → A	GAG→GAA		Pif-2		SNP (Transition)	ORF 45
*UV_4	45853	G → A	GTG→ATG	V → M	39K	Substitution	SNP (Transition)	ORF 57
*UV_5	79840	T → G	TTG→GTG	L → V	HP	Substitution	SNP (Transversion)	ORF 94
UV_6	104395	G → A	AAG→AAA		Lef-8		SNP (Transition)	ORF 119
*UV_7	104574	T → C	ATG→ACG	M → T	HP	Start Codon Loss	SNP (Transition)	ORF 120

*SNPs identified are the same as those identified from Mwanza (2019)

Pif-2: Per os infectivity factor-2, 39K: 39K protein, HP: Hypothetical protein, lef-8: Late expression factor-8

Amino Acid Change: I = Isoleucine, T= Threonine, V = Valine, M = Methionine, L= Leucine

Nucleotide: T = Thymine, C = Cytosine, G = Guanine, A = Adenine

ORF = Open reading frame

Three of the SNPs identified did not result in amino acid changes and these were at position 21222, 38366 and 104395. The four SNPs that resulted in amino acid changes were at position 38194, 45853, 79840 and 104574. Additionally, four out of the seven identified SNPs were identical to those identified by Mwanza (2019), as indicated in Table 2.3; these were at position 38194, 45853, 79840 and 104574.

2.3.2 Transmission electron microscopy

Transmission Electron Microscopy was used to examine the OBs of the CrleGV-SA-C5 virus sample and the CrleGV-SA virus sample to determine the purity of each. Image results are shown in Figure 2.1 for both the CrleGV-SA-C5 and the CrleGV-SA sample. Little debris was observed for both virus samples and the OBs were roughly oval shaped. For the CrleGV-SA-C5 sample the average length of the OB was 344.7 ± 49.4 nm and average width 205.7 ± 32.3 nm (n=30). For the CrleGV-SA sample, the average OB length was 364.9 ± 30.1 nm and average width 215 ± 26.5 nm (n=30).

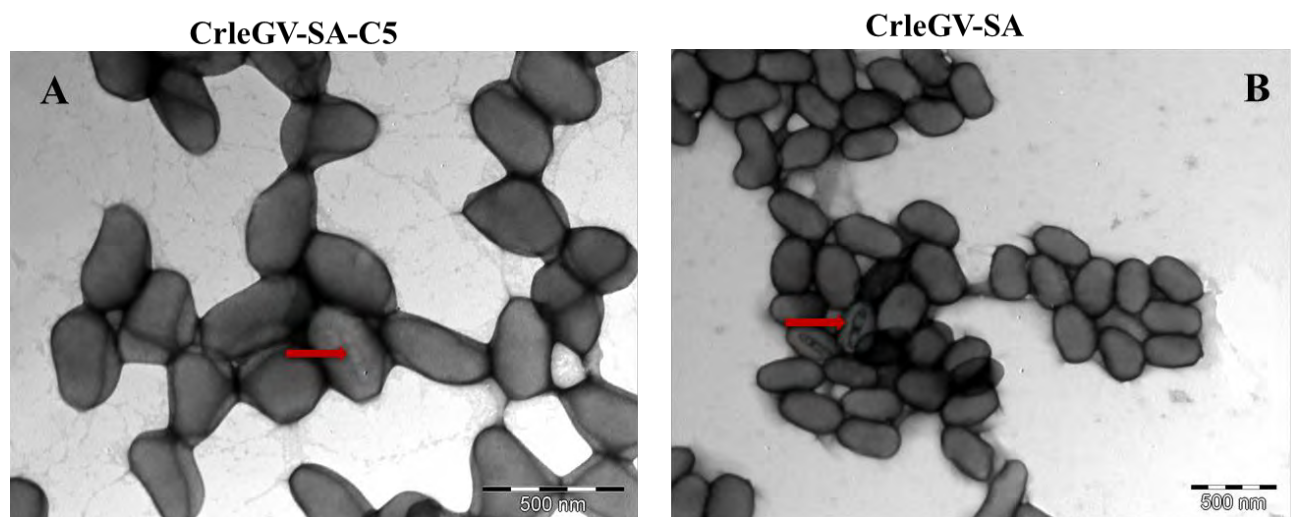


Figure 2.1: Transmission Electron Micrograph of A: CrleGV-SA-C5 and B: CrleGV-SA. The red arrow is indicating the nucleocapsid within the OB (CrleGV-SA TEM images courtesy of Thuthula Mela).

2.3.3 Genomic DNA extraction

Genomic DNA was extracted from CrleGV-SA OBs and CrleGV-SA-C5 OBs. Genomic DNA was analysed by 1 % AGE (Figure 2.2) and used as template DNA for the PCR reactions. Both the CrleGV-SA and CrleGV-SA-C5 samples produced bands greater than 10000 bp (Figure 2.2).

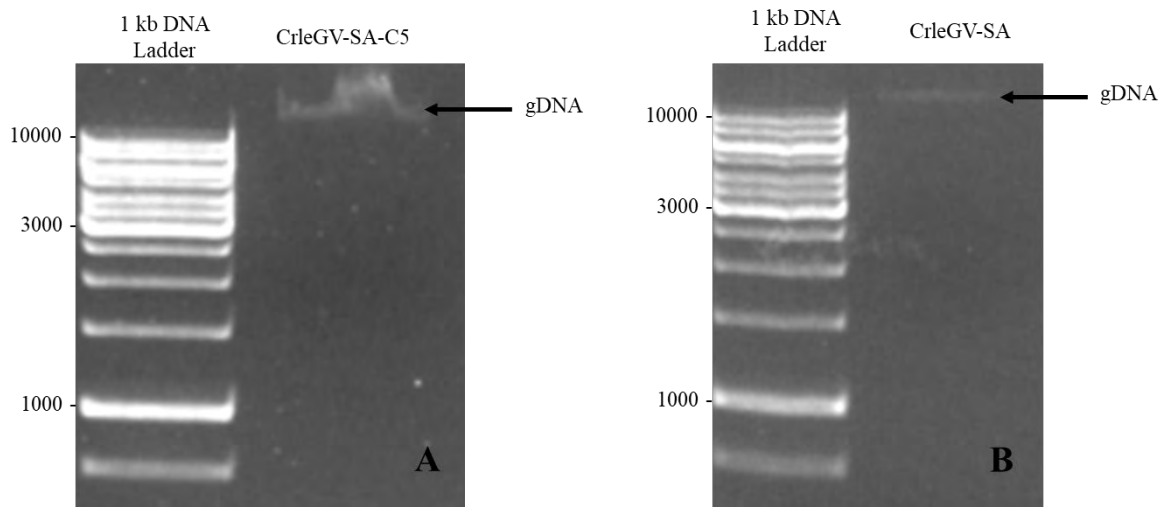


Figure 2.2: Agarose gel electrophoresis of extracted genomic DNA. A: CrleGV-SA-C5. B: CrleGV-SA.

2.3.4 Oligonucleotide design and PCR amplification of genomic regions

2.3.4.1 Oligonucleotide design and *in silico* testing

Three sets of oligonucleotides were designed targeting the regions where the SNPs have been identified between the CrleGV-SA-C5 and CrleGV-SA isolates (Table 2.1). The three sets of oligonucleotides were tested *in silico* (Figure 2.3). The first oligonucleotide set, Pif-2, incorporated two SNPs (UV_2 and UV_3) at position 38194 and 38366. The HypoP oligonucleotide set encompassed one SNP (UV_5) at position 79840 and the Lef-8/HP oligonucleotide set encompassed two SNPs (UV_6 and UV_7) at positions 104395 and 104574. A schematic diagram showing the binding positions of each oligonucleotide set on the CrleGV-SA genome is shown below in Figure 2.3.

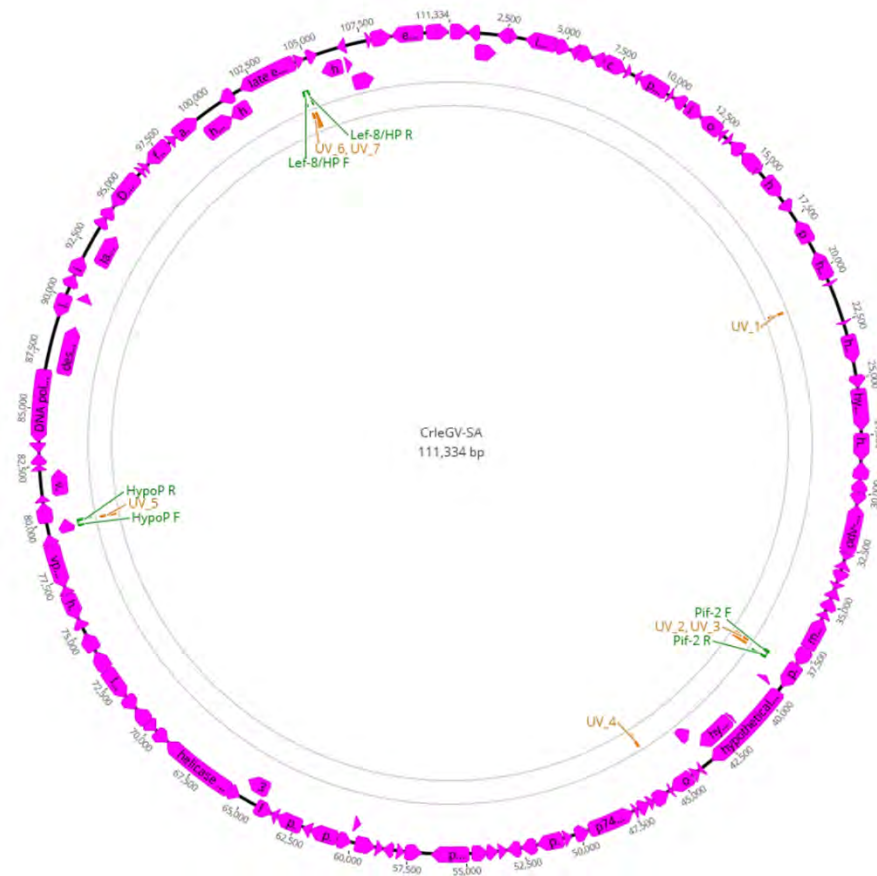


Figure 2.3: *In silico* test conducted on the CrleGV-SA using the three sets of oligonucleotides designed targeting five different SNPs identified. The binding sites are shown in green, with the various SNPs indicated in yellow. The CrleGV-SA genes are shown in purple.

2.3.4.2 PCR amplification of regions containing SNPs

Following the *in silico* test, the designed oligonucleotides were tested by PCR amplification using CrleGV-SA gDNA as the template, to amplify the identified regions where the SNPs have been detected. A schematic diagram illustrating where the oligonucleotide sets bind to the target regions relative to the identified SNPs is shown in Figure 2.4. The oligonucleotide sets were optimised by PCR amplification at three different annealing temperatures, 50 °C, 53 °C and 55 °C (Figure 2.5). All three oligonucleotide sets annealed correctly at the different temperatures. The annealing temperature chosen for downstream experiments was at 55 °C.

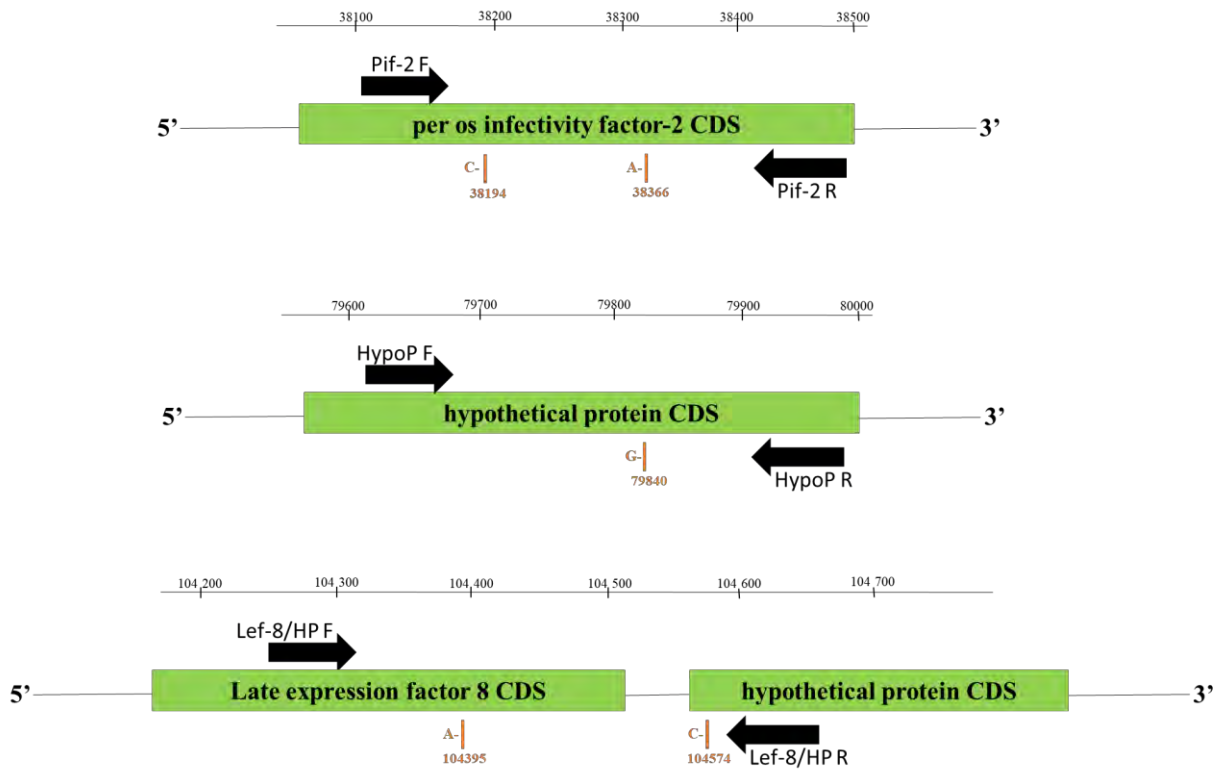


Figure 2.4: Schematic diagram indicating where the oligonucleotides bind to the target regions relative to the identified SNPs

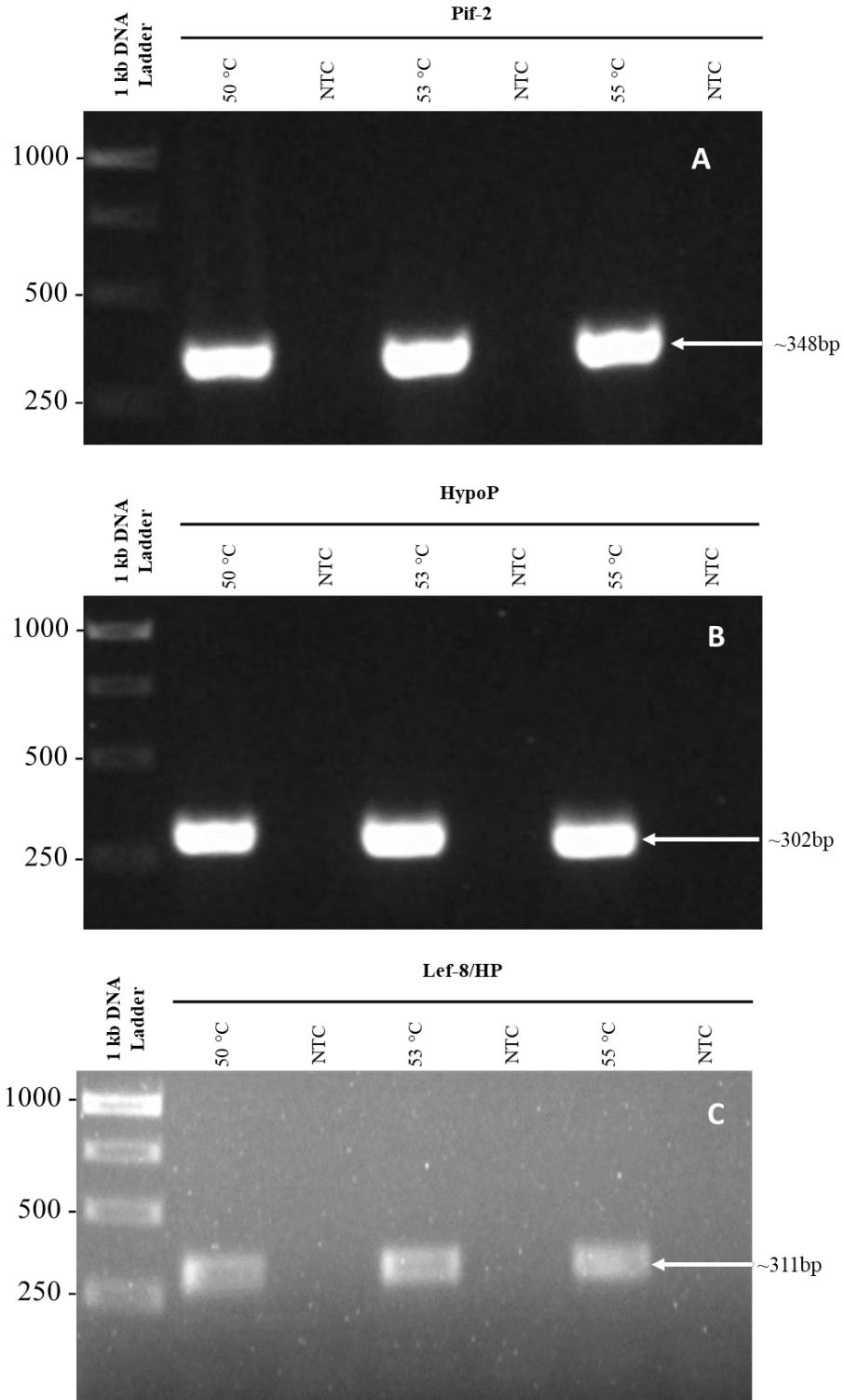


Figure 2.5: AGE with ethidium bromide staining of PCR amplicons, using three different oligonucleotide sets at three different annealing temperatures. A) Pif-2 PCR amplicons of 348 bp in size. B) HypoP PCR amplicons of 302 bp in size. C) Lef-8/HP PCR amplicons of 311 bp in size.

After optimisation, the amplicons of the approximate expected sizes for all three oligonucleotide sets were obtained. The oligonucleotide sets were then applied to the CrleGV-SA-C5 gDNA and CrleGV-SA gDNA. Figure 2.6 shows PCR amplification using the oligonucleotide sets on CrleGV-SA-C5 gDNA and CrleGV-SA gDNA with an annealing temperature at 55 °C. Amplification of the target regions was successfully achieved for all samples, and the sizes of the amplicons amplified were at the expected band sizes.

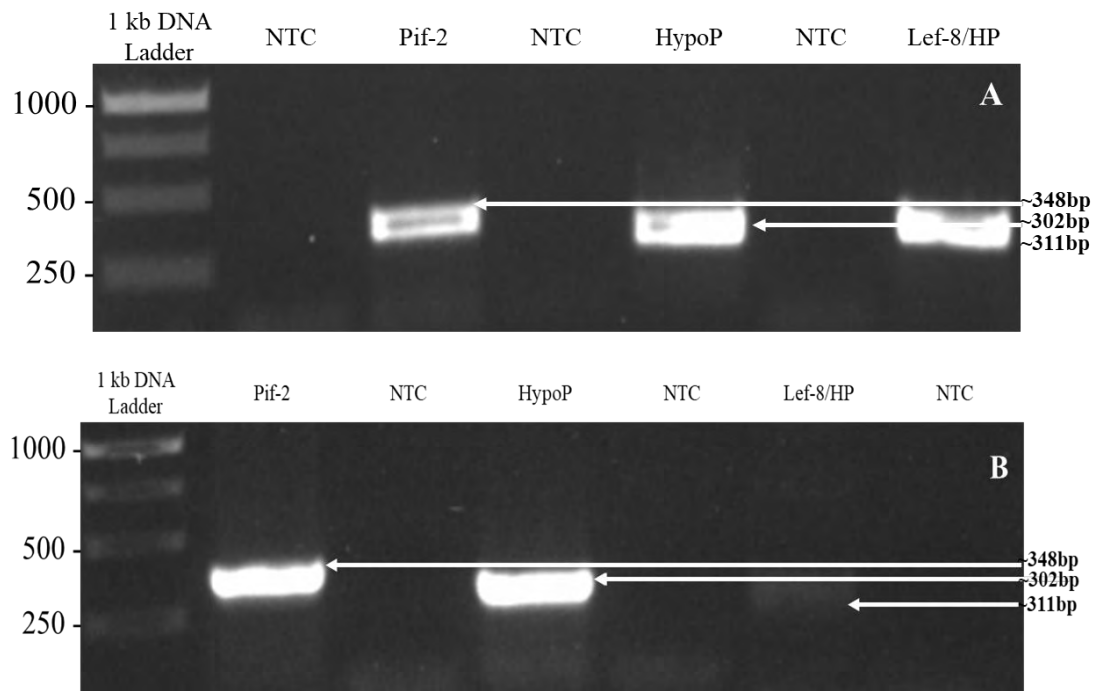


Figure 2.6: AGE with ethidium bromide staining of PCR amplicons resulting from gDNA extracted from A: CrleGV-SA and B: CrleGV-SA-C5. The Pif-2 amplicon size is 348bp, the HypoP amplicon size is 302bp and the Lef-8/HP amplicon size is 311bp.

2.4 DISCUSSION

Next generation sequence data of a UV-tolerant CrleGV-SA-C5 isolate was provided by Mwanza (2019). The genome of the CrleGV-SA-C5 was reassembled by *de novo* assembly followed by a sequence comparison with the CrleGV-SA genome. The length of the assembled consensus CrleGV-SA-C5 sequence is consistent with the length of the genome sequence assembled by van der Merwe et al. (2017), both being 111334 bp in length. Both the current study and the study by Mwanza (2019) obtained the same pairwise identity after sequence comparison with the published CrleGV-SA. Several SNPs were detected after sequence comparison. Four of the SNPs detected were the same as those reported by Mwanza (2019) and Mwanza et al. (2022). Two out of the seven SNPs detected were unique to the current study

and the seventh SNP detected was previously reported by van der Merwe et al. (2017). During the NGS process, millions of small DNA fragments are sequenced in parallel (Behjati & Tarpey, 2013). The most vital application of NGS according to Wadapurkar & Vyas (2018), is mutation identification. the most important NGS application. Firstly, the NGS reads are mapped to a reference genome, thereafter variations are identified from the mapped data (Wadapurkar & Vyas, 2018). The NGS data set from the current study had just over a million reads, with the analysis conducted on the NGS data involving a sequence alignment and identification of SNPs. The SNPs detected that are unique to the current study are possibly due to a different portion of the data being analysed in comparison to the portion of data analysed by Mwanza (2019).

The remove duplicate, error correcting and *de novo* assembly step of the data analysis may have resulted in a slightly different portion of the NGS data set being selected, compared to Mwanza (2019). Therefore, the consensus sequence generated after *de novo* assembly may have been slightly different to the consensus sequence generated by Mwanza (2019), as demonstrated by the unique SNPs detected.

The identified SNPs in the previous and current studies are possibly introduced due to the UV radiation. It is known that UV radiation induces mutations (Shibai et al., 2017). UV radiation also results in the inactivation of OBs (Beas-Catena et al., 2014). DNA molecules absorb UV light, which as a result, causes pyrimidine dimers in the DNA chain (Yoon et al., 2000). Additionally, the viability of baculoviruses is reduced significantly by direct UV irradiation (Jones et al., 1993). The effect of UV irradiation was tested on *Galleria mellonella* nucleopolyhedrovirus (GmNPV) (Witt & Stairs, 1975). The study found that part of the virus population was susceptible to high dosages of UV, while the other part of the population was only susceptible to low doses. As a result, Witt & Stairs (1975) predicted that genetic variability of the virus populations could be the cause of the heterogeneity in the UV-response, and therefore a UV-tolerant strain of the virus could be selected for. As a result of what was observed by Witt & Stairs (1975), a near UV-tolerant strain of *Autographa californica* MNPV (AcMNPV) was successfully isolated by Witt & Hink (1979) after five selection cycles.

Additionally, the SNPs detected could have been introduced due to the UV radiation selecting for a different genotype of the same virus. Baculoviruses exist as mixtures of different genotypes (Herniou & Jehle, 2007; Opoku-Debrah et al., 2013). It was indicated by Clavijo et al. (2010) that in numerous MNPV, like AcMNPV, that a single OB can have several genotypes

occluded within it. The genetic diversity of baculoviruses is very high. Diverse genotypes are present in a given virus population and these genotypes have different biological characteristics (Escribano et al., 1999). Baculovirus isolates consist of variation in the genetic variants which are caused by multiple mechanisms such as horizontal gene transfer, point mutations, deletion, and insertions. The variation enables the variants to compete and cooperate in environmental conditions that modulate their survival (Aguirre et al., 2019). Virulence may additionally be affected by the genetic variation of baculovirus populations found in the field. The variation includes recombination events or mutations within the genes (Erlandson, 2009; Pijlman et al., 2003; Serrano et al., 2015). Opoku-Debrah et al. (2013) bioprospected for new CrleGV isolates, with the use of overcrowding of host populations as an induction method for latent infections. The host populations of *T. leucotreta* were geographically distinct and five new isolates of CrleGV were recovered from these populations. Each isolate comprised of a mixture of greater than one CrleGV-SA genotype, which was evidence of genotypic variation between samples. The DNA profiles of the different isolates were shown to be different after single restriction endonuclease (REN) analysis was conducted. The *egt* and *granulin* genes were PCR amplified and sequenced from the various isolates and SNPs were identified after multiple nucleotide sequence alignments were conducted (Opoku-Debrah et al., 2013). The phylogenetic analysis of the sequence data revealed that two separate groups were present, based on the evolutionary relationship of the seven SA isolates reported in the study. The Cape Verde isolate (CrleGV-CV3) appeared to be phylogenetically distinct, whereas the CrleGV-SA isolates from both groups appeared to have emerged from a common ancestor. The existence of two distinct CrleGV-SA groups was supported by the results, based on the *granulin* and *egt* gene sequences and the REN profiles (Opoku-Debrah et al., 2013).

A study by van der Merwe et al. (2017) generated seven full genome sequences of the isolate CrleGV-SA selected over 15 years. These isolates were compared with one another to investigate the genetic stability of CrleGV-SA since 2000 when it was first produced and applied in the field. The SNP detected at position 21222 in the current study is the same nucleotide observed in the 2000, 2003, 2005, 2007, 2009, and 2012 sequences by van der Merwe et al. (2017). The SNP at position 38194 in the current study, is the same as the nucleotide observed by van der Merwe et al. (2017) in the 2012 sequence reported. The SNPs detected at these positions in the CrleGV-SA-C5 isolate sequence, therefore, may not be mutations introduced due to exposure to UV radiation, but rather a selection of a different pre-existing genotype of the virus, which exhibits improved tolerance to UV stress. Such genetic

variation may naturally exist within baculovirus populations, offering improved fitness to changing environmental conditions. After a baculovirus infection cycle, millions of genomes are produced, and several of these genomes may harbour mutations. The genetic variability allows for the response of these viruses to natural selection and therefore are able to adjust to varying environmental conditions (Herniou & Jehle, 2007).

Transmission electron microscopy results showed CrleGV OBs that were consistent with the size and morphology of GV OBs as described in Herniou et al. (2011), who state that the diameter of GV OBs range from 120-300 nm and the length of GV OBs range from 300-400 nm. Therefore, the measured CrleGV-SA-C5 and CrleGV-SA OBs fall within the size range of GV OBs. The shape of GVs is ovoid (Ackermann & Smirnoff, 1983), which is consistent with the results observed in the current study. A study by Nakai et al. (2015) aimed to identify and characterize the OB morphology of a new variant of AdorGV isolated from Japan (AdorGV-M). The study found that the morphology of the OBs were cuboidal in shape and significantly larger, which is in contrast to the morphology of GVs which are ovo-cylindrical in shape. The unusual OB morphology of AdorGV-M was suggested to be linked to UV resistance (Nakai et al., 2015). Additionally, Mwanza (2019) aimed to determine whether UV irradiation had an effect on the morphology of CrleGV-SA OBs. Transmission electron microscopy was conducted on an unexposed CrleGV-SA virus sample, on a 72 h UV-exposed CrleGV-SA cycle 5 virus sample and a 72 h UV-exposed CrleGV-SA at cycle 1 virus sample. The TEM results for the unexposed CrleGV-SA sample revealed that the dimensions of the OBs were consistent with those of other granuloviruses. In comparison to the unexposed control OBs, the nucleocapsid cavities and mean length of the OBs of the 72 h UV-exposed CrleGV-SA cycle 1 virus sample were notably smaller and the mean nucleocapsid cavity width was notably larger. The mean OB length was notably smaller for the 72 h UV-exposed CrleGV-SA cycle 5 virus OBs and the mean OB width of the Cycle 5 OBs showed no significant difference in comparison with the unexposed control OBs (Mwanza 2019). The AGE results for the DNA extraction showed that the extracted DNA for both CrleGV-SA and CrleGV-SA-C5 gDNA had a high molecular weight, greater than 10000 bp in size. Genomic DNA was therefore successfully extracted, as baculovirus genomes range between 80 to 180 kbp.

Oligonucleotides were designed flanking SNPs that were in close proximity to each other, instead of flanking the SNPs individually. The *Pif-2* set flanked two SNPs that were 172 bp apart and the *Lef-8/HP* set flanked two SNPs that were 179 bp apart. The oligonucleotide sets were successfully tested *in silico*, encompassing the correct SNPs.

The three sets of oligonucleotides targeting the regions where the SNPs occur were tested against CrleGV-SA gDNA by PCR amplification with an annealing temperature ~5 °C lower than the melting temperature for each oligonucleotide set. The amplicons with the expected sizes were generated for the *Pif-2* and *HypoP* oligonucleotide sets. Non-specific PCR bands were observed after amplification using the *Lef8/HP* oligonucleotide set (data not shown). Non-specific PCR bands consisting of different lengths are a result of PCR stringency being extremely low. To mitigate this, PCR conditions that increase stringency should be chosen (Lorenz, 2012). PCR reactions can be enhanced by optimizing the annealing temperature and in combination with either adjusting the cycle parameters or with additional additives (Lorenz, 2012). Optimisation at three different annealing temperatures was then performed using all three oligonucleotide sets for consistency. AGE results after PCR optimisation were successful, as amplicons of the expected size for each oligonucleotide set were generated at all three temperatures. The higher annealing temperature was therefore chosen for downstream experiments after PCR optimisation. The temperature chosen was influenced by the desired specificity as well as the strand-melting temperature of the oligonucleotides. Higher temperatures are however suggested for greater stringency (Erjavec, 2020). The next objective was to apply the oligonucleotide sets by PCR amplification on the CrleGV-SA-C5 and CrleGV-SA gDNA. The amplification was successful as the amplicons were of the expected sizes.

In conclusion, the objectives of the study reported in this chapter were achieved. Variations between the CrleGV-SA-C5 and CrleGV-SA were identified and oligonucleotide sets were successfully designed and tested. Target regions where the SNPs were identified were amplified by PCR. In the next chapter, ligation of the PCR amplicons into the pJET1.2/blunt cloning vector for sequencing, to determine if the SNPs remain detectable in the genome is reported.

Chapter 3

Screening for the presence of SNPs using plasmid cloning and qPCR melt curve

3.1 INTRODUCTION

In the previous chapter, three sets of oligonucleotides (Pif-2, HypoP and Lef-8/HP) were designed to target three regions of the CrleGV-SA-C5 genome. The PCR amplification was conducted separately on CrleGV-SA-C5 and CrleGV-SA gDNA generating six amplicons. The next step was to develop a method for screening to differentiate between CrleGV-SA-C5 and CrleGV-SA isolates and confirming/verifying that the identified single nucleotide polymorphisms (SNPs) were detectable. The two screening methods of choice were, construction of six plasmids and sequencing and the second was quantitative polymerase chain reaction (qPCR) melt curve analysis.

The pJET1.2/blunt cloning vector, supplied by Thermo Fisher Scientific, USA, was chosen for cloning of the six amplicons. It consists of a T7 promoter, an ampicillin resistant gene, a multiple cloning site (MCS), and a lethal gene among other features (Thermo Fisher Scientific, 2015). The lethal gene is located between nucleotides 753 and 16 and the MCS is located between nucleotides 422-328. When a DNA insert is ligated into the pJET1.2/blunt vector MCS, the lethal gene is disrupted and as a result, cells have the ability to propagate (Daryaei et al., 2017). Where no DNA insertion occurs, the lethal gene remains intact leading to cell death and consequently enabling positive selection of recombinant plasmids. Deoxyribonucleic acid fragments that can be cloned into pJET1.2/blunt vector are those with either sticky-ends or blunt ends. Additionally, inserts ranging between 6 bp to 10 kb may be cloned into this cloning vector (Thermo Fisher Scientific, 2015). The pJET1.2/blunt cloning vector is a positive blunt-end cloning vector and is 2974 bp in length. Prior to ligation a DNA blunting enzyme must be used to blunt PCR products which contain nucleotide overhangs that are being cloned (Lloyd, 2017).

To select colonies containing the recombinant plasmid it is vital to always conduct screening (Casali & Preston, 2003). Transformant colonies can be rapidly screened by several methods; these include colony PCR and rapid screening by direct electrophoresis. Restriction enzyme

digestion and sequence analysis are desirable methods to use for screening transformants for possible candidate recombinant plasmids and for confirming the identification of purified plasmid DNA (Casali & Preston, 2003). An essential part of DNA cloning is the ability of transformed cells being selected by means with an antibiotic because of the antibiotic resistant gene of the plasmid (Lodish et al., 2000). The drug resistant gene of a plasmid enables transformed cells to be selected for from those without the presence of a plasmid, when grown in a medium containing a specific antibiotic such as ampicillin (Lodish et al., 2000). Colonies of bacteria grown on selective media, after a transformation step, can be screened rapidly by the colony PCR method (Bergkessel & Guthrie, 2013). Studies such as Daryaei et al. (2017) and Bozorgkhoo et al. (2014) both conducted molecular cloning and sequencing of different genes into the pJET1.2/blunt vector. Both studies conducted colony PCR using the universal pJET1.2/blunt primers for confirming the presence of the insert. Colony PCR was one of the methods selected in the current study to confirm the presence of the insert due to the primer binding sites that flank the insert region.

Double-enzyme digest may be used to excise cloned inserts by using restriction enzymes with sites located in the MCS (Lloyd, 2017). The MCS allows for screening, mapping and excision of the insert being cloned (Thermo Fisher Scientific, 2015). The restriction enzymes *XhoI* and *XbaI* were chosen for the current study, as these restriction sites flank the insert region in the vector and can therefore be used to confirm the presence of the cloned PCR products.

A method that has been demonstrated to be highly sensitive for SNP genotyping and mutation discovery is the melt curve analysis using fluorescent dyes (Cho et al., 2008; G. D. Smith et al., 2008). These fluorescent dyes, such as SYBR Green I, preferentially bind to double stranded DNA (dsDNA) enabling accurate detection and quantification (Zipper et al., 2004). During the melt analysis, changes in fluorescence are monitored, with an increase in temperature leading to denaturation of dsDNA and consequently a decrease in fluorescence levels. Differences in nucleotide composition affect the rate at which dsDNA molecules denature, resulting in unique melting temperatures and rates of fluorescence drop-off. This enables the differentiation of these dsDNA molecules by their resulting characteristic melt curves (Zhou et al., 2004).

The study by Krejmer-Rabalska et al. (2019) reported a reliable and fast method based on a real-time polymerase chain reaction technique with melting point curve analysis in order to detect new GV species and for previously analysed GV species to be differentiated. The results

showed that there were different melting temperatures in a single run for each single pair of primers, indicating that the nucleotide sequences for the real-time PCR products were different and therefore the method may be used for GV differentiation. The study by Krejmer-Rabalska et al. (2019) demonstrated that small variations between baculovirus isolates can be differentiated by melt curve analysis. Therefore, for the current study melt curve analysis was selected to differentiate between CrleGV-SA-C5 and CrleGV-SA.

The aim of the chapter was to develop screening methods to distinguish between CrleGV-SA-C5 and CrleGV-SA isolate regions. The specific objectives were to (i) ligate the amplicons into the pJET1.2/blunt vector and transform the ligations into competent *E. coli* cells, (ii) perform colony PCR to screen transformants for presence of the insert, (iii) to extract the plasmids and perform restriction enzyme digestion, (iv) to sequence the plasmid DNA and analyse the sequence data for the presence of the SNPs, and (v) qPCR melt curve analysis using PCR amplicons to differentiate between CrleGV-SA-C5 and CrleGV-SA isolates.

3.2 METHODS

3.2.1 Recombinant plasmids

Six recombinant plasmids containing amplicons generated using Pif-2, HypoP and Lef-8/HP oligonucleotides were constructed, as seen in Table 3.1.

Table 3.1: Details of the recombinant pJET1.2/blunt plasmids following ligation of the Pif-2, HypoP and Lef-8/HP inserts, indicating the insert size, SNPs encompassed and the resulting size of each recombinant plasmid.

Plasmid name	PCR amplicon cloned in pJET1.2/blunt vector	Insert size	Plasmid backbone	SNPs encompassed	Size of recombinant plasmid
pC5_Pif-2	CrleGV-SA-C5 Pif-2	348	pJET1.2/blunt vector	UV_2 & UV_3	3322
pSA_Pif-2	CrleGV-SA Pif-2	348			3322
pC5_HypoP	CrleGV-SA-C5 HypoP	302		UV_5	3276
pSA_HypoP	CrleGV-SA HypoP	302			3276
pC5_Lef-8/HP	CrleGV-SA-C5 Lef-8/HP	311		UV_6 & UV_7	3285
pSA_Lef-8/HP	CrleGV-SA Lef-8/HP	311			3285

3.2.2 Ligation of amplicons into pJET1.2/blunt and transformation into *E. coli*

Ligations were performed following the manufacturer's protocol for the CloneJET PCR Cloning Kit (Thermo Fisher Scientific, USA). The blunting enzyme mixture was set-up on ice in a total volume of 18 μl . In a 1.5 ml microcentrifuge tube, 10 μl of 2 \times reaction buffer, 6 μl ddH₂O, 1 μl PCR product (20 ng. μl) and 1 μl DNA blunting enzyme was added. The tube was gently mixed and incubated for 5 min at 70 °C. Thereafter the tube was placed back on ice and 1 μl pJET1.2/blunt cloning vector and 1 μl T4 Ligase was added to the blunting enzyme mixture, having a new total volume of 20 μl . The microcentrifuge tube was gently mixed and briefly centrifuged for 5 s, followed by incubation for 5 min at room temperature. This process was repeated for each of the six PCR amplicons (Table 3.1). The ligation mixtures were then used directly to perform transformation.

For each ligation reaction, competent TOP10 *E. coli* cells were thawed on ice and all the ligation mixture was added to 100 μl of the competent cells in a 1.5 ml microcentrifuge tube. A control was used for the reaction setup by adding 100 μl ddH₂O to 100 μl of the competent cells. The tube was then gently mixed and then incubated on ice for 15 min. The mixture was then subjected to heat shock for 45 s at 42 °C and incubated on ice for 2 min. 900 μl Luria Broth (LB) (1.25 g NaCl, 1.25 g Yeast Extract, 2.5 g Tryptone and 250 ml ddH₂O, autoclaved) was added, and the mixture was then incubated for 30 min at 37 °C. An initial 100 μl of the sample was spread-plated on Luria agar (LA) (1.25 g NaCl, 1.25 g Yeast Extract, 2.5 g Tryptone, 5 g Agar and 250 ml ddH₂O, autoclaved) (with 100 $\mu\text{g}\cdot\text{ml}^{-1}$ Ampicillin) plate, and the tube was then centrifuged for 3 min at 1000 $\times g$. The supernatant was gently poured out, leaving \sim 100 μl sample in the tube. The pellet was gently re-suspended and the remaining cells were spread-plated on an LA (with 100 $\mu\text{g}\cdot\text{ml}^{-1}$ Ampicillin) plate, followed by incubation overnight at 37 °C. The transformation process was repeated for each of the six ligation mixtures.

3.2.3 Colony PCR

Following the manufacturer's protocol of the CloneJET PCR Cloning kit (Thermo Fisher Scientific, USA), colony PCR reactions were set-up in PCR tubes as described in Table 3.2. A distinct colony was selected for each transformation and transferred into separate PCR mixtures using a toothpick. A SimpliAmp™ Thermal Cycler (Thermo Fisher Scientific, USA) was used to carry out the PCR amplification, which consisted of an initial denaturation period of 3 min

at 95 °C, followed by 94 °C for 30 s, 60 °C for 30 s, 72 °C for 1 min, all for 25 cycles each and a final elongation at 72 °C for 2 min. Amplicons were visualised by 1 % agarose gel electrophoresis with ethidium bromide staining in 1 × TAE buffer (1 mM EDTA, 20 mM acetic acid, 40 mM Tris-acetate) run at 80 V for 30 min.

Table 3.2: Reaction set-up for colony PCR of recombinant plasmids in transformed TOP10 *E. coli* cells.

Reagents	Sample	NTC
2 × Amplicon <i>Taq</i>	10 µl	10 µl
pJET1.2 Forward primer (10 µM)	0.4 µl	0.4 µl
pJET1.2 Reverse primer (10 µM)	0.4 µl	0.4 µl
ddH ₂ O	9.2 µl	9.2 µl
Transformed colony (Template DNA)	✓	—
Total	20 µl	20 µl

3.2.4 Plasmid extraction

Colonies identified as positive by colony PCR were inoculated in 5 ml LB containing ampicillin (100 µg.ml⁻¹) followed by incubation with shaking at 37 °C overnight. Plasmids were extracted from 3 ml of the cultured cells following the manufacturer’s protocol of the GeneJET Plasmid Miniprep Kit (Thermo Fisher Scientific, USA). All centrifugation steps were carried out at 12000 ×g, and plasmid DNA was eluted with 50 µl Elution buffer. Samples were stored at -20 °C.

3.2.5 Restriction enzyme digestion

Restriction enzyme digestion reactions were setup on ice in 0.2 ml tubes according to Table 3.3, using FastDigest restriction enzymes (Thermo Fisher, USA). The reaction was gently mixed and then centrifuged for ~5 s, followed by incubation at 37 °C for 15 min. Digests were visualised by 1 % agarose gel electrophoresis with ethidium bromide staining in 1 × TAE buffer at 80 V for 30 min. A GeneRuler™ 1 kb DNA ladder (Thermo Fisher, USA) was used to estimate band sizes. A ChemiDoc™ XRS+ System with Image Lab™ Software (Bio-Rad Laboratories, USA) was used to visualise the agarose gel.

Table 3.3: Reaction setup for restriction digestion of recombinant plasmid DNA

Components	Volume
ddH ₂ O	14 µl
10 × FastDigest Buffer	2 µl
Plasmid DNA (51.0 – 159.9 ng/µl)	2 µl
FastDigest <i>Xba</i> I (10 U/µl)	1 µl
FastDigest <i>Xho</i> I (10 U/µl)	1 µl
Total Volume	20 µl

3.2.6 Plasmid sequencing and sequence alignment

Successfully extracted plasmids were sent for sequencing by Inqaba Biotechnical Industries (Pty) Ltd (South Africa). All plasmids were sequenced in the forward direction only using the pJET1.2 forward oligonucleotide. The CrleGV-SA Lef-8/HP PCR product was also sequenced in both the forward and reverse direction using the Lef-8/HP F and Lef-8/HP R oligonucleotides. A pairwise alignment was performed using the forward and reverse CrleGV-SA Lef-8/HP PCR sequences and the consensus sequence from the PCR product alignment was used for the alignment against the CrleGV-SA and CrleGV-SA-C5 sequences. A multiple alignment was performed using the resulting sequence data, the reference CrleGV-SA (Accession number: MF974563.1) sequence and the CrleGV-SA-C5 sequence using the ClustalW method in Geneious R11.

3.2.7 Melt curve analysis

The CrleGV-SA-C5 HypoP and CrleGV-SA HypoP PCR products were used for the melt curve analysis. Each 20 µl SYBR melt curve reaction was setup according to Table 3.4. No Template controls (NTC) were used for each reaction setup, replacing the template DNA with ddH₂O. The cycle parameters had an initial denaturation set at 95 °C for 3 min followed by the melt curve generation starting at 65 °C increasing up to 95 °C with a 0.5 °C increment and 5 s hold at each temperature. The samples were setup in triplicate. Melt curve analysis was viewed using the CFX Manager™ Software v3.1 (Bio-Rad Laboratories, USA).

Table 3.4: SYBR Melt Curve reaction setup

Reagents	Setup	NTC
SYBR <i>Taq</i>	10 μ l	10 μ l
PCR Product template (12.5 ng/ μ l)	1 μ l	-
ddH ₂ O	9 μ l	10 μ l
Total Volume	20 μl	20 μl

3.3 RESULTS

3.3.1 Cloning of PCR amplicons into pJET1.2/blunt plasmid vector and colony PCR

The CrleGV-SA-C5 Pif-2, HypoP and Lef-8/HP and the CrleGV-SA Pif-2, HypoP and Lef-8/HP PCR amplicons were ligated into the pJET1.2/blunt vector following the blunt cloning protocol, resulting in recombinant pJET1.2 plasmids with inserts being created. Figure 3.1 shows the pSA/pC5_Pif-2 plasmid map, representing the common layout present in each of the six constructs.

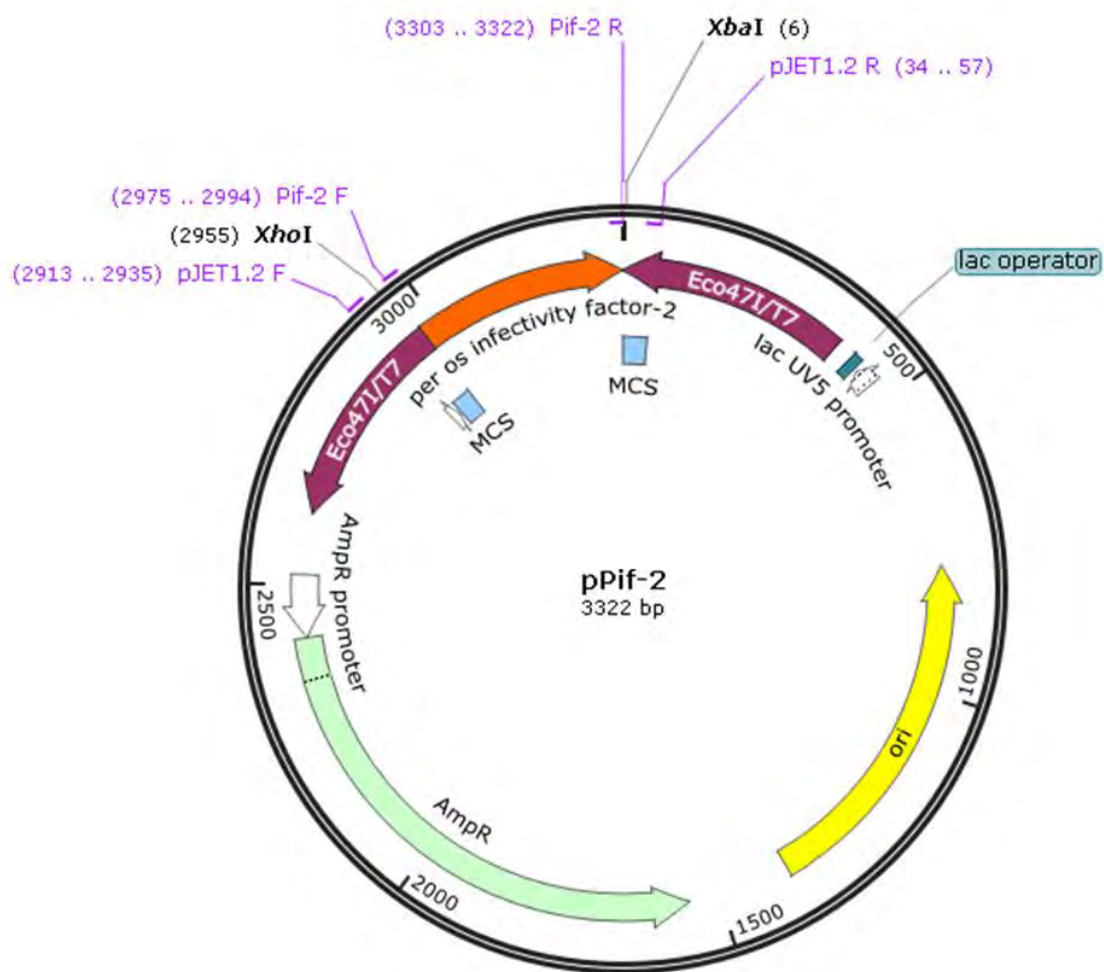


Figure 3.1: A generalised plasmid map of the recombinant vectors that were created using Pif-2, the insert (Orange) represents the target gene that was ligated into the pJET1.2/blunt cloning vector. Annotations: The disrupted lethal gene (Eco47I/T7) in maroon, the Ampicillin resistance gene (AmpR) in green, and the multiple cloning site (MCS) in blue. Oligonucleotide and restriction enzyme binding sites are labelled in purple and black text respectively.

Following ligation and transformation, colony PCR was performed using the pJET1.2 oligonucleotides. The expected sizes of the colony PCR amplicons were determined using the constructed plasmid maps and are reported in Table 3.5. The expected amplicon size for Pif-2 was 467 bp, 421 bp for the HypoP amplicon and 430 bp for the Lef-8/HP amplicon. The amplicons of the approximate expected sizes were obtained after conducting colony PCR amplification using the recombinant plasmids as the template (Figure 3.2).

Table 3.5: Expected sizes of the colony PCR amplicons

Plasmid Name	pJET1.2 Oligonucleotide binding position	Expected Colony PCR amplicon size (bp)
pC5_Pif-2		467
pSA_Pif-2		
pC5_HypoP	pJET1.2 F: 2913→2935	421
pSA_HypoP	pJET1.2 R: 34→57	
pC5_Lef-8/HP		430
pSA_Lef-8/HP		

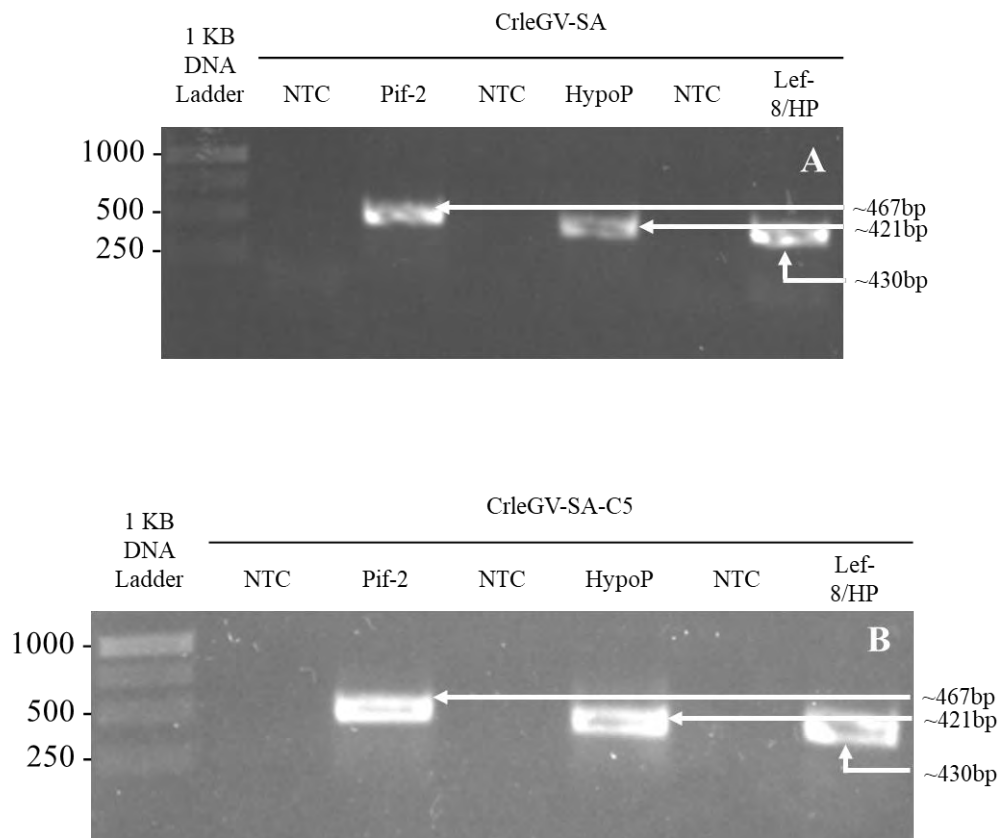


Figure 3.2: A 1% agarose gel with ethidium bromide staining of the colony PCR amplification of the cloned CrleGV-SA and CrleGV-SA-C5 PCR amplicons.

3.3.2 Plasmid extraction and restriction digestion

To further confirm the presence of the insert, recombinant plasmids were extracted and digested with the FastDigest *XhoI* and *XbaI* restriction enzymes. The undigested along with digested plasmids were then analysed by agarose gel electrophoresis (Figure 3.3, panels A, B and C). In the undigested samples, in lanes 1 and 3, the different conformations of the plasmid were observed with the open circular, linear and supercoiled conformations all visible. The size of the linear bands for these plasmids were 3322 bp for pC5_Pif-2 and pSA_Pif-2, 3276 bp for pC5_HypoP and pSA_HypoP and 3285 bp for pC5_Lef-8/HP and pSA_Lef-8/HP. For the digested samples in lanes 2 and 4, a large band with vector backbone and a smaller band of the insert was observed. Bands of approximately 2974 bp and 348 bp for plasmids pC5_Pif-2 and pSA_Pif-2, 2974 bp and 302 bp for plasmids pC5_HypoP and pSA_HypoP and 2974 bp and 311 bp for plasmids pC5_Lef-8/HP and pSA_Lef-8/HP were visible and these included the insert which resolved lower down (Figure 3.3).

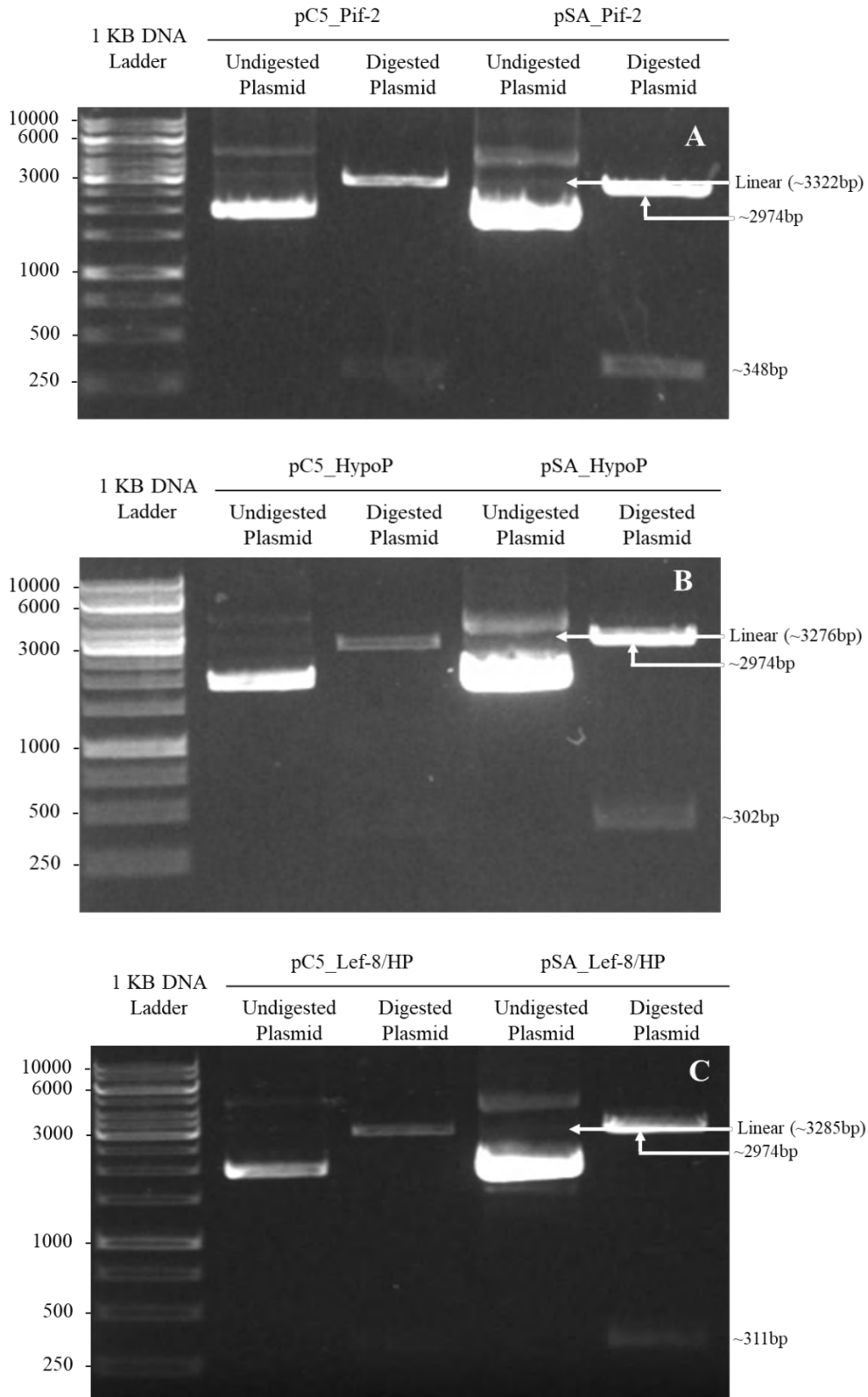


Figure 3.3: Agarose gel electrophoresis (1 %) with ethidium bromide staining showing the results with undigested and digested plasmids. A) pC5_Pif-2 and pSA_Pif-2. B) pC5_HypoP and pSA_HypoP. C) pC5_Lef-8/HP and pSA_Lef-8/HPs.

3.3.3 Sequencing of recombinant plasmids

3.3.3.1 Multiple alignment of Pif-2 region

Six recombinant plasmids were constructed, confirmed for the presence of the insert by colony PCR and restriction enzyme digestion and then Sanger sequenced. Plasmids pC5_Pif-2 and pSA_Pif-2 were aligned to the CrleGV-SA-C5 Pif-2 and CrleGV-SA Pif-2 genes, this is shown in Figure 3.4. The first SNP (UV_2) was identified at position 153, this was a Thymine to Cytosine and the second SNP (UV_3) was identified at position 325, this was a Guanine to Adenine change, as observed in the alignment, which were both identified in the initial bioinformatics analysis.

3.3.3.2 Multiple alignment of the HypoP region

The sequence results from plasmid pC5_HypoP and pSA_HypoP were aligned against the HypoP gene from CrleGV-SA-C5 genome and the HypoP gene from CrleGV-SA genome with the results shown in Figure 3.5. The SNP can be seen at position 243, with a Thymine to Guanine change present, this SNP represents UV_5 as identified during the initial bioinformatics analysis.

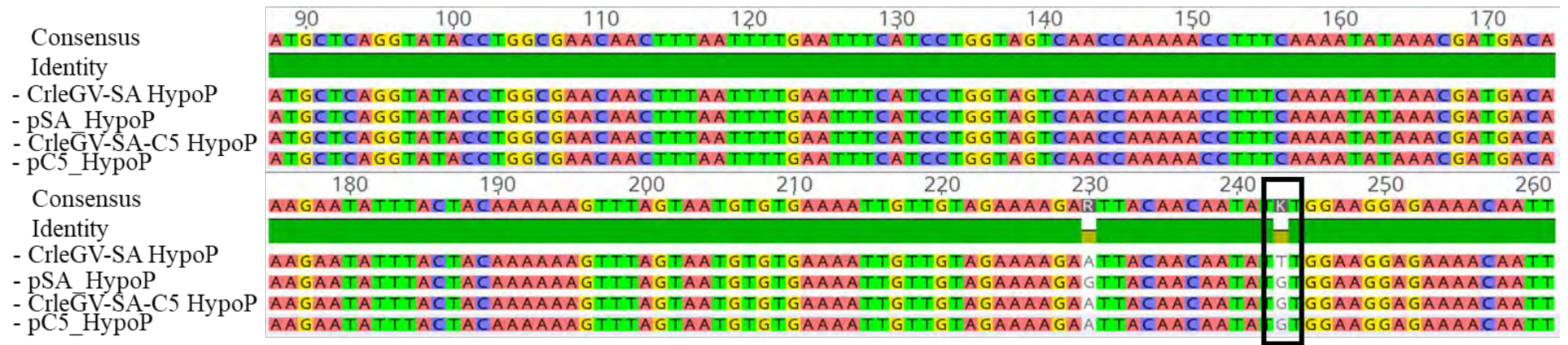


Figure 3.5: Multiple Sequence alignment of the CrleGV-SA-C5 and CrleGV-SA HypoP region against the plasmid sequence of pC5_HypoP and pSA_HypoP. The targeted SNP, UV_5 is highlighted by the black box.

3.3.3.3 Multiple alignment of the Lef-8/HP region

Sequences of pC5_Lef-8/HP and the CrleGV-SA Lef-8/HP PCR amplicon were aligned to the CrleGV-SA-C5 Lef-8/HP and CrleGV-SA Lef-8/HP reference gene sequences, the result is shown in Figure 3.6. The SNP can be observed at position 362, with a Thymine to Cytosine change present. This represents SNP UV_7 as was identified during the initial bioinformatics analysis. The SNP UV_6 identified during the initial bioinformatics analysis was a Guanine to Adenine change, which is not observed in the sequence alignment at position 183.

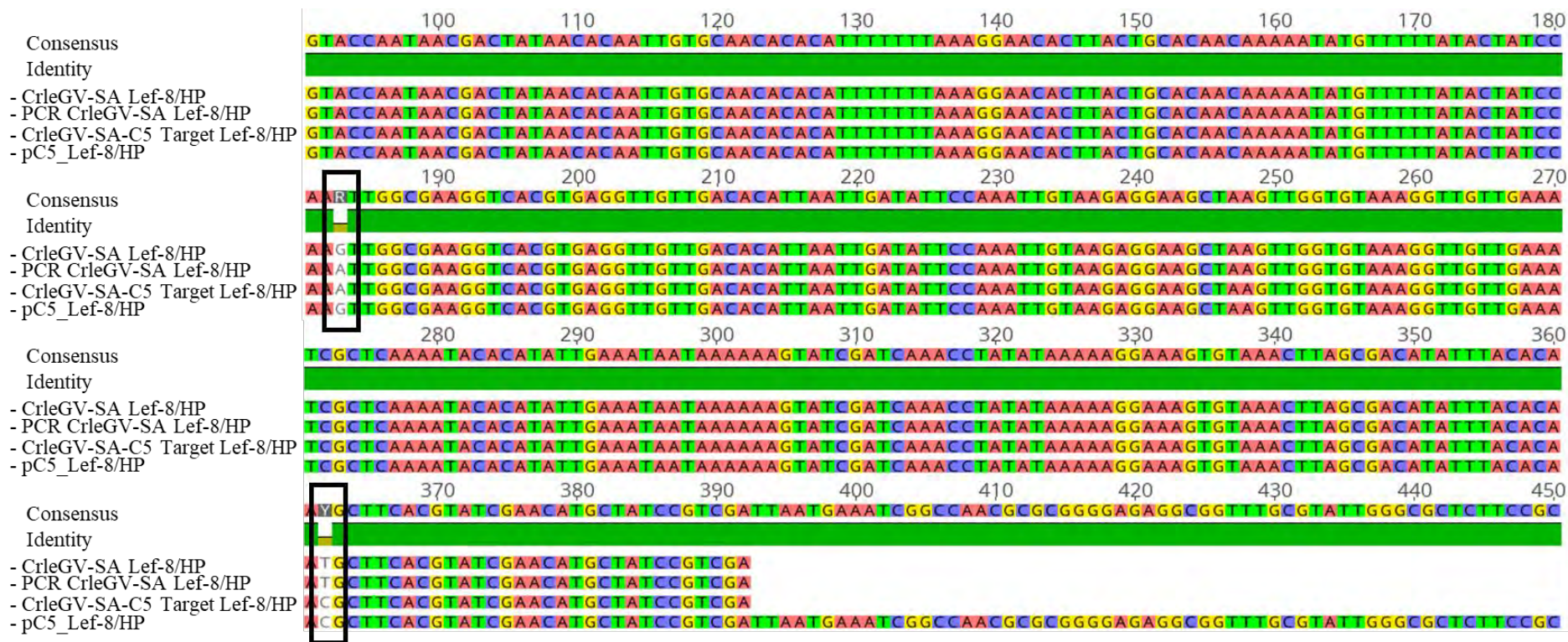


Figure 3.6: Multiple sequence alignment of the CrleGV-SA-C5 and CrleGV-SA Lef-8/HP region against the plasmid sequence of pC5_Lef-8/HP and the sequence of the CrleGV-SA Lef-8/HP PCR amplicons. The targeted SNPs, UV_6 and UV_7, are highlighted in with the black box.

3.3.4 SYBR melt curve analysis

The CrleGV-SA-C5 and CrleGV-SA HypoP PCR products were used for qPCR Melt curve analysis. The results are presented in Figure 3.7, the average T_m for the CrleGV-SA-C5 samples was 79.3 ± 0.28 °C (n=3) and the T_m for the CrleGV-SA samples were 79.5 ± 0.0 °C (n=2).

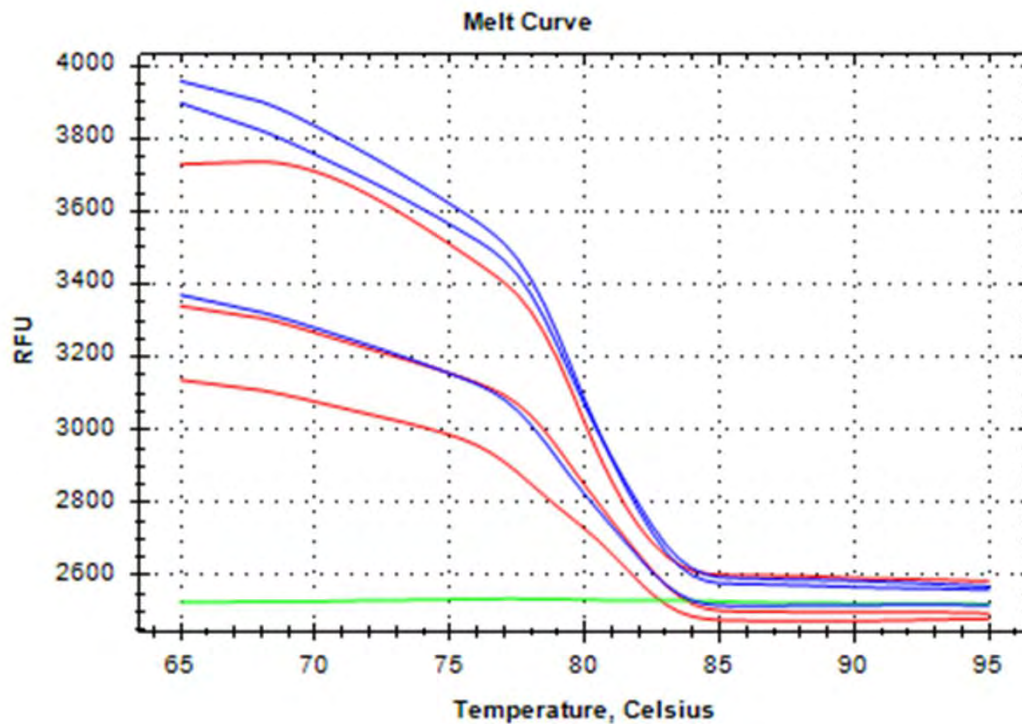


Figure 3.7: Melt Curve generated using the CrleGV-SA-C5 HypoP PCR product and the CrleGV-SA HypoP PCR Product. The blue curves represent the CrleGV-SA-C5 HypoP PCR products, the red curves represent the CrleGV-SA HypoP PCR products, and the green line the NTC reaction.

3.4 DISCUSSION

The aim of the study reported in this chapter was to develop screening methods for differentiating the CrleGV-SA-C5 isolate from the CrleGV-SA isolate by two different methods. The two approaches were sequencing and qPCR melt curve analysis. The objectives for the study were (i) ligation of PCR amplicons into pJET1.2/blunt vector and transformation of the ligations, (ii) colony PCR to confirm the presence of the inserts, (iii) plasmid extraction and restriction digestion, (iv) plasmid DNA sequencing, and (v) qPCR melt curve analysis. The CrleGV-SA-C5 and CrleGV-SA Pif-2, HypoP, and Lef-8/HP PCR amplicons were PCR amplified using three oligonucleotide sets as described in Chapter 2. The PCR amplicons were successfully cloned into pJET1.2/blunt cloning vector. Plasmid maps were successfully constructed and used to determine the expected colony PCR amplicon sizes. Colony PCR was performed to screen for plasmids containing the cloned inserts, with the resulting AGE images showing the successful amplification and the ligated inserts producing amplicons of the expected size for each cloned insert.

The third objective was the extraction of plasmids and restriction digestion. These plasmids were constructed to confirm the presence of the SNPs identified in the previous chapter which could then be compared against CrleGV-SA. All six plasmids were successfully extracted, undigested plasmids were analysed by AGE and the amplicon size of the linear band produced was of the expected size for all the constructed plasmids. Plasmids were further analysed by restriction digestion to identify the presence of the inserts. The restriction enzymes *XhoI* and *XbaI* were selected for restriction digestion because the restriction sites of these enzymes are located on either end of where the PCR product was ligated into the pJET1.2/blunt vector. All restriction digest fragments were of the expected sizes, suggesting that ligation of inserts into pJET1.2/blunt vector were successful.

The successfully generated recombinant plasmids were then sent for Sanger sequencing. Five out of the six plasmids were successfully sequenced. After sequencing of the pSA_Lef-8/HP plasmid, the sequence data generated was not satisfactory (data not shown) and therefore the CrleGV-SA Lef-8/HP PCR amplicon was sequenced directly. A vital limitation of Sanger sequencing automation is that the sequences within the first 15-40 bp is of low-quality because of primer binding and the inability of single base pair differences being distinguishable in longer segments (Crossley et al., 2020). The loss of sequence data due to these limitations of

Sanger sequencing was of concern when directly sequencing the PCR products, as the sequence results may be affected.

Furthermore, the reverse sequence read was of low quality in this region and as a result, the SNP was poorly identified. To mitigate this, the CrleGV-SA Lef-8/HP PCR amplicon was sequenced in both the forward and reverse directions to overcome these limitations and to ensure that the SNPs were accurately identified. Whereas the entire sequence of the insert was successfully generated when sequencing from the plasmid DNA with only the forward direction required. An advantage of cloning the PCR amplicons into the pJET1.2/blunt vector followed by sequencing, is that the vector consists of sequencing sites that flank the insert region and would therefore provide additional nucleotides on either side of the insert for the machine when sequencing. Four out of the five targeted SNPs remained detectable in the C5 genome, with the SNP UV_6 in the Lef-8/HP region not being detected. Mistakes that occur during PCR amplification emerge in the sequence data and contribute to false mutations (Potapov & Ong, 2017). During DNA synthesis the *Taq* DNA polymerase does not have the ability to rectify misincorporated nucleotides that occur, as a result of the polymerase not having a 3'→5' exonuclease activity (McInerney et al., 2014). The published error rate of *Taq* polymerase enzyme is $1-20 \times 10^{-5}$ errors/bp/duplication (McInerney et al., 2014). The targeted SNPs were also present in the sequences of the CrleGV-SA isolate. The mismatches in the CrleGV-SA isolate sequences may be as a result of an error in the sequencing process or misincorporation of nucleotides during PCR amplification. It has been observed within various baculovirus species that there is considerable genotypic variation (López-Ferber et al., 2003). The SNPs present in the CrleGV-SA isolate could be due to genotypic variation within the sample. The SNP at position 153 in the pSA_Pif-2 is the same as the nucleotide identified at position 38194 in van der Merwe et al. (2017).

The SNPs UV_2, UV_3, and UV_5 were identical to the SNPs at the same position identified in the pSA_Pif-2 and pSA_HypoP sequences respectively, and UV_6 was the same as the SNP identified at the same position in the CrleGV-SA Lef8/HP sequence which may be a variation that is unstable. This indicates that UV_2, UV_3, UV_5 and UV_6 are not ideal markers to use for differentiating between the CrleGV-SA-C5 and CrleGV-SA isolates. The SNP UV_7 was the only SNP that was different from the CrleGV-SA sequences, resulting in the only suitable marker to differentiate between the CrleGV-SA-C5 isolate and the CrleGV-SA isolate. Therefore, four of the five SNPs did not render markers that could be selected and UV_7 is the

only marker that will be used is next chapter to differentiate between the CrleGV-SA-C5 and CrleGV-SA isolates.

Two approaches were conducted to differentiate between CrleGV-SA-C5 and CrleGV-SA isolate regions, the one approach was sequencing and the other qPCR melt curve analysis. At the initial observation of melt curve data, the melt curve was not successful at differentiating between the two isolate regions. The melt curve analysis does however show potential, but the technique may need to be optimised, either by decreasing the size of the amplicon, or using a machine with a high-resolution melt analysis. High-resolution melting (HRM) analysis is a closed tube method used for quick analysis of genetic differences that occur in PCR amplicons (Reed & Wittwer, 2004). Using the melting temperature to correctly differentiate between wild-type and homozygous mutant samples, requires closely controlled reaction conditions and high-resolution melting (Seipp et al., 2007). When probes are not used during HRM, reducing the amplicon size and using internal temperature standards can increase the sensitivity of the genotyping (Seipp et al., 2007). Due to the CrleGV-SA-C5 and CrleGV-SA HypoP isolates not being differentiated by melt curve analysis, this method was not conducted for the Lef-8/HP and Pif-2 PCR amplicons. It was later identified upon sequencing analysis that the melt curve may have been successful as it supports the sequencing results shown that there was no difference between the CrleGV-SA-C5 HypoP and CrleGV-SA HypoP regions as UV_5 was identical to the SNPs at the same position identified in the pSA_HypoP sequences. This technique would need further evaluation.

In conclusion, six recombinant plasmids were successfully constructed and confirmed for the presence of the insert by colony PCR and restriction enzyme digestions. Sanger sequencing confirmed the presence of SNPs originally detected in regions of the CrleGV-SA-C5 genome. Melt curve analysis was unsuccessful at distinguishing between the CrleGV-SA-C5 and CrleGV-SA isolates. The next chapter aims to bulk up CrleGV-SA-C5 in 4th instar *T. leucotreta* larvae and to investigate the genetic stability of the virus following infection and recovery.

Chapter 4

Investigating the genetic stability of CrleGV-SA-C5 during propagation in *T. leucotreta* larvae

4.1 INTRODUCTION

Chapter 2 described a bioinformatics analysis which revealed seven SNPs in the CrleGV-SA-C5 genome when compared to the CrleGV-SA genome. Three sets of oligonucleotides were designed to flank five of the identified SNPs to detect their presence by PCR. Further investigation is required on the CrleGV-SA-C5 isolate because it is not yet known whether these genetic changes directly contribute to the UV tolerance of the CrleGV-SA-C5 isolate. If the SNPs do indeed contribute to UV tolerance, it is necessary for commercial purposes and important that during the bulk-up of the virus the genetic changes are stable and are retained. Therefore, the next step of the study was to passage the CrleGV-SA-C5 through *T. leucotreta* larvae and for the virus genome to be analysed for the presence of the identified SNPs.

Prior to conducting bioassays, it was necessary to rear the *T. leucotreta* to the life stage required for the study. The artificial diet on which *T. leucotreta* are reared is described by Moore et al. (2014). According to Jones (2000) there is a positive correlation between larval weight and amount of virus produced per insect. Therefore, for the purpose of this chapter the fourth instar *T. leucotreta* was chosen for virus propagation to obtain sufficient yield of the virus. After rearing of larvae, it is necessary to determine the lethal concentration (LC) estimates for the later propagation of CrleGV-SA-C5 in *T. leucotreta* larvae. For the purpose of propagation, the LC₉₀ value was important to obtain sufficient virus for further propagation and analysis. Lethal concentrations were determined through surface-dose bioassays whereby one of five dilutions of the CrleGV-SA-C5 was spread on the surface of the *T. leucotreta* diet in a 24-well bioassay plate and an individual insect was placed on the diet surface and incubated. According to Jones (2000) the aim of all *in vivo* dose-response assays should have a dose range that will cause between 10 – 90 % insect mortalities and generally, there should be five doses. The design of surface dose bioassays is essentially for the feeding pattern of insects that burrow into the fruit or eat the fruit surface to be mimicked (Jones, 2000).

For the purpose of the study, it was important to determine the LC₉₀ for the virus propagation, however the LC₅₀ was also determined. The LC₉₀ is the concentration required for 90 % of larvae in a sample to be killed (Moore et al., 2011a). The LC₅₀ is the concentration of virus required for 50 % of the larvae in a sample to be killed (Thomas & Elkinton, 2004). According to Jones (2000) it is vital to accurately determine the concentration of virus suspensions that are used in bioassays and the most suitable method to determine the concentration of purified viruses is to use a haemocytometer. The use of a haemocytometer was chosen for determining the concentration of all the virus samples in the chapter. The propagation was conducted following the propagation method described by Mwanza (2019) with slight modifications.

It is important to analyse the propagated CrleGV-SA-C5 for the presence or absence of the identified SNPs. Polymerase chain reaction rapidly and selectively amplifies a target sequence of DNA, generating millions of copies (Green & Sambrook, 2019). Therefore, the PCR amplification method was selected for amplifying the target regions which flank the identified SNPs. Sanger sequencing is used when it is required for the sequencing of fragment of genes or for sequencing of specific genes (Vernet, 2017). Sanger sequencing was used in Chapter 3 for sequencing of samples, based on the results obtained Sanger sequencing was selected in the current chapter to confirm the presence of the SNPs in the amplified target regions.

The overall aim of the chapter was to determine whether the genetic integrity of the CrleGV-SA-C5 isolate is retained when bulked up *in vivo*. The specific objectives were (i) to enumerate CrleGV-SA-C5 OBs (ii) to rear *T. leucotreta* fourth instars on artificial diet (iii) to perform surface dose-response bioassays in fourth instars and evaluate LC₅₀ and LC₉₀ (iv) to propagate CrleGV-SA-C5 in fourth instar *T. leucotreta* larvae (v) to extract CrleGV-SA-C5 genomic DNA from purified OBs and PCR amplify the target regions for Sanger sequencing to determine the presence of the original SNPs.

4.2 METHODS

A schematic flow diagram of the procedure conducted to achieve the various objectives is shown in Figure 4.1.

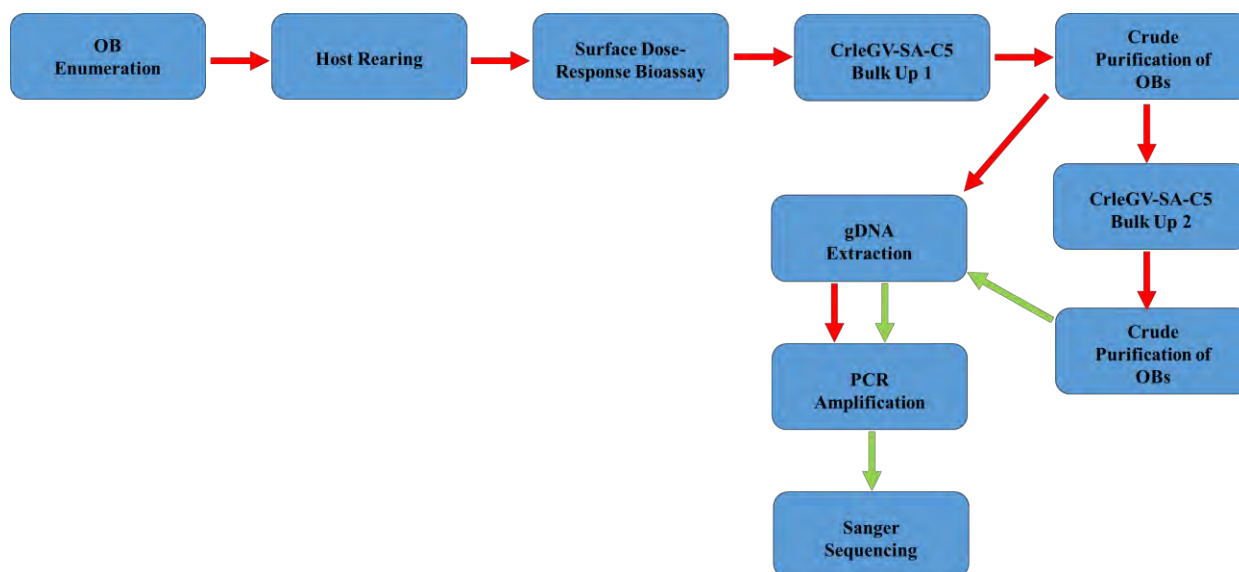


Figure 4.1: Schematic diagram describing the various steps of the study

4.2.1 Occlusion body enumeration

Light microscopy was used to determine the concentration of the OBs from the CrleGV-SA-C5 sample and the bulked up CrleGV-SA-C5 samples. A 1:5 dilution of the virus suspension was made by adding 10 μl of the purified OBs to 40 μl of ddH₂O in a 1.5 ml tube, making a total volume of 50 μl , and this was followed by mixing to homogenise the suspension. 200 μl of SDS (0.07 % w/v) solution was added to the 50 μl virus suspension making a further 1:5 dilution (total 25 \times dilution). The suspension was mixed until homogenous. The sample was sonicated at 60 Hz for four 15 s pulses (ear protection was worn). A further four dilutions, were prepared using the sonicated suspension in four 2 ml tubes, whereby 1975.0, 1971.4, 1966.7 and 980.0 μl ddH₂O was added to 25.0, 28.6, 33.3 and 20.0 μl of the sonicated suspension, respectively, resulting in dilutions ranging from 1:80 to 1:50 (total 1:2000 to 1:1250). The suspensions were mixed to ensure homogenous dilutions. A Thoma bacterial counting chamber with a 0.02 mm depth (Marienfeld, Germany) and cover slip were cleaned using 70 % ethanol solution and tissue paper. The cover slip was partially placed over the counting chamber for the virus suspension to be pipetted. The dilutions were tested, starting with the most diluted virus suspension, and working up until the most concentrated. The virus suspension that had \pm 7 OBs per small square (0.0025 mm²) of the grid was used for counting and 5 μl was pipetted onto the counting chamber. The cover slip was placed completely over the counting chamber. The slide was then left to stand for 5 min prior to counting. This allows Brownian movement

of non-virus particles to settle. The CrleGV-SA-C5 OBs were counted under the light microscope at 400 × magnification by phase contrast. The bulk-up 1 (CrleGV-SA-C5_BU1) and bulk-up 2 OBs (CrleGV-SA-C5_BU2) were observed at 400 × magnification using dark field. A Helber counting chamber with a Thoma ruling and a 0.02 mm depth (Hawksley, United Kingdom) was used for the dark field microscopy. The OBs in the top right and left, bottom right and left and a central large square of the main 4 × 4 grid (each square consisting of 16 smaller squares of 0.0025 mm²) were counted. Equation 4.1 was used to calculate the concentration of OBs.

Equation 4.1: Equation to determine the concentration of the virus sample using a counting chamber

$$\text{Concentration (OBs per ml)} = (D \times x) \div (N \times V)$$

Where D = dilution factor, x = Average number of OBs counted, N = Number of small squares and V= volume

4.2.2 *Thaumatotibia leucotreta* diet preparation

In a baking tray, 200 g of the dry FCM diet (210 g maize meal, 36.5 g milk powder, 100 g Brewer's yeast, 200 g wheat germ, 6.5 g sorbic acid and 15 g nipagin) (Moore et al., 2014) was homogenised in 200 ml ddH₂O and baked for 20 min at 200 °C.

4.2.3 Rearing of *Thaumatotibia leucotreta* larvae

Thaumatotibia leucotreta eggs laid on wax paper were provided by the Centre for Biological Control (CBC), Department of Zoology and Entomology, Rhodes University and were reared on artificial *T. leucotreta* diet. *Thaumatotibia leucotreta* diet was baked in a baking tray and placed in a laminar flow hood to cool down. In the laminar flow hood, the eggs were sterilised with 5 % formaldehyde and then placed on the surface of the diet. A small piece of paper towel was placed on the surface of the diet to reduce condensation. A glass cover was placed on the baking tray and secured with crocodile clips. The baking tray was incubated for ~11 days at 25 °C with a 16h:8h (L:D) photoperiod, until larvae reached fourth instar (Figure 4.2).



Figure 4.2: Rearing of *T. leucotreta* larvae in artificial diet in baking trays, incubated at 25 °C with 16 h:8 h (L:D) photoperiod.

4.2.4 Surface dose-response bioassays to determine the lethal concentration estimates

Surface-dose bioassays were performed in 24-well bioassay plates to estimate specific LCs. *Thaumatotibia leucotreta* diet was prepared and baked in a Pyrex dish and placed under a laminar flow hood to cool down. A modified 10 ml syringe was used to cut the diet, then pressed down into each well and covered with bioassay plate covers. A 10-fold dilution series was conducted with five concentrations made from the CrIeGV-SA-C5 OB stock in ddH₂O (Figure 4.3). 50 µl of each virus dilution or the control was evenly pipetted on the surface of the diet in each well and a glass lid was used to cover the plates. A single fourth instar larva was placed on the surface of the diet in each well. A sample of 10 larvae from the insect batch was collected, the larval head capsule width was measured using the Leica EZ4 D microscope (Leica Microsystems) and Hofmeyr et al. (2016) was used for reference to confirm the larval instar. The mean head capsule width of the larvae used was 0.8416 mm (n=10) which confirmed the larvae were 4th instar. Bioassay plates were securely closed with masking tape and incubated at 25 °C. After 7 days, diet was carefully dissected and larval survival was recorded. The data from the dose-response bioassays were subjected to probit analysis in ToxRat Professional to determine the LC₅₀ and LC₉₀.

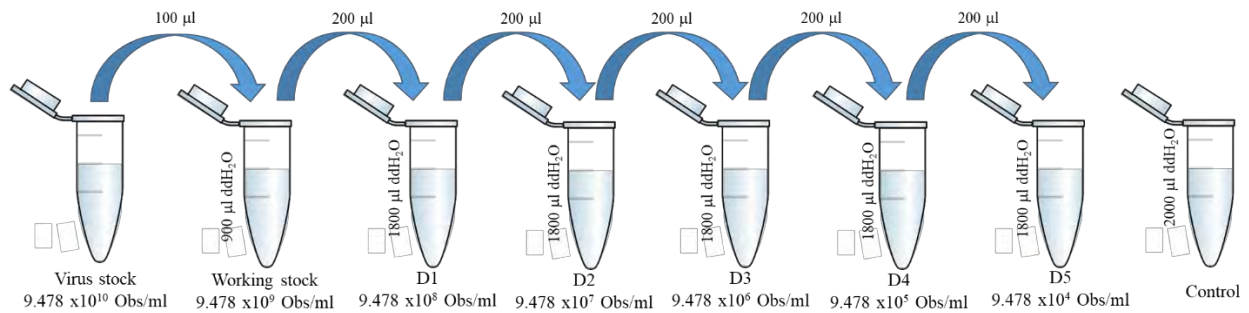


Figure 4.3: Dilution series of CrleGV-SA-C5 for surface dose-response bioassays against *T. leucotreta* fourth instars to determine LC₉₀.

4.2.5 CrleGV-SA-C5 bulk-up in fourth instar *T. leucotreta*

CrleGV-SA-C5 was bulked up using a modified protocol described by Mwanza (2019). CrleGV-SA-C5 was bulked up in fourth instar *T. leucotreta* larvae carried out in 24-well bioassay plates. *Thaumatotibia leucotreta* diet was prepared and baked in a Pyrex dish and placed under a laminar flow hood to cool down. A modified 10 ml syringe was used to cut the diet, then pressed down into each well and covered with bioassay plate covers. The surface of the diet in each well was inoculated with 50 µl CrleGV-SA-C5 with an adjusted LC₉₀ concentration of 8.75×10^9 OBs/ml. A single fourth instar larva (mean head capsule width: ~ 0.875 mm, n=10) was placed on the surface of the diet in each well. Bioassay plates were securely closed with masking tape and incubated at 25 °C. Bioassay plates were inspected after 7 days for infected or dead larvae, and larvae were collected in a microcentrifuge tube. Occlusion bodies were extracted from larval cadavers as described in section 4.2.6. Purified virus was stored at -20 °C for future use in subsequent bulk-up. The purified virus from bulk-up 1 was used to conduct a second bulk-up in fourth instar *T. leucotreta* larvae (mean head capsule width: ~ 0.863 mm, n=10). Virus was extracted and purified from larval cadavers collected from bulk-up 2 and stored at -20 °C. Three bioassay plates were used for bulk-up 1 and ten bioassay plates were used for bulk-up 2.

4.2.6 Crude purification of occlusion bodies

Purification of OBs from larval cadavers collected from bulk-up 1 and from bulk-up 2 was conducted following the protocol described in Jukes (2017), originally adapted from Wennmann & Jehle (2014). Larval cadavers collected from bulk-up 1 were pooled together and larval cadavers collected from bulk-up 2 were pool together. Into sterile 2 ml tubes, larval cadavers and were homogenised in 1 ml 0.1 % SDS (w/v) using a sterile mortar, followed by vortexing for 1-2 min. Homogenised samples were centrifuged for 60 s at 100 ×g and the

supernatants were collected in a new 2 ml tube. 1 ml of 0.1 % SDS was used to resuspend the pellets followed by centrifugation for 60 s at 100 ×g. The supernatants were collected and pooled together, followed by centrifugation at 2500 ×g for 5 min. The supernatants were discarded, and the pellet was resuspended in 1 ml ddH₂O. A final centrifugation was performed at 12000 ×g for 5-10 min and the supernatant was removed. The pellets were resuspended in 500 and 1500 µl ddH₂O for bulk-up 1 and 2 respectively and stored at -20 °C for future use.

4.2.7 Genomic DNA extraction

100 µl of purified OBs was mixed with 45 µl Na₂CO₃ followed by incubation for 30 min at 37 °C. The pH was neutralised by the addition of 55 µl 1M Tris-HCl (pH 6.8). Thereafter DNA was extracted following the manufacturer's instructions of the Quick-DNA™ Miniprep Plus kit (Zymo Research, USA). All centrifugations were performed at 12000 × g. DNA was eluted in 50 µl pre-heated (70 °C) DNA elution buffer and stored at -20 °C for future use.

4.2.8 Polymerase chain reaction of target regions

Each 25 µl PCR reaction was set up following the method described in Chapter 2, section 2.2.5. Template DNA with concentration between 40.9 – 64.8 ng/µl was used. No template controls (NTC) were used for each PCR, replacing the template gDNA with ddH₂O. Positive controls were used for each PCR, using the plasmid DNA from pC5_Pif-2, pC5_HypoP and pC5_Lef-8/HP as template DNA for the respective PCR reaction set ups. The PCR products were analysed by 1% agarose gel electrophoresis (AGE) with ethidium bromide staining in 1 × TAE buffer (1 mM EDTA, 20 mM acetic acid, 40 mM Tris-acetate) for 30 min at 80V. The GeneRuler™ 1 kb DNA ladder (Thermo Fisher, USA) was used to estimate amplicon size. A ChemiDoc™ XRS+ System with Image Lab™ Software (Bio-Rad Laboratories, USA) was used to visualise the agarose gel.

4.2.9 Sanger sequencing of polymerase chain reaction amplicons

Amplicons from bulk-up 2 were sent for sequencing by Inqaba Biotechnical Industries (Pty) Ltd (South Africa) in both the forward and reverse direction using the Pif-2, HypoP and Lef-8/HP oligonucleotide sets. A pairwise alignment was conducted using the ClustalW method, aligning the forward and reverse sequences for each of the three regions generating a consensus sequence. A pairwise alignment was then performed using the generated consensus sequence and the CrleGV-SA-C5 sequence using the ClustalW method in Geneious R11.

4.3 RESULTS

4.3.1 Occlusion body enumeration

The OB enumeration of CrleGV-SA-C5 was determined by phase contrast on a light microscope. The concentration of the stock of CrleGV-SA-C5 was 9.478×10^{10} OBs/ml. The OB enumeration of the CrleGV-SA-C5_BU1 was determined by dark field microscopy and the concentration of the stock was 4.075×10^{11} OBs/ml.

4.3.2 Surface dose-response bioassays to determine the lethal concentration estimates

Surface dose bioassays were performed in triplicate using CrleGV-SA-C5 OBs against fourth instar *T. leucotreta* larvae. Each bioassay setup consisted of a control treatment using ddH₂O and five dose treatments ranging from 1.481×10^6 OBs/mm² to 1.481×10^2 OBs/mm². The percentage larval mortality, regression probit and percentage corrected mortality for the conducted for the first two bioassay replicates are shown in Table 4.1 and for all three bioassay replicates are shown in Table 4.2.

Table 4.1: *Thaumatotibia leucotreta* larval mortality in surface dose-response bioassay after 7 days for the first two bioassay replicates

Treatment (OBs/mm ²)	Mortality (%)	Corrected Mortality (%)	Reg. Probit
D1 (1.481×10^6)	85.4	82.5	0.911
D2 (1.481×10^5)	70.8	65.0	0.527
D3 (1.481×10^4)	68.8	62.5	0.143
D4 (1.481×10^3)	50.0	40.0	-0.240
D5 (1.481×10^2)	37.5	25.0	-0.624
Control	16.7	0.0	—

Table 4.2: *Thaumatotibia leucotreta* larval mortality in surface dose-response bioassay after 7 days for all three bioassay replicates

Treatment (OBs/mm ²)	Mortality (%)	Corrected Mortality (%)	Reg. Probit
D1 (1.481 × 10 ⁶)	80.6	76.7	0.750
D2 (1.481 × 10 ⁵)	69.4	63.3	0.430
D3 (1.481 × 10 ⁴)	66.7	60.0	0.110
D4 (1.481 × 10 ³)	52.8	43.3	-0.211
D5 (1.481 × 10 ²)	38.9	26.7	-0.531
Control	16.7	0.0	—

The mortality for the third bioassay replicate was lower than 90 % and for the first two replicates the mortality was greater than 90 %. An LC₉₀ could not be determined when probit analysis was conducted on all three bioassay replicates and was only determine with the analysis conducted on the first two bioassay replicates. The concentration-effect and survival rate curves for the first two bioassay replicates are shown in Figure 4.4. A linear regression was performed using the first two bioassay replicate data, resulting in a chi-squared value of 1.57627 and a p(Chi²) value of 0.665 and a statistically significant concentration p(F) of 0.004. The probit analysis indicated a LC₅₀ of 6.266 × 10³ OBs/mm², a LC₇₅ of 3.578 × 10⁵ OBs/mm² and a LC₉₀ of 1.367 × 10⁷ OBs/mm² (Table 4.3).

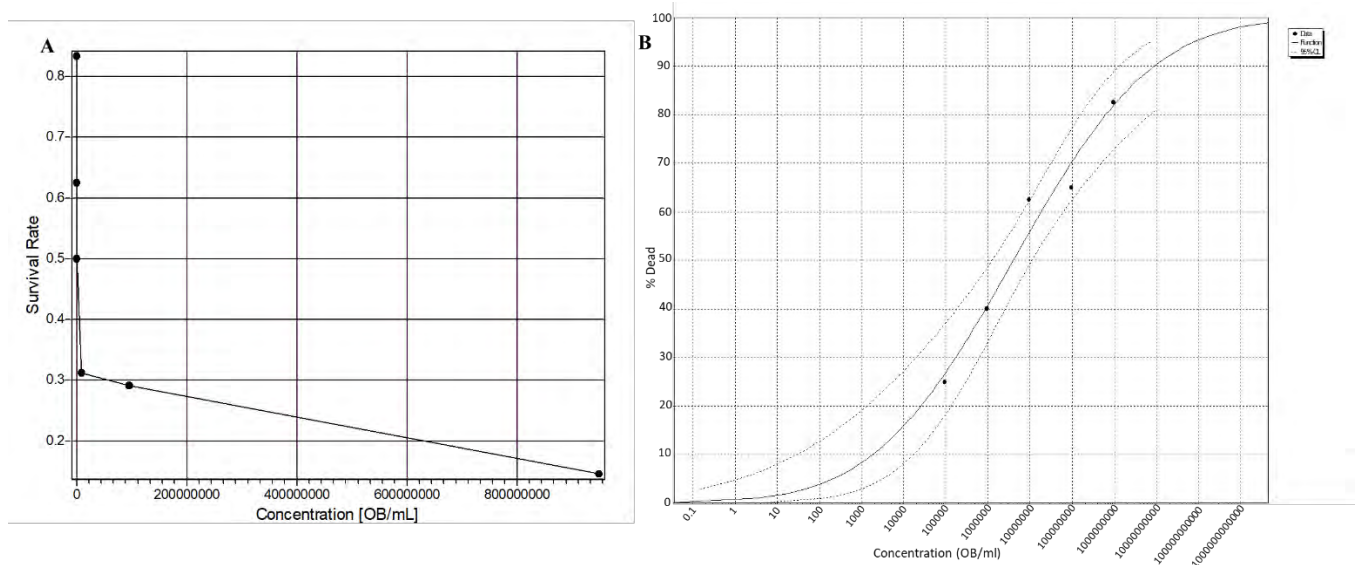


Figure 4.4: Analysis of the first two bioassay replicates. A: The larval survival rate against concentration rate of UV-tolerant C5 CrleGV OBs (OBs/ml). B: Probit analysis of the percentage mortality against the concentration rate of UV-tolerant C5 CrleGV OBs (OBs/ml), with the response curve (—) and 95 % confidence intervals (---) shown.

Table 4.3: The LC₅₀ and LC₉₀ for the CrleGV-SA-C5 bioassay against fourth instar *T. leucotreta* larvae for the first two bioassay replicates

Lethal Concentration	Concentrations (OBs/mm ²)	95 % Confidence limits	
		Upper	Lower
LC ₅₀	6.266×10^3	1.719×10^4	1.953×10^3
LC ₉₀	1.367×10^7	n.d.	2.016×10^6

4.3.3 CrleGV-SA-C5 bulk-up 1 and bulk-up 2

The CrleGV-SA-C5 was bulked up twice in fourth instar *T. leucotreta* larvae. Three 24-well bioassay plates were used for the first bulk-up to get enough virus to use for the second bulk-up. The second bulk-up was conducted in 10 24-well bioassay plates to obtain sufficient virus to conduct semi-field trials reported in Chapter 5. Table 4.4 shows the results of the bulk-up after crude purification of the larvae collected from each bulk-up procedure. An example of the 24-well plates and of two infected larvae collected after one of the virus bulk-up process is shown in Figure 4.5.

Table 4.4: CrleGV-SA-C5 bulk-up results showing the amount of tissue from which the OBs were extracted from, the concentration of the OBs and the final volume obtained.

Sample	Number of larvae collected	Total tissue mass (g)	Concentration (OBs/mm ²)	Mean OBs per larva	Volume (μl)
CrleGV-SA-C5_BU1	72	0.995	6.367×10^8	2.830×10^8	500
CrleGV-SA-C5_BU2	240	2.510	1.607×10^9	2.143×10^8	1500



Figure 4.5: Images from the virus bulk-up of A & B: 24-well plates and C & D: Infected *T. leucotreta* larvae that were collected.

4.3.4 Genomic DNA extraction

Genomic DNA was successfully extracted from purified CrleGV-SA-C5_BU1 OBs (Results not shown) and CrleGV-SA-C5_BU2 OBs and visualised by 1 % AGE stained with ethidium bromide. The CrleGV-SA-C5_BU2 sample produced a band greater than 10,000 bp in size (Figure 4.6).

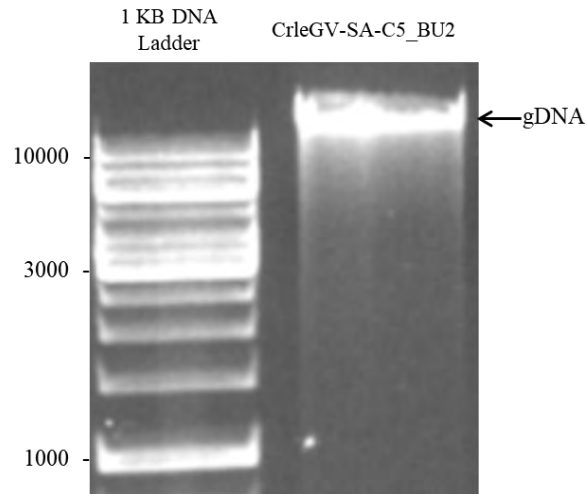


Figure 4.6: AGE with ethidium bromide staining of genomic DNA extractions from CrleGV-SA-C5_BU2 OBs.

4.3.5 Polymerase chain reaction of target regions

Polymerase chain reaction amplifications were conducted using CrleGV-SA-C5_BU1 (data not shown) and CrleGV-SA-C5_BU2 gDNA as template DNA and the three oligonucleotide sets. The PCR results from the amplification using CrleGV-SA-C5_BU2 gDNA was visualised by 1 % AGE stained with ethidium bromide. Amplicons of approximately 348 bp, 302 bp and 311bp were produced for the Pif-2, HypoP and Lef-8/HP regions respectively. These sizes were of the expected band sizes (Figure 4.7, panels A, B and C).

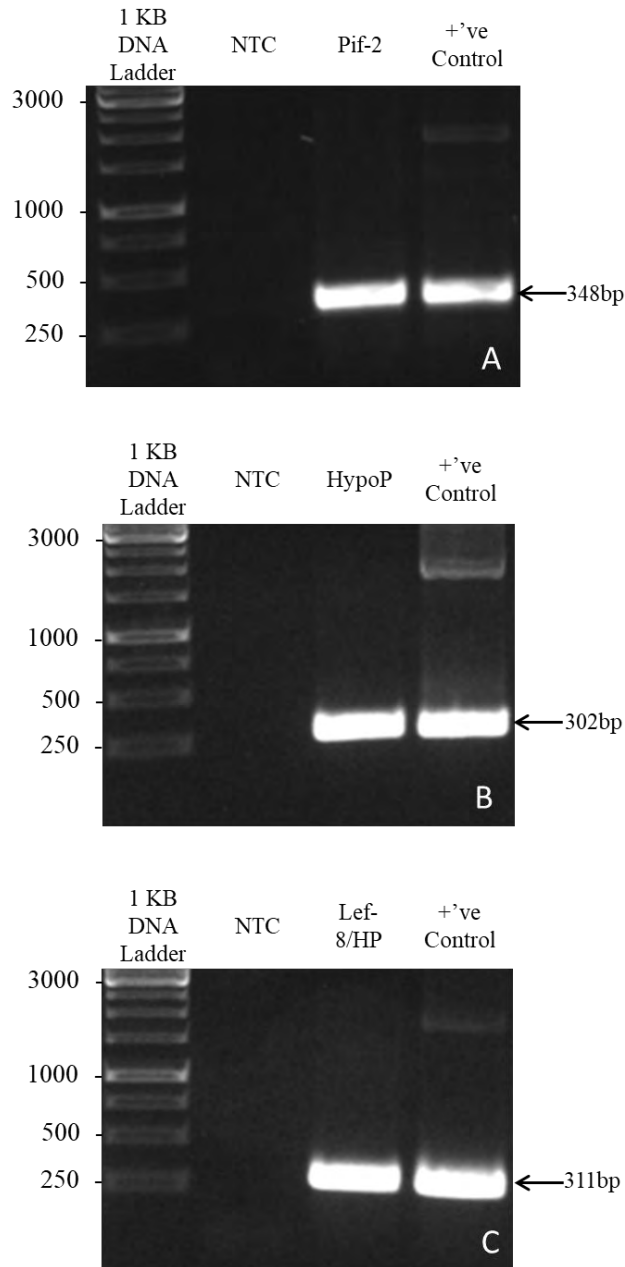


Figure 4.7: AGE with ethidium bromide staining of PCR amplicons resulting from gDNA extracted from CrleGV-SA-C5_BU2. A) Pif-2 oligonucleotide set, B) HypoP oligonucleotide set and C) Lef-8/HP oligonucleotide set. The Pif-2 amplicon size is 348bp, the HypoP amplicon size is 302bp and the Lef-8/HP amplicon size is 311bp.

4.3.6 Sanger sequencing of polymerase chain reaction amplicons

Polymerase chain reaction amplicons from CrleGV-SA-C5_BU2 were Sanger sequenced. The consensus sequence, from the alignment of the CrleGV-SA-C5_BU2 Pif-2 forward and reverse sequences, was aligned to the CrleGV-SA-C5 *Pif-2* gene, shown in Figure 4.8. The first SNP (UV_2) was identified at position 94, which was a Cytosine and the second SNP (UV_3) was

identified at position 266, which was an Adenine change; both were identified in the initial bioinformatics analysis.

The sequence results from CrleGV-SA-C5_BU2 HypoP forward and reverse sequences were aligned generating a consensus sequence. The consensus sequence was aligned to the CrleGV-SA-C5 *HypoP* gene; the result is shown in Figure 4.9. The SNP UV_5 was identified at position 213, this was a Thymine to Guanine change as identified during the initial bioinformatics analysis.

The consensus sequence generated from the pairwise alignment of the CrleGV-SA-C5 Lef-8/HP forward and reverse sequences was aligned to the CrleGV-SA-C5 *Lef-8/HP* genes, as observed in Figure 4.10. The SNPs UV_6 and UV_7 were observed at positions 102 and position 281 respectively. These were identified during the initial bioinformatics analysis, where the first SNP was an Adenine, and the second SNP was a Cytosine.

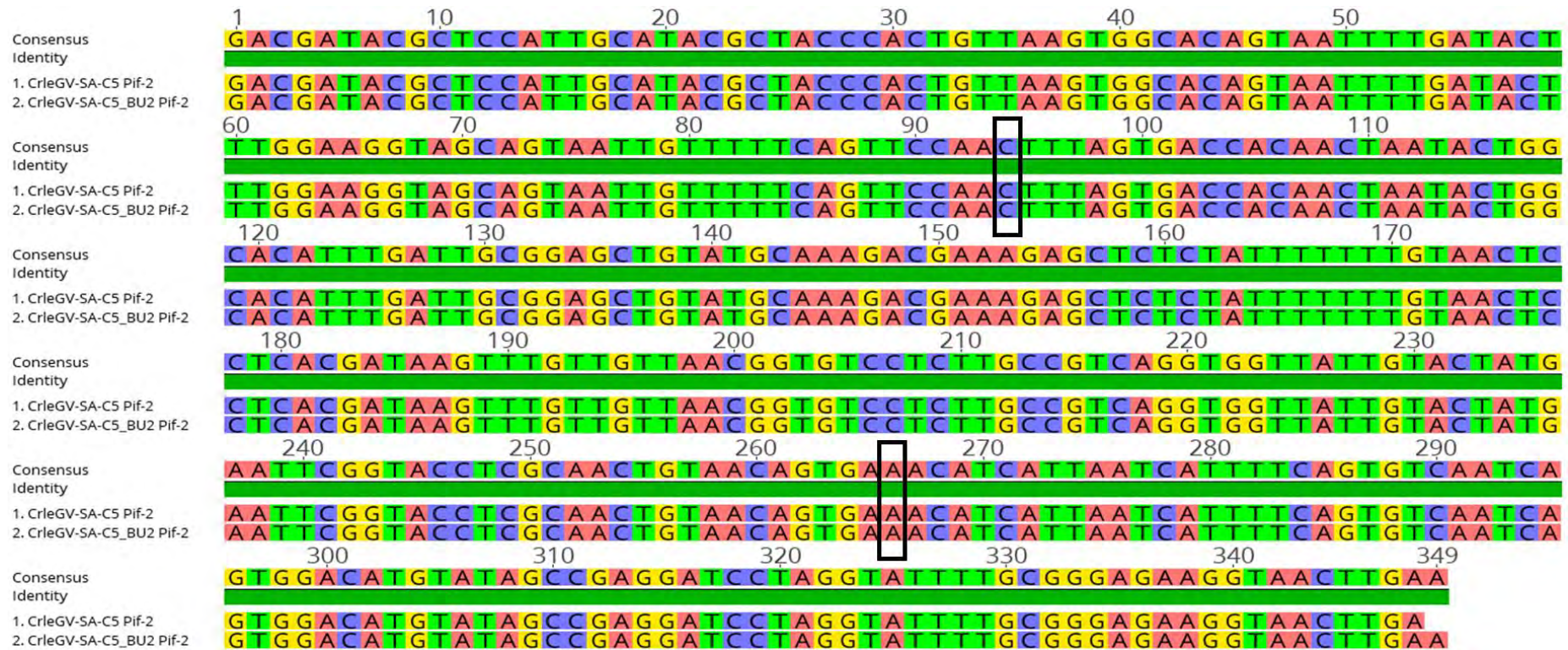


Figure 4.8: Pairwise sequence alignment of the consensus sequences generated of the CrleGV-SA-C5_BU2 Pif-2 PCR amplicons against the CrleGV-SA-C5 *Pif-2* gene. The targeted SNPs, UV_2 and UV_3, are highlighted within the black boxes.

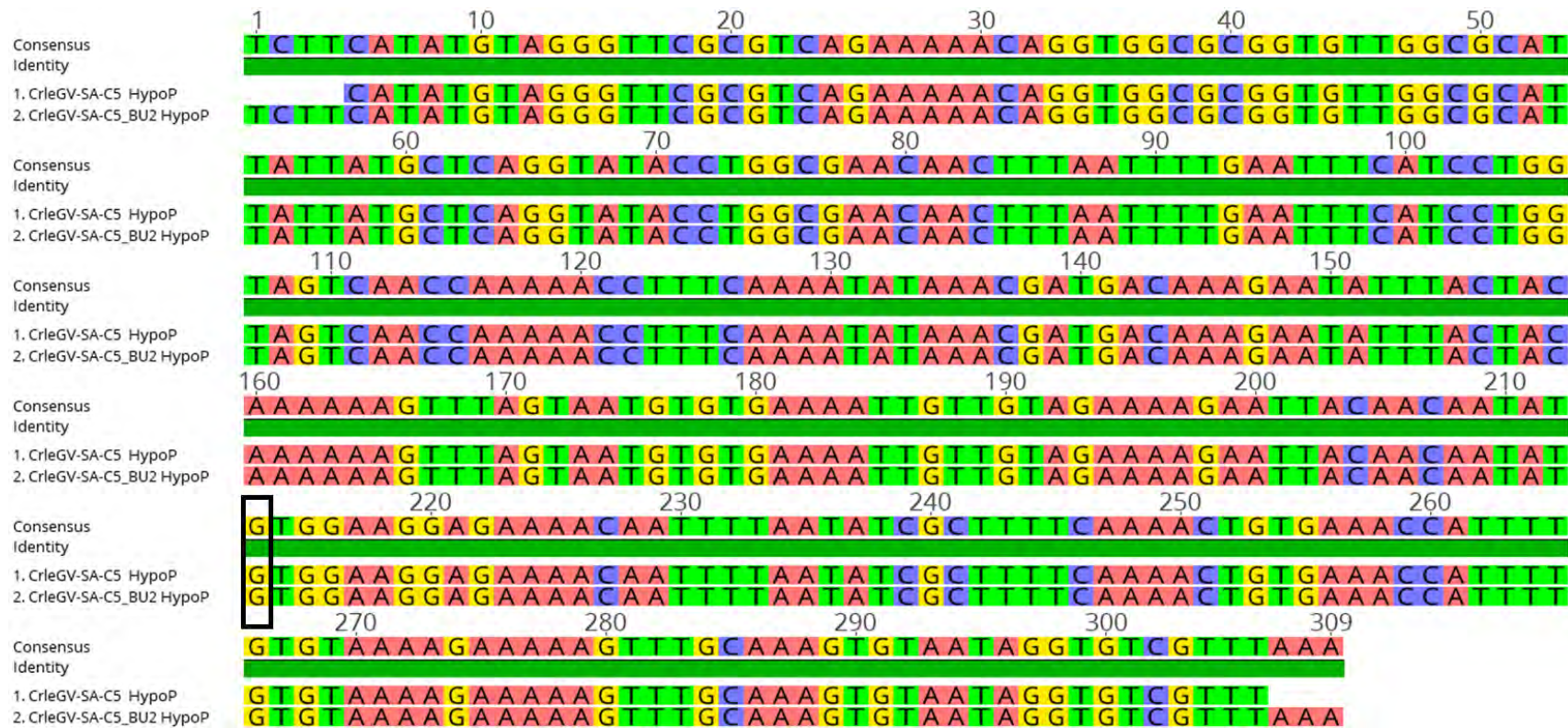


Figure 4.9: Pairwise sequence alignment of the CrleGV-SA-C5_BU2 HypoP consensus sequence, aligned against the CrleGV-SA-C5 *HypoP* gene. The targeted SNP, UV_5, is highlighted within the black box.

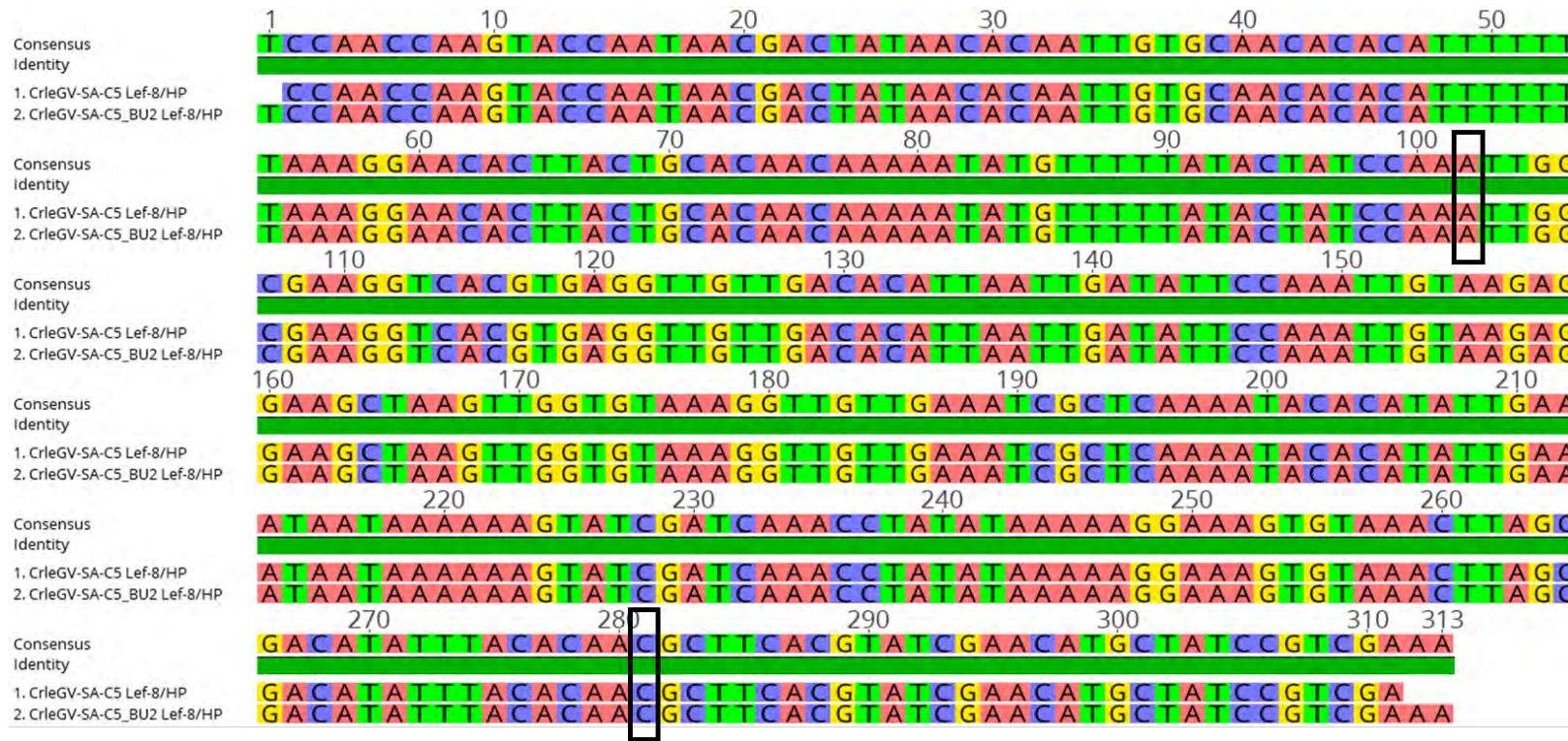


Figure 4.10: Pairwise sequence alignment of the CrleGV-SA-C5_BU2 Lef-8/HP consensus sequence aligned against the CrleGV-SA-C5 *Lef-8/HP* genes. The black boxes highlight the targeted SNPs UV_6 and UV_7.

4.4 DISCUSSION

The aim of the chapter was to determine if the genetic changes are retained in the CrleGV-SA-C5 genome after bulking up *in vivo*. This was achieved by firstly evaluating the LC₅₀ and LC₉₀ by conducting surface dose-response bioassays using fourth instar *T. leucotreta* larvae. The resultant LC₉₀ value was used to bulk-up the CrleGV-SA-C5 in fourth instar *T. leucotreta* larvae. The OBs from CrleGV-SA-C5_BU1 and CrleGV-SA-C5_BU2 were purified, gDNA was extracted and analysed by PCR amplification of the target regions. Polymerase chain reaction amplification was followed by Sanger sequencing of the target regions from only CrleGV-SA-C5_BU2 to determine the presence of the original SNPs.

The surface dose-response bioassays were conducted in triplicate, however a LC₉₀ could not be determined when the data from all three replicates were analysed (Data not shown). Therefore, the LC₉₀ was successfully obtained after analysing the data from two of the dose-response replicates, albeit no upper 95 % confidence limit could be calculated. The study by Mwanza (2019) indicated the LC₅₀ and LC₉₀ to be 1.73×10^6 and 6.22×10^9 OBs/ml respectively for the CrleGV-SA-C5. These are 2.3-fold and 1.4-fold lower in comparison to the current study despite the bioassays conducted by Mwanza (2019) being against neonates. This difference may be due to the use of different *T. leucotreta* colonies from which larvae were sourced, or minor differences in bioassay technique. It was found that over a 16 month period the LC₅₀ of *Spodoptera littoralis* NPV against neonate larvae, obtained with the droplet bioassay of standard suspension, varied from 0.96×10^5 to 7.67×10^5 PIB.ml⁻¹ (PIB more recently referred to as OBs) (Jones, 1988). Variation between separate insect batches may also occur (Jones, 2000). According to Burges & Thompson (1971) assays conducted by different researchers and in different laboratories can cause variation between assays.

Insects susceptibility to virus also differs with insect instar and age (Jones, 2000). An example is that an isolate of *Spodoptera exigua* NPV had a LD₅₀ that ranged from 1.3×10^6 PIB per larva for fifth instar larvae to the LD₅₀ for the first instar larvae being 4 PIB per larva (Smits, 1987). In Addition, the study by Abulkadir (2014) aimed to evaluate the biological activity of *Plutella xylostella* granulovirus (PlxyGV-SA) against the neonate and fourth instar *P. xylostella* larvae. Abulkadir (2014) stated that when comparing the LC₅₀ values of the various larval instars that the larval instar that were the most susceptible to virus infection were the neonate larvae. The study also stated that a higher concentration of virus is required to elicit mortality in older larvae in comparison to a lower dose required to kill neonate larvae. This study

however, was conducted on cabbage leaves where larvae do not burrow in comparison to the current study where larvae burrow into the diet.

The CrleGV-SA-C5 was successfully bulked up in fourth instar *T. leucotreta* larvae and sufficient virus was obtained which was used in detached field trials reported in the next chapter. The study by Moore (2002) found that the mean number of OBs produced per larva was 1.158×10^{11} , this is 409-fold and 540-fold greater than the number of CrleGV-SA-C5 OBs produced after bulk-up 1 and bulk-up 2 respectively. However, the mean number of CrleGV-SA-C5 OBs produced after each bulk-up in the current study was produced in fourth instar *T. leucotreta*, which is in contrast with the study by Moore (2002), where CrleGV-SA was produced in fifth instar *T. leucotreta* larvae. The CrleGV-SA-C5_BU1 and CrleGV-SA-C5_BU2 OBs were successfully purified, and the extraction of the genomic DNA was successful for both the CrleGV-SA-C5_BU1 and CrleGV-SA-C5_BU2 gDNA. It was previously shown (Chapter 3) that the constructed plasmids pC5_Pif-2, pC5_HypoP and pC5_Lef-8/HP consist of the target insert. Therefore, these plasmids were used as positive controls for the PCR amplifications. All PCR amplifications were successful, and the amplicons were of the expected sizes. The next objective was Sanger sequencing of the PCR amplicons in both the forward and reverse direction. Sequencing was successful and results confirmed the stability of the SNPs after virus bulk-up. Although all SNPs were present after virus bulk-up, as discussed in Chapter 3, only UV_7 can be used as a genetic marker to differentiate between the CrleGV-SA-C5 and the CrleGV-SA isolate. It was previously shown (Chapter 3) that the two approaches, cloning the PCR products followed by sequencing and sequencing PCR products directly, were both able to detect the SNPs. However, sequencing of the PCR products directly would require sequencing in both the forward and reverse direction to mitigate limitations of Sanger sequencing.

A UV-tolerant baculovirus pesticide with longer field persistence may potentially be developed with the existence of a UV-tolerant strain. As a result, the potential of the pathogen against the pest may be enhanced and the cost of UV protectants and the number of applications required may be reduced (Jeyarani et al., 2013). For the commercial production of a virus into a biopesticide, large quantities of the virus need to be obtained, likely requiring multiple passages of the virus through susceptible host larvae (Grzywacz et al., 2003). It is not known if the identified SNPs directly contribute to the isolate being UV-tolerant. The current results indicate that the CrleGV-SA-C5 isolate is genetically stable after two bulk-ups, suggesting that the CrleGV-SA-C5 isolate has the potential to be used on a commercial scale, particularly if these

genetic changes do indeed directly contribute to the UV tolerance measured by Mwanza (2019). However, further analysis would have to be conducted to determine if the CrleGV-SA-C5 isolate will remain stable after bulking the virus up multiple times.

In conclusion, the objectives for the chapter were successfully attained. The CrleGV-SA-C5 was bulked up, genomic DNA was extracted from the virus samples and target regions were PCR amplified. Sanger sequencing confirmed the presence of the target SNPs in the genome of CrleGV-SA-C5_BU2 after bulking up of the virus. The next chapter aims to test the efficiency of the CrleGV-SA-C5 isolate in semi-field trials.

Chapter 5

Comparing the UV-tolerance of the CrleGV-SA-C5 isolate to the CrleGV-SA isolate in detached fruit bioassays

5.1 INTRODUCTION

The UV-tolerant CrleGV-SA-C5, isolated by Mwanza et al. (2022) and Mwanza (2019), has the potential to improve the control of *T. leucotreta*. However, the efficacy of the CrleGV-SA-C5 isolate has not been tested in the field. Therefore, this chapter will focus on comparing the degree of UV-tolerance of the CrleGV-SA-C5 isolate in comparison to the CrleGV-SA isolate by detached fruit bioassays under natural UV irradiation.

The use of CrleGV for the biological control of *T. leucotreta* on agricultural crops was not exploited until 2004 (Moore et al., 2015b). According to Moore et al. (2015b) more than 50 trials have been conducted, since 2000, extensively testing CrleGV in the field. The efficacy of 13 field trials sampled during this time ranged from 30 % to 92 %. Additionally, it was observed that after the application of CrleGV, the efficacy persisted for up to 17 weeks at a level of 70 % mortality (Moore et al., 2015b). However, this was a best case scenario and the persistence of baculoviruses in the field is limited by the natural environmental factors such as heat, plant architecture, UV irradiation, wind, rain, and plant chemistry (Moore & Jukes, 2020). UV irradiation is the most important environmental factor affecting baculovirus persistence (Fuller et al., 2012; Mwanza, 2015; Shapiro et al., 2002). Therefore, it was important to test the UV-tolerance of the CrleGV-SA-C5 isolate under semi-field conditions, in comparison to the CrleGV-SA isolate, for its potential development as a biological control agent for improved management of *T. leucotreta*.

In the development of improved or new biological control options, it is crucial to conduct appropriate bioassays. Field trials and laboratory assays often have disparities between them (Moore et al., 2011a). There are important environmental differences between field and laboratory conditions, with conditions in the field having large variation and often involving factors not typically included in laboratory-based assays, such as rain or UV. Additionally, the biology of the pathogen and the host similarly differ between the laboratory and the field

(Evans, 1999). Field conditions are represented more through detached fruit bioassays in comparison to other laboratory-based assays, exposing treatments to natural variation in the environment as would be experienced during application as a formulated biopesticide. Moore et al. (2011a) stated that the LC₉₀ obtained during detached fruit bioassays, could theoretically be used as a reference for determining the ranges of concentrations that would be used in field trials. Detached fruit bioassays under natural UV irradiation was the method of choice, to determine the UV tolerance of the CrleGV-SA-C5 isolate in comparison to the CrleGV-SA isolate.

In order to measure the effect that control options have on a pest and to ensure optimal timing of treatments, it is important to monitor pest populations in the field (Moore, 2021). Monitoring pest populations is used to also determine if there is adequately low presence in an orchard (Hattingh et al., 2020). Therefore, if the pest population is either too high or too low it could affect the outcome of a field trial, in comparison to using a predetermined level of infestation in a laboratory assay. According to Boardman et al. (2012), neonates can be negatively affected and may die due to unstable environmental conditions, such as humidity and temperature. As a result, to limit the environmental stresses against neonates, detached fruit bioassays can be conducted in a CE room, as was done by van der Merwe et al. (2022). Certain variables, such as virus treatments and the life stage of the pest, need to be controlled in order to obtain laboratory results that represent what may be seen in the field (van der Merwe et al., 2022). The treatment applied should mimic the application used in the field. Additionally, the life stage of the pest targeted in the field should be the same as the life stage used for laboratory assays. Detached fruit bioassays provide for a way of mimicking the natural environmental conditions of a field trial, while providing the benefit of reduced interference from external factors (abiotic and biotic factors), such as farm spray programmes, enabling the level of infestation to be predetermined and controlled, whereas the level of infestation may vary in the field.

However, the disadvantages of conducting a detached fruit bioassay over a field trial are that the fruit are detached and the natural lifecycle of the pest is not represented. According to Newton (1998), in nature the adult will lay the eggs on the fruit, the larvae will hatch and for a protracted period, the larvae will wander on the fruit before penetrating into the fruit. Whereas with detached fruit bioassays the eggs or neonates are placed on the fruit, which does not represent the lifecycle under natural conditions.

Moore et al. (2011a), Fullard & Hill (2013), and van der Merwe et al. (2022) reported conducting detached fruit bioassays in their studies. Moore et al. (2011a) conducted detached fruit bioassays using the CrleGV-SA isolate. van der Merwe et al. (2022) aimed to evaluate the efficacy of CrleGV-SA combined with gut-associated yeasts isolated from *T. leucotreta* larvae by conducting a series of detached fruit bioassays and semi-field trials. Detached fruit bioassays were conducted to test all isolated yeasts in combination with CrleGV-SA, to determine the optimal yeast:virus ratio and to further enhance yeast-virus formulation by the addition of a surfactant and an adjuvant. Fullard & Hill (2013) conducted topical insecticide applications and detached fruit bioassays to screen various new insecticides for their potential negative impacts on *T. leucotreta*'s reproduction.

Therefore, the method chosen for the determination of the efficacy of the CrleGV-SA-C5 isolate was through detached fruit bioassays. A sufficient quantity of the CrleGV-SA-C5 required for detached fruit bioassays was obtained through virus bulk-up, reported in Chapter 4 of the study. An important component of the detached fruit bioassays was to expose the treated oranges to natural UV irradiation by sunlight, while monitoring the weather data during the UV exposure period. Mwanza (2019) and Mwanza et al. (2022) identified that the CrleGV-SA-C5 isolate has significant tolerance to UV irradiation for up to 72 h exposure. According to David et al. (1968), in numerous cases UV irradiation reduces the viral activity within 24-48 h. Therefore, for the purpose of the current study 48 h of UV irradiation from sunlight per hemisphere of the orange was chosen for the time of exposure.

The overall aim of the chapter was to compare the UV tolerance of the CrleGV-SA-C5 and CrleGV-SA isolates under natural UV irradiation via detached fruit bioassays. The specific steps in the study were (i) preparation of oranges and virus treatments, (ii) UV exposure and non-UV exposure set-up with appropriate controls, (iii) monitoring weather conditions, (iv) inoculation of fruit with *T. leucotreta* eggs, (v) evaluating the degree of infestation of oranges post detached fruit bioassay and (vi) statistical analysis of data.

5.2 METHODS

5.2.1 Collection and preparation of oranges and virus treatment preparation

Oranges were collected in the Sundays River Valley, Eastern Cape Province. Oranges were thoroughly washed, to remove any residue or contaminants on the orange, in water with a small amount of dishwashing liquid, followed by a rinse in water, wiped down and left to dry overnight. Three treatments, two of which were the viruses CrleGV-SA-C5 and CrleGV-SA,

and a ddH₂O control were used for the two detached fruit bioassays set-ups, the UV exposure (UV_DFB) and Non-UV exposure control (Non-UV_DFB) detached fruit bioassays (Table 5.1). Each virus treatment was applied at a concentration of 5×10^5 OBs/ml (being the registered concentration for Cryptogran) in a total of 1 litre.

Table 5.1: Treatments applied to oranges for each UV_DFB and Non-UV_DFB set-up to determine the UV tolerance of the CrleGV-SA-C5 isolate in comparison to the CrleGV-SA isolate.

	Treatments	Concentration (OBs/ml)	Number of infected oranges per treatment
UV Exposure	ddH ₂ O Control	—	30
	CrleGV-SA-C5	5×10^5	
	CrleGV-SA		
Non-UV Exposure	ddH ₂ O Control	—	30
	CrleGV-SA-C5	5×10^5	
	CrleGV-SA		

5.2.2 Detached fruit bioassay

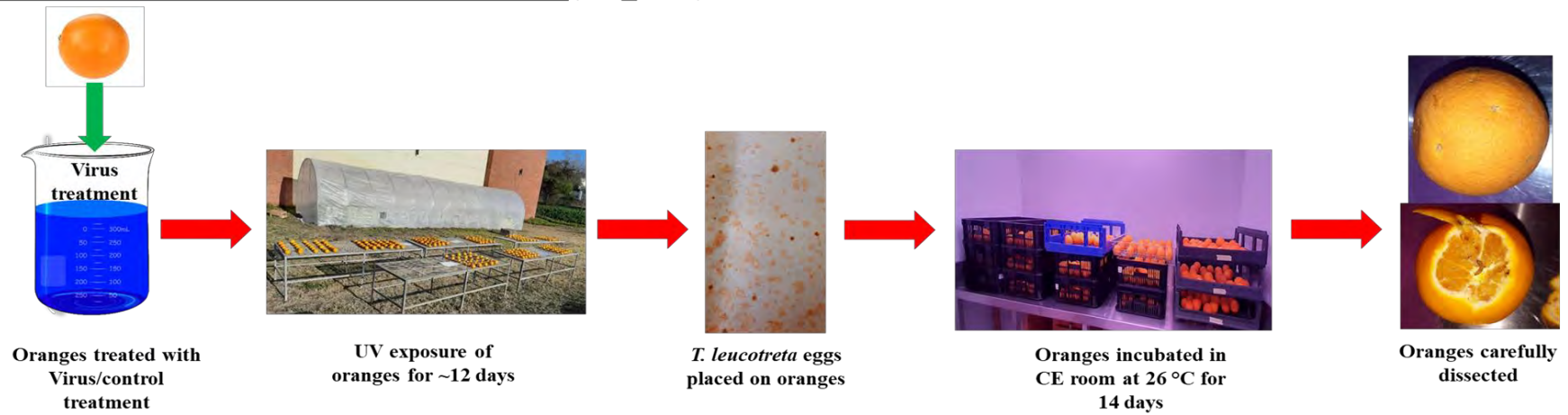
Two detached fruit bioassay set-ups, a UV_DFB and Non-UV_DFB were used (Figure 5.1). The same virus treatment and ddH₂O control were used for each detached fruit bioassay set-up and a total of 30 oranges was used per virus treatment and for the control treatment (Table 5.1). Oranges were dipped into the treatment for full coverage, thereafter treated oranges for the UV_DFB set-up were placed onto galvanized steel tables that were placed outside for natural UV exposure from sunlight. Oranges were exposed to UV for 48 h per hemisphere, equating to oranges being exposed for a total of 96 h and ~8 h exposure per day (total ~12 days), therefore oranges were taken outside in the morning and taken indoors in the late afternoon. Oranges treated for the Non-UV_DFB set-up were placed on galvanized steel tables placed indoors and left for ~12 days with no exposure to sunlight.

Thaumatotibia leucotreta egg sheets were provided by River Bioscience (Pty) Ltd. Ten *T. leucotreta* eggs were placed onto each of the treated oranges from both bioassay set-ups, oranges were placed into crates and incubated in a CE room set to 26 °C for 14 days. Following

incubation, oranges were carefully dissected and inspected for the presence of live *T. leucotreta* larvae (Figure 5.2). The infestation of *T. leucotreta* was identified by the presence of the larva and oranges were considered infested if it contained a larva. Each detached fruit bioassay set-up, UV_DFB and Non-UV_DFB set-up was replicated three times.

Weather data for each day of UV exposure for the UV_DFB was collected from the Rhodes University Geography Department weather station (33°18'00" S, 26°30'00" E) which was approximately 500 m from the study site. GraphPad Prism v 9.3.1 (GraphPad Software, San Diego, California USA) was used to perform all statistical analyses. A Kruskal-Wallis nonparametric test was performed on the data from both UV_DFB and Non-UV_DFB for the average total infested oranges from all three replicates from the virus treatments. A Mann-Whitney test was performed on the data from the control treatments for both the UV_DFB and Non-UV_DFB for the average total infested oranges from all three replicates from the control treatments.

UV Exposure Detached Fruit Bioassay Set-up (UV_DFB)



Non-UV Exposure Detached Fruit Bioassay Set-up (Non-UV_DFB)

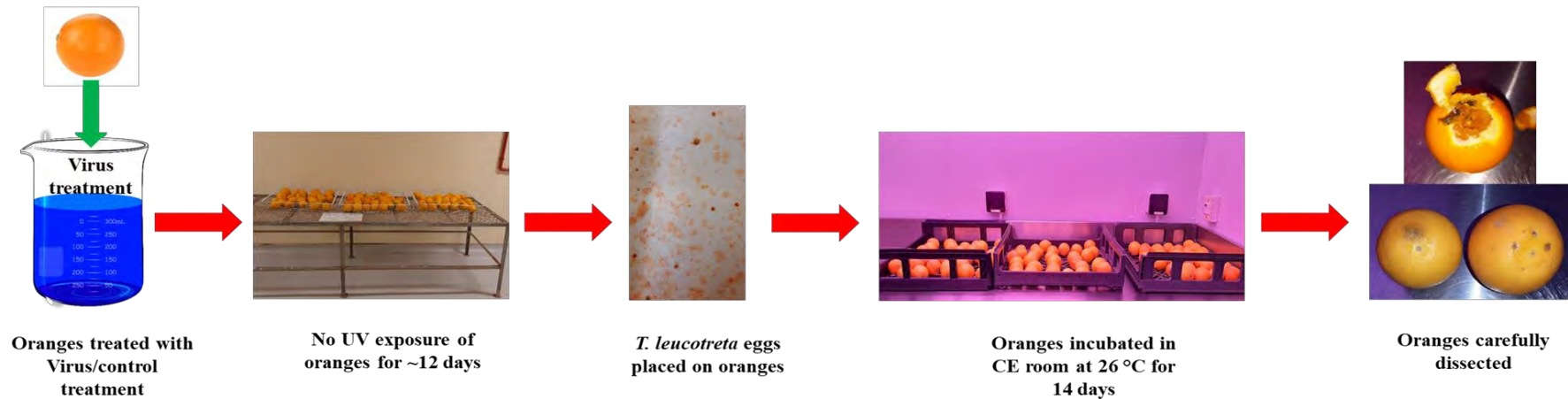


Figure 5.1: A schematic flow diagram of the UV exposure and Non-UV Exposure detached fruit bioassay setup.

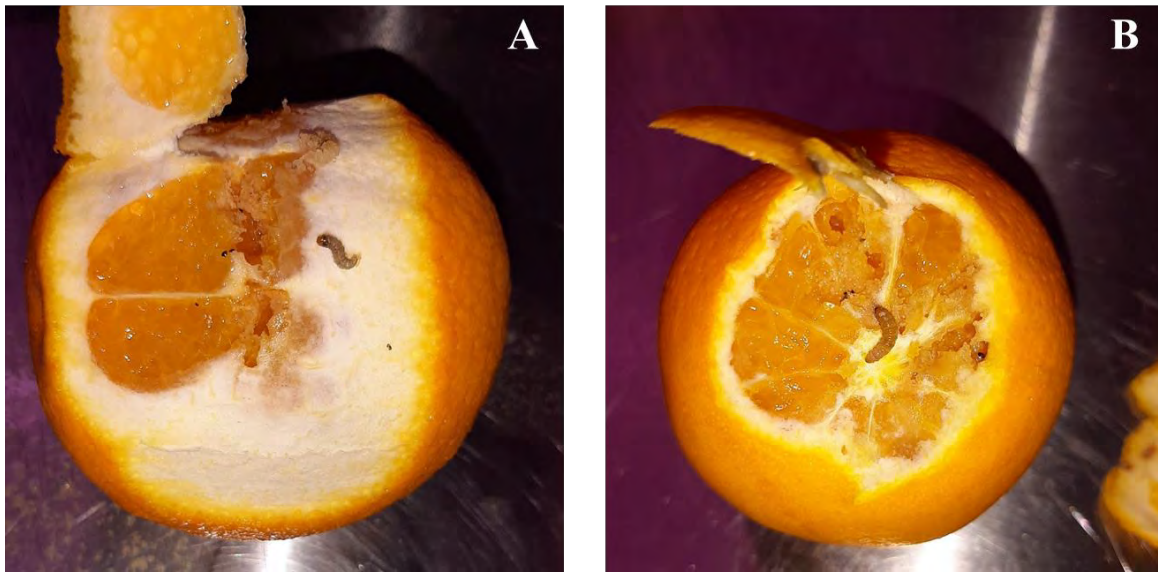


Figure 5.2: Oranges infested with *T. leucotreta* larvae. A: Orange from UV_DFB replicate 2 CrleGV-SA-C5 treatment and B: Non-UV_DFB replicate 3 control treatment.

5.3 RESULTS

5.3.1 Detached fruit bioassay

The weather data for the duration of the UV_DFB for all three replicates was obtained from Rhodes University Geography Department. The temperature, rain and UV Index was recorded for each day. For UV_DFB replicate 1, the highest temperature was 25.5 °C on the 8th day and rainfall was recorded on the 2nd, 3rd, and 4th day of 0.002, 0.030, and 0.009 mm respectively. The highest temperature was 25.8 °C recorded for UV_DFB replicate 2 and UV_DFB replicate 3 (Figure 5.3). Rainfall of 0.006 mm was recorded on the 8th and 7th day for UV_DFB replicate 2 and replicate 3 respectively. The highest UV Index recorded for UV_DFB replicate 1, replicate 2 and replicate 3 was 1.1 recorded on the 10th day, on the 4th day and on the 3rd day respectively (Figure 5.4).

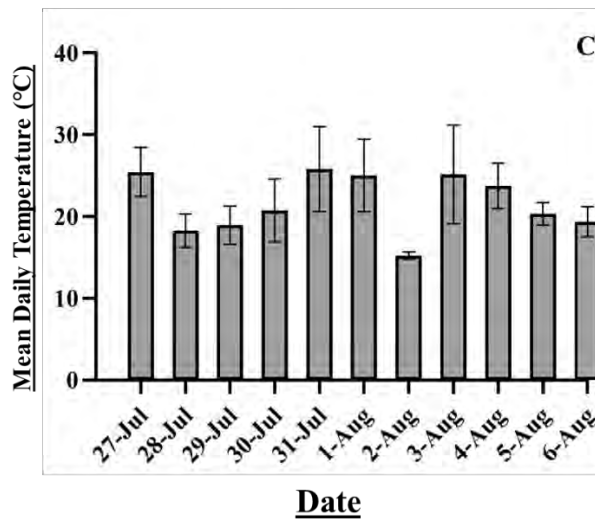
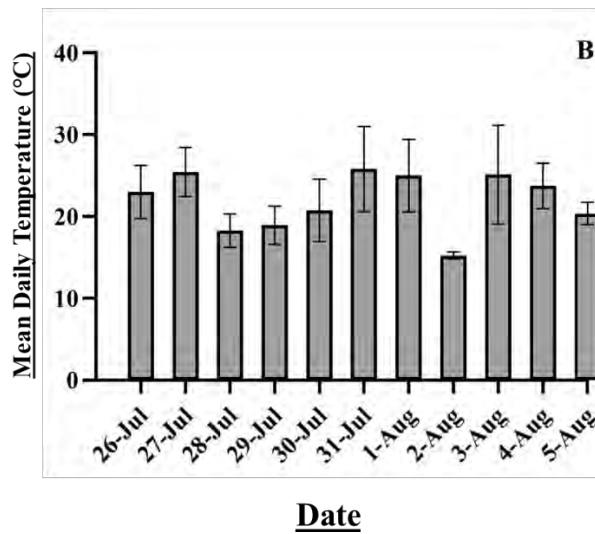
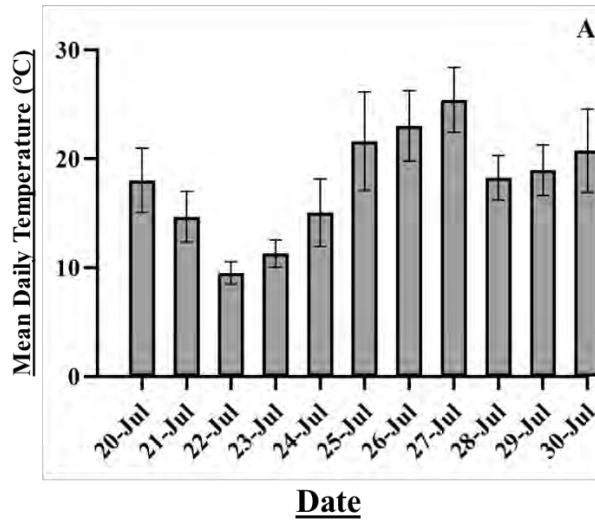


Figure 5.3: Mean (\pm SE) temperature recorded for the UV exposure period per day for each UV exposure detached fruit bioassay replicate set-up. Weather data from A: bioassay replicate 1, B: bioassay replicate 2 and C: bioassay replicate 3.

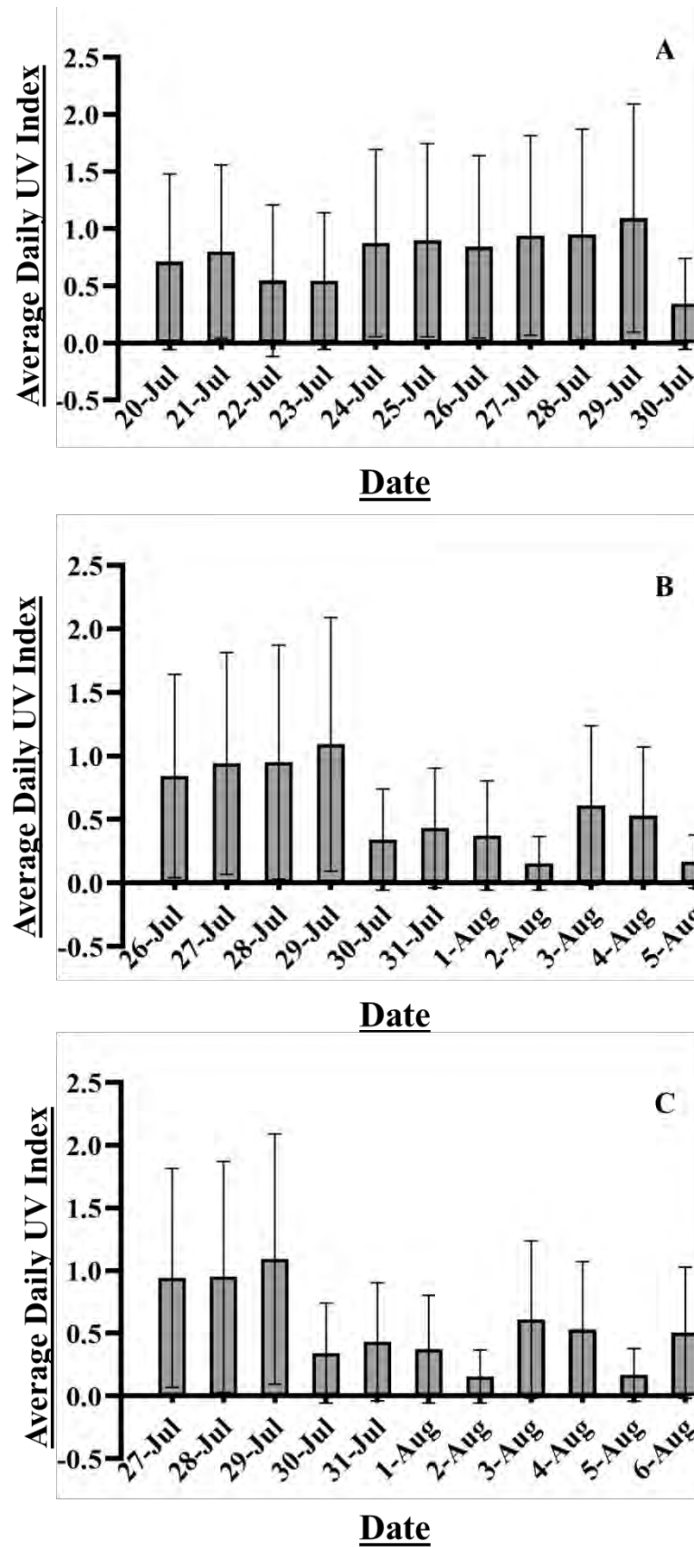


Figure 5.4: Average (\pm SE) UV Index recorded per day for each UV exposure detached fruit bioassay replicate set-up. A: UV Index data from bioassay replicate 1, B: UV Index data from bioassay replicate 2 and C: UV Index data from bioassay replicate 3.

The UV_DFB bioassay was conducted by exposing the treated oranges to UV irradiation from sunlight to determine the efficacy of the CrleGV-SA-C5 isolate when exposed to UV compared to the CrleGV-SA isolate. The Non-UV_DFB bioassay was conducted by not exposing the treated oranges to UV irradiation, this setup was a non-exposure control. There was no significant difference in larval infestation of fruit between CrleGV-SA-C5 and CrleGV-SA for the UV_DFB ($p = 0.9036$). For the Non-UV_DFB there was also no significant difference in infestation between CrleGV-SA-C5 and CrleGV-SA treated fruit ($p > 0.9999$) (Figure 5.5).

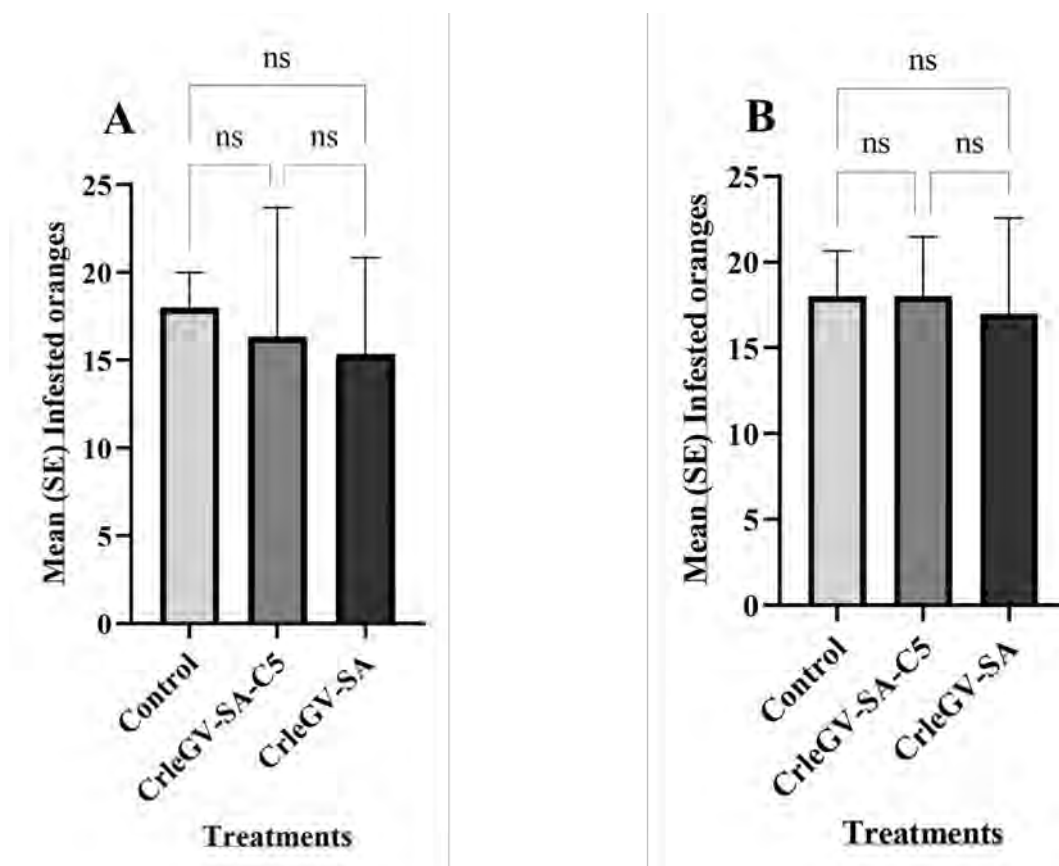


Figure 5.5: Analysis of the infested oranges from all three bioassay replicates from both UV_DFB and Non-UV_DFB. The oranges that were not infested by *T. leucotreta* larvae from both UV_DFB and Non-UV_DFB were also recorded (data not shown). There was no significant difference between the UV_DFB and Non-UV_DFB Control treatments ($p > 0.9999$)

5.4 DISCUSSION

The aim of the chapter was to evaluate the UV tolerance of the CrleGV-SA-C5 isolate in comparison to the CrleGV-SA isolate under natural UV irradiation via detached fruit bioassays.

To achieve the aim, oranges were firstly prepared and treated by dipping into the either of the virus treatments or the ddH₂O control. Two detached fruit bioassays were set up, including a UV exposure bioassay, where treated oranges were subjected to natural UV irradiation from sunlight and a Non-UV exposure bioassay, where treated oranges were not subjected to UV irradiation.

The outcome was not as anticipated, as statistical analysis indicated that there was no significant difference between the virus treatments in both UV_DFB and Non-UV_DFB. The lack of difference between treatments in UV_DFB could theoretically be as a result of UV irradiation, rainfall, virus OBs not attaching to the oranges or low virus concentration and therefore warrant investigation.

One of the major drawbacks affecting the persistence of baculoviruses in the field is UV irradiation. UV irradiation inactivates baculoviruses, resulting in short residual activity (Cory & Evans, 2007; Shapiro, 1995). DNA molecules actively adsorb UV light and as a result induce pyrimidine dimer formation in DNA chains (Yoon et al., 2000). Gendall (2005) demonstrated that Cryptogran, a commercial CrleGV formulation, is affected by UV. A field trial showed that on fruit on the northern side of citrus trees, Cryptogran broke down to 50 % of its original activity within 5 days (Moore et al., 2001). When OBs are still wet they are more susceptible to UV inactivation as a result of UV being able to refract onto the OB, which is located in the droplet (Grzywacz & Moore, 2017). After dipping the oranges in the relevant treatments, the oranges were not completely dry when placed outside for UV exposure or when placed indoors to be subjected to no UV exposure. As a result, the poor efficacy of the virus treatments in UV_DFB could have been due to UV possibly refracting onto the OBs in the droplet on the orange rind making the OBs more susceptible to UV inactivation. UV irradiation may have inactivated the virus OBs when the treated oranges were subjected to UV exposure, contributing to the CrleGV-SA-C5 and CrleGV-SA isolates' poor efficacy in the UV_DFB. However, given the lack of a significant difference between the UV and Non-UV treatments and their controls, UV irradiation may not have affected the efficacy of the virus.

For each bioassay replicate in the UV_DFB, during the period of UV exposure, as observed from the weather data, there was at least one day where rainfall was recorded. It was emphasised by Evans (1994) that products need to be tested under laboratory and under field conditions. Despite there being rain during the period of UV exposure, oranges were still left outside to expose them to the most natural environmental conditions as possible. It is therefore

necessary to explore the possibility that rain could have washed the virus off the oranges and therefore be a possible contributing factor to the outcome in results. However, Kirkman (2007) conducted laboratory bioassays to determine the degree of rainfastness of Cryptogran. The study found that rainfall did not have any detrimental effect on the virus efficacy. It was stated that if Cryptogran was able to control FCM after the exposure of rainfall applied at a very high intensity, then for practical purposes it was deemed rainfast. It was also suggested that rain did not easily wash deposits of *Trichoplusia ni* NPV from foliage (Jacques, 1972). Therefore, given the fact that Kirkman (2007) showed that Cryptogran has a high degree of rainfastness and the detached fruit bioassay results in the current study showed that there was no difference between the UV_DFB and Non-UV_DFB, rain is not likely to have been a contributing factor affecting the outcome of the results.

According to Silva & Moscardi (2002), biological products used during the 1993/94 soybean season were reported to have low quality and efficacy, which could have been in relation to various factors affecting the efficacy and stability under field conditions. Some of the factors include: relative humidity and precipitation (Jacques, 1977), solar radiation (Silva, 1987), temperature (Ignoffo, 1985), age and population intensity of the host insects (Silva, 1987), pH of the aqueous viral suspension in the spray tanks (Batista, 1997) and viral formulation, equipment and application technology (Silva, 1986). Therefore, the low efficacy of the virus treatment in both Non-UV_DFB and UV_DFB could have been due to complications in the preparation of the virus treatments or the application of the treatments. Possibilities include: the pH of the ddH₂O used in the virus preparation (could have been either too high or too low), the OBs may not have adhered to the surface of the oranges, the concentration of the virus applied was too low, or there could have been a contaminant on the surface of the oranges as a result of the oranges not being properly cleaned prior to being treated.

Gotoh et al. (2008) examined the inactivation of baculoviruses under various conditions by ELVA (envelope-labelled virus assay). The ELVA method was used to examine the effect pH had on the inactivation of baculoviruses. They found that the virus titre significantly decreased by the pH being altered from neutral to a higher or lower pH. Additionally, Silva & Moscardi (2002) evaluated the parameters affecting the field efficacy of AgMNPV, including the pH of the viral aqueous suspension, application time and the mixture of mineral oil with the virus, to name a few. They found that the pH of the aqueous spray suspension significantly affected the efficacy of AgMNPV. Soybean plots treated with AgMNPV viral suspension at pH 2 and 10 had a significantly lower number of infected or dead larvae compared to plots treated at pH 6

which had significantly higher number of infected or dead larvae. A pH of about 6.4 is optimal for the storage of baculoviruses (Gotoh et al., 2008). The pH of the water could be a drawback, subsequent evaluation of the pH of the water (pH 7.63) was within the given range, therefore, it is likely not to have affected the results. However, this issue cannot be fully resolved, because the pH of the solutions used in the study was not tested. Therefore, the pH of the water used in the current study could have either been too high or low, and as a result inactivating the virus.

The concentration of the virus used in the current study could have been too low, therefore resulting in the lack of significant efficacy. Studies by van der Merwe (2021) and Moore et al. (2011a) conducted detached fruit bioassays using CrleGV-SA respectively. Detached fruit bioassays conducted by van der Merwe (2021) had CrleGV-SA included in treatments at a LC_{50} concentration of 9.31×10^7 OBs/ml and those conducted by Moore et al. (2011) had five CrleGV-SA concentrations prepared as a series of two-fold dilutions, with the concentration of the stock suspension of the virus being 5.4×10^{11} OBs/ml. In comparison to the current study, the virus concentrations used by van der Merwe (2021) and Moore et al. (2011) were higher. The concentration of the treatments used in the current study was the concentration registered for Cryptogran. A 70 % reduction in *T. leucotreta* infestation over a 17-week period was recorded in a semi-commercial block trial conducted using Cryptogran to combat pre-harvest fruit loss. A similar level of infestation was expected in the current study.

Another possibility is that the virus OBs may not have adhered to the oranges, thus contributing to the poor results recorded. It was shown that the efficacy of Cryptogran is enhanced and improved by the addition of molasses (Moore et al., 2004). Molasses acts as a feeding attractant for *T. leucotreta* larvae and improves virus adhesion, thus improving the efficacy of the biopesticide (Kirkman, 2007a). It was also shown that the medial lethal exposure time (LET_{50}) for neonate codling moth, *Cydia pomonella*, larvae was dramatically decreased by the incorporation of 15 % cane molasses in a formulation of purified CpGV and it was also found that the damage caused by codling moth in field trials, where molasses was added to the virus, was reduced (Ballard et al., 2000). Additionally, it has been shown that the efficacy of the virus may be significantly improved with the addition of surfactants and adjuvants into the CrleGV-SA formulations, such as BREAK-THRU® S 240 (250 g/L Polyether, 750 g/L Polyether modified trisiloxane) (Evonik Industries AG, Germany) (Moore et al., 2015b). Cryptogran is registered to be applied with molasses and an adjuvant. Neither were used in this study and consequently their addition in future trials may improve the outcome.

In summary, the results were not significant and consequently, we were not able to reach a conclusion on the UV-tolerance of the virus in a semi-field detached fruit setup. There was no difference between the treatments used in both UV_DFB and Non-UV_DFB. It is recognised that further detached fruit bioassays and field trials are required, but with improved protocols in order to conclusively determine the efficacy and UV-tolerance of the CrleGV-SA-C5 isolate. The results from this study will be discussed further in the next chapter.

Chapter 6

General Discussion

6.1 Thesis Overview

A UV-tolerant *Cryptophlebia leucotreta* granulovirus isolate was isolated after successive cycles of exposing the CrleGV-SA virus to UV (Mwanza, 2019; Mwanza et al., 2022). The current study aimed to investigate the biological and genetic stability of the UV-tolerant CrleGV-SA-C5 isolate, which has the potential to improve the control of *T. leucotreta*. A *de novo* assembly alignment was conducted for the reassembly of the CrleGV-SA-C5 genome, followed by a sequence comparison with the CrleGV-SA genome for the identification of any SNPs (Chapter 2). Following the identification of SNPs, oligonucleotides were designed, flanking the SNPs that were in close proximity to each other. Genomic DNA extraction from purified CrleGV-SA-C5 and CrleGV-SA OBs was extracted and PCR amplification of the target regions was conducted (Chapter 2). Two methods were conducted for the screening of the presence of SNPs (Chapter 3). For the first screening method, six plasmids were constructed, followed by sequencing to confirm the presence of SNPs originally detected in regions of the CrleGV-SA-C5 genome. Quantitative polymerase chain reaction melt curve analysis was the second screening method conducted. Following the screening for the presence of SNPs, CrleGV-SA-C5 virus bulk-up was conducted and prior to the bulking up, the LC₉₀ and LC₅₀ for CrleGV-SA-C5 against fourth instar *T. leucotreta* was evaluated. Once the LC₉₀ concentration was determined, it was used to conduct virus bulk-up using fourth instar *T. leucotreta* as hosts (Chapter 4). Following virus bulk-up, the genome of the CrleGV-SA-C5_BU2 virus was analysed for the presence of the identified SNPs. Lastly, the bulked up CrleGV-SA-C5 virus was used to conduct detached fruit bioassays under natural UV irradiation to determine the degree of UV tolerance of the CrleGV-SA-C5 isolate in comparison to the CrleGV-SA isolate.

6.2 CrleGV-SA-C5 Genomic Analysis and SNP Screening

Seven SNPs were identified following *de novo* assembly and sequence comparison. Out of the 7 SNPs, two were unique to this study and four were previously reported by Mwanza et al. (2022). The seventh SNP was detected by van der Merwe et al. (2017). As previously stated, the identified SNPs could have been introduced as a result of the UV irradiation, as UV light

contributes to damage in virus genomes and also damage to structural proteins (Akhanaev et al., 2017). Alternatively, the identified SNPs may have arisen as a result of UV exposure selecting a different genotype of the same virus. A typical feature of numerous natural baculovirus isolates are genotype mixtures and genetic diversity, representing a population of various genotypes (Fan et al., 2020). Natural baculovirus isolates are usually composed of heterogeneous or homogeneous populations of genotypes (Fan et al., 2020). In a population, a new mutation has a low chance of reaching high frequency, as it may be eliminated through stochastic evolutionary events (Masel, 2011). Beneficial mutations within a genome conferring high fitness should be favoured by natural selection. Therefore, in a given population best-adapted genomes will remain at high frequency. The UV irradiation could have selected for different genotypes that are better adapted to UV exposure. The CrleGV-SA genome sequence was generated a few years prior to the isolation of the CrleGV-SA-C5 isolate and as a result, mutations could have emerged within the CrleGV-SA genome after the generation of the published CrleGV-SA genome but at low frequencies. The identified SNPs could have been at a low frequency in the CrleGV-SA genome and when the virus was subjected to UV irradiation by Mwanza (2019) and Mwanza et al. (2022), the frequency of these SNPs increased, as the genotypes containing the identified SNPs may be more adapted to UV exposure.

Intra species variation analysis by mapping and reassembly of Illumina reads to the complete CpGV-SA genome sequence revealed that the wild type CpGV-SA isolate is composed of a mixture of genotypes. The study by Motsoeneng et al. (2019) reported on the genome analysis of a novel CpGV isolate. Single nucleotide polymorphism comparison of the novel CpGV isolate with five previously sequenced CpGV isolates, revealed 67 unique events. It was found that the CpGV-SA isolate consisted of a mixture of genotypes, after conducting single nucleotide variation analysis. The study concluded that the CpGV-SA isolate is a genetically distinct unique isolate, which is likely a representative of a new genogroup (Motsoeneng et al., 2019). Using the consensus sequences to determine SNP specificities can however be considered a bottleneck because there is risk of a decrease in the intraspecific variation at the first step, when a consensus sequence is generated. The presence of intraspecific variation by ambiguous nucleotides can be determined by a consensus, however, the ratio of the nucleotides present at these positions stay hidden. Tools for SNP quantification and identification are very helpful to properly characterise and analyse complex genotype mixtures. Minor mutations and submolar genotypes are frequently ignored in sequence data assembly as only the most frequent nucleotides are represented by consensus sequences (Day & McMorris, 1992). The published

CrleGV-SA genome was a single consensus sequence, generated from tens of thousands of sequence reads (van der Merwe et al., 2017). The identified SNPs could have been a minor mutation or part of a submolar genotype of the published CrleGV-SA genome, which could have been ignored when the consensus sequence was generated and may have been a more frequent nucleotide in the CrleGV-SA-C5 genome. The NGS data set from the current study had just over a million reads before analysis, with the analysis conducted on the NGS data, involving a sequence alignment against the published CrleGV-SA genome and identification of SNPs. Therefore, the SNPs detected in the current study are possibly due to a selection of a different genotypic variation.

The remapping of short-read sequencing data against their consensus sequence for the evaluation of intraspecific genetic variation within the sequenced baculovirus population (Harrison et al., 2017) or the alignment of consensus sequences, generated previously from the same data (Wennmann et al., 2017), are used in the majority of cases to determine SNP position. The detection of intraspecific variation within sequenced baculovirus samples, is enabled by the well-established method of mapping reads against their own consensus sequence. The combination of both methods, SNP specificity determination by alignments of consensus sequences and using the specific positions in order to quantify the presence of a specific isolate (Gueli et al., 2017) or comparing SNP patterns using a single consensus sequence to draw conclusions about the similarity and relatedness of sequenced isolates (Larem et al., 2019), are the most current approaches used. The SNPs detected in the current study are possibly due to a different portion of the data being analysed, due to limited computational power, in comparison to the portion of data analysed by Mwanza (2019) indicating the need for additional analysis of the genetic variability within the CrleGV-SA-C5 genome. The study by Wennmann et al. (2020) focused on determining an analysis method for firstly avoiding the determination of a consensus sequence available from data and secondly enabling the determination of unknown and previously known detection. The study reported how isolate or specimen-specific SNPs positions can be detected using a consensus sequence free method and how these may be used for identifying isolates' genotypic composition. The method used in the study enables SNP specificity determination across several sequenced isolates. The method allows for intraspecific genetic variability of a single baculovirus isolate to be determined as well as supports the hypothesis that genotypes of equal frequency are represented by SNP positions with similar frequencies and as a result can be used for the characterisation and determination of the homogeneity and heterogeneity of isolates (Chateigner et al., 2015).

It was further determined in Chapter 3, that out of the five SNPs used to distinguish between the CrleGV-SA-C5 and CrleGV-SA isolates only one, UV_7, rendered a good marker. After plasmid construction and sequencing, the CrleGV-SA Pif-2, HypoP and Lef-8/HP sequence data was compared to the CrleGV-SA-C5 Pif-2, HypoP and Lef-8/HP sequences. It was found that the SNPs UV_2, UV_3, and UV_5 were present in both the CrleGV-SA and CrleGV-SA-C5 sequences, in comparison to when the SNPs were initially identified, they were not present in the reference CrleGV-SA genome (Chapter 2). As a result, these are not suitable markers for the differentiation of CrleGV-SA-C5 isolate from wild-type virus. These SNPs are still valuable, however, not all are suitable for differentiation of isolates. López-Ferber et al. (2003) highlighted that the pathogenicity of a viral population is increased by the mutualistic interactions between genotypes of an insect baculovirus. Phenotype of increased pathogenicity is a result of a combination of a deletion mutant unable to be transmitted orally and a complete genotype able to be transmitted orally. Mixed genotype infections are more infectious than single genotype infections (López-Ferber et al., 2003). Distinct SNPs of specific genome groups may be used as genetic markers for the genotype of new isolates to be quantified (Fan et al. 2020). The genetic variability within a large DNA virus population would need to be examined in order to explore the potential breadth of viral diversity (Chateigner et al., 2015). For virus adaptation, viruses depend on large population size and widespread genetic variation. The study by Chateigner et al. (2015) deep sequenced a natural strain of AcMNPV to determine the genetic variation in the dsDNA virus population and established a technique for the delimitation of large deletions present in next generation sequencing data. The study detected low frequency mutations (0.025 %) within the 124221× average genome coverage of the 133926 bp long consensus, and 60 high frequency non-synonymous mutations under balancing selection were found distributed in the functional classes. Altogether, a wide breadth of genomic variation in the baculovirus population was established, indicating a high adaptive potential (Chateigner et al., 2015).

6.3 CrleGV-SA-C5 Virus Propagation and UV tolerance comparison

6.3.1 Propagation of CrleGV-SA-C5 in *T. leucotreta* larvae and genome analysis

A wide variety of crops have been protected globally against various lepidopteran pests with the use of commercial products successfully formulated with several dozen species of

baculoviruses (Moore & Jukes, 2020). The application of CrleGV is used commercially over thousands of hectares every year (Moore et al., 2015b). One of the major drawbacks with using baculoviruses as biopesticides is UV degradation, which affects the persistence of viruses in the field (Moore & Jukes, 2020). Here, the CrleGV-SA-C5 virus was bulked up by conducting two virus bulk-ups through *T. leucotreta* larvae, after which genome analysis of the CrleGV-SA-C5_BU2 virus results confirmed the presence of the target SNPs in the genome, including UV_7 as a potential marker, indicating the genetic stability after two bulk-ups. The stability of the SNPs provides the potential for larger scale production of the virus. Baculoviruses are produced either in isolated insect cell culture lines (*in vitro*) or in whole insects (*in vivo*) (Grzywacz et al., 2003). However, the industrial production of NPV is currently only done *in vivo* for use as biopesticides, by rearing, infecting, and harvesting whole insects. The production of *Helicoverpa armigera* NPV (HearNPV) is conducted on artificial diet in production trays inoculated with OBs on which third instar *H. armigera* larvae feed. A 1×10^5 fold return on the inoculum used is a possible gain when using this virus production method. About 500 larvae are placed into each production tray, with 1×10^8 OBs of inoculum used and the dose rate applied at 2×10^5 OBs/larva. The production stages of HearNPV include: production tray preparation, inoculation of production trays and loading larvae, harvesting the larvae that are infected and processing of infected larvae (Grzywacz et al., 2003). This study used a similar method of production to the described for HearNPV.

6.3.2 Comparing the UV-tolerance of the CrleGV-SA-C5 isolate

The UV tolerance of the CrleGV-SA-C5 isolate was tested by detached fruit bioassay, following the bulk-up of the virus. As described in Chapter 5, statistical analysis indicated that there was no significant difference between the virus treatments within the detached fruit bioassay set-ups. The lack of difference was not due to UV exposure or weather conditions but rather as a result of external linked to the methodology. There are a range of potential reasons for lack of meaningful results in the bioassays. These should be determined and resolved, by adjusting the bioassay protocol, before being repeated.

The application of crude virus preparations can improve the baculovirus persistence (Burgess & Jones, 1998). The persistence of baculoviruses can also be improved by the application of virus at higher rates or more frequent virus application (Grzywacz & Moore, 2017; Moore et al., 2015b) and early morning or late afternoon application of the virus (Kirkman, 2007). For commercial products, it is recommended to have operational CpGV dosages of 10^{13} - 10^{14} OBs/ha. During detached fruit bioassays using CrleGV-SA, an LC_{50} of 9.31×10^7 OBs/ml and

an LC₉₀ of 1.515×10^9 OBs/ml were established (Moore et al., 2011). Therefore, in future detached fruit bioassays conducted to determine the UV tolerance of the CrleGV-SA-C5 isolate, the concentration of the virus applied (5×10^5 OBs/ml) should be increased. Additionally, Cryptogran is recommended to be used at a concentration of 5×10^6 OBs/ml for citrus and avocados (Moore et al., 2004). The commercial CrleGV products are applied at 5×10^{13} OBs/ha for Cryptogran and 6.6×10^{12} OBs/ha for Cryptex and Gratham (Moore et al., 2004). Therefore, an increase in the concentration of CrleGV-SA-C5 is recommended for future field trials, requiring the production of more virus for preparation of treatments at higher concentrations.

In contrast to the detached fruit bioassay described in the current study, the detached fruit bioassay described by van der Merwe et al. (2022) indicated that the specific treatment was sprayed onto the oranges until thoroughly covered and once the oranges were dry, five *T. leucotreta* neonates were added to each fruit. van der Merwe et al. (2022) demonstrated that the efficacy of CrleGV-SA seemed to be enhanced by the addition of yeast. The overall best-performing yeast species isolated from the gut of *T. leucotreta* larvae, were determined by neonate behaviour (fruit penetration) in detached fruit bioassays and used to conduct semi-field trials. The treatments used for the detached fruit bioassays conducted by van der Merwe et al. (2022), included ddH₂O alone, CrleGV-SA alone, CrleGV-SA combined with *Pichia kudriavzevii* and CrleGV-SA, *P. kudriavzevii*, and *Saccharomyces cerevisiae* combined with molasses and the adjuvant, BREAK-THRU[®] S 240 (250 g/L Polyether, 750 g/L Polyether modified trisiloxane). The efficiency of *P. kudriavzevii*, and *S. cerevisiae* formulations were significantly enhanced with the addition of molasses and BREAK-THRU[®] S 240 compared to CrleGV-SA (van der Merwe et al., 2022). Kirkman (2007) conducted bioassays to determine the rainfastness of Cryptogran. Treatments included: a Cryptogran and molasses treatment, a distilled water treatment and a treatment with a combination of Cryptogran, molasses and simulated rainfall. Fruit were dipped into treatments and allowed to dry, followed by simulating the effect of rainfall by placing the fruit under a shower and then allowed to dry. Three neonate *T. leucotreta* larvae were placed onto each fruit and incubated for two weeks. The study found that the virus efficacy was not affected by rainfall (Kirkman, 2007). The detached fruit bioassay methodology described by Moore et al. (2011) included the addition of an adjuvant containing spreading agents, pH indicator, wetting agents, acidifier, and penetrating agents, to all virus dilutions for the spreading of the virus particles on the fruit, onto which two neonate larvae were placed. In comparison, no additional agents were added to the treatments in this current

study, as described in Chapter 5. The addition of adjuvants, surfactants, spreading agents, wetting agents and feeding attractants or stimulants could improve the efficacy of the CrleGV-SA-C5 virus and improve results in such bioassays.

The survival of the virus in the field is largely limited by UV radiation from sunlight (Cory & Evans, 2007). Akhanaev et al. (2017) aimed to compare the UV tolerance of two strains of *Lymantria dispar* multiple nucleopolyhedrovirus (LdMNPV) isolated in spatially different regions (LdMNPV-27/0 and LdMNPV-45/0) to the effects of UV sunlight radiation. Different durations of exposure, 0.25, 0.5, 1 and 2 h, of the virus on the surface of a leaf to direct sunlight were used to measure the level of tolerance of the virus strains to sunlight UV. Comparison of equal effects (i.e., virus-induced mortality) and equal doses, were the two comparison methods used for the applied virus. Virus treatments were dropped onto the leaves and left for the solvent to evaporate. Thereafter leaves were exposed to sunlight, followed by cutting small leaf discs that were individually given to fourth instars. The study found significantly different tolerances to UV sunlight exposure between the two strains. The study also conducted a comparison between the main structural protein sequences of the two strains. It was found that the loss of the virus enhancing factor-1 (*vef-1*) gene in the LdMNPV-27/0 strain, was the most prominent difference between the strains (Akhanaev et al., 2017). Additionally, viruses can potentially desiccate. The lipid bilayer envelopes of baculovirus virions make viruses more susceptible to loss of viability and desiccation outside the host (Cox, 1989). The tolerance of *Baculovirus penaei* virus to various environmental parameters such as desiccation was investigated by (LeBlanc & Overstreet, 1991). The study found that the viral suspension was completely inactivated after 48 h of desiccation. However, this is a shrimp virus, rather than a baculovirus of an insect.

6.4 Conclusion and Future Work

In conclusion, the overall aim of this study was to determine the biological and genetic stability of the UV-tolerant CrleGV-SA-C5 isolate, which can potentially improve *T. leucotreta* control. Variations were successfully identified between the CrleGV-SA-C5 and CrleGV-SA isolates. Six amplicons were PCR amplified, targeting three regions of the CrleGV-SA-C5 genome which encompass five SNPs. The construction of six recombinant plasmids were successful and the presence of the SNPs originally detected in the regions of the CrleGV-SA-C5 genome were confirmed by Sanger sequencing, with one suitable marker identified. Surface dose response bioassays and virus bulk-up were conducted, and the presence of the target SNPs in

the genome of the CrleGV-SA-C5_BU2 virus was confirmed by Sanger sequencing. This led to testing the UV tolerance of the CrleGV-SA-C5 isolate by detached fruit bioassays. Results confirmed that there was no significant difference in the treatments in both the Non-UV_DFB and UV_DFB. Future research into the UV tolerance of the CrleGV-SA-C5 isolate is required for the development of this isolate into a biopesticide formulation for the control of *T. leucotreta*.

The ultimate objective of the study was to evaluate the CrleGV-SA-C5 isolate, which could be incorporated into novel formulations of CrleGV-SA for improved field efficacy and enhanced control of *T. leucotreta* in IPM programmes. According to Moore (2002a), extensive field trials need to be conducted to assess a control agent's efficacy and persistence against the abiotic and biotic factors encountered in the field, prior to the potential incorporation into IPM programmes. Therefore, future research projects could conduct extensive field trials testing the UV-tolerance of the CrleGV-SA-C5 isolate, with the possibility of incorporating the isolate into the *T. leucotreta* IPM programme. A repeat of the detached fruit bioassay with adaptations to the current methodology, such as the addition of surfactants and adjuvants such as BREAK-THRU[®] S 240 and molasses, the testing of pH for all prepared solutions, and an increase in the virus concentrations used, should be considered. Additionally, conducting a preliminary assay with the CrleGV-SA at varied UV exposure times should also be considered prior to the detached fruit bioassays, to determine the UV exposure time required to degrade the treatment from 90 % to 50 % mortality.

Massive parallel sequencing techniques are the most generally applied methods established for the fragmentation of genomic DNA, the selection of fragment size, PCR amplification followed by large scale sequencing, and as a result millions of short sequenced reads are generated (Wennmann et al., 2020). In studying genotypic composition, the position and number of SNPs from data obtained by sequencing are generally used as suitable markers (Wennmann et al., 2020). Therefore, future studies can investigate intraspecific genetic variability in the CrleGV-SA-C5 isolate with the identification of other possible SNPs present within the genome that can be used as suitable markers to differentiate it from other isolates such as CrleGV-SA, as having only one suitable marker is not adequate. Additionally, the role of the identified SNPs in baculovirus tolerance to UV should be investigated in future studies.

Desiccation of the CrleGV-SA-C5 virus before inoculating the oranges with *T. leucotreta* eggs during the detached fruit bioassay may have affected the efficacy of the virus. Future research

could potentially assess the effect of desiccation by adding a potential control setup for the detached fruit bioassays. Potential methodology could include the dipping of oranges into the virus treatments and add larvae to fruit immediately after fruit have dried, to ensure the treatments are working.

Commercial baculovirus insecticides such as Cryptogran with CrleGV-SA and Madex with CpGV-M are only formulated with a single isolate. As a result of the registration requirements and/or the production guidelines, the specific genotypes that these insecticides are comprised of remain consistent. Mixtures of isolates, distinct virus species or genotypes have been shown by several studies to result in interactions giving rise to improved activity (Carballo et al., 2017; Jukes et al., 2017). Future research could potentially assess and compare the effects of the UV-tolerance of a mixture of CrleGV-SA-C5 and CrleGV-SA viruses with the UV-tolerance of each virus alone.

REFERENCES

- Abulkadir, F. (2014). Genetic and biological characterisation of a novel South African *Plutella xylostella* granulovirus (PlxyGV) isolate. Master's Thesis, Rhodes University.
- Ackermann, H.W., & Smirnoff, W.A. (1983). A morphological investigation of 23 baculoviruses. *Journal of Invertebrate Pathology*, 41(3), 269–280.
- Aguirre, E., Beperet, I., Williams, T., & Caballero, P. (2019). Genetic variability of *chrysodeixis includens* nucleopolyhedrovirus (ChinNPV) and the insecticidal characteristics of selected genotypic variants. *Viruses*, 11(7). <https://doi.org/10.3390/v11070581>.
- Akhanaev, Y.B., Belousova, I.A., Ershov, N.I., Nakai, M., Martemyanov, V.V., & Glupov, V.V. (2017). Comparison of tolerance to sunlight between spatially distant and genetically different strains of *Lymantria dispar* nucleopolyhedrovirus. *PLoS ONE*, 12(12), 1–13. <https://doi.org/10.1371/journal.pone.0189992>.
- Altschul, S., & Pop, M. (2017). Sequence Alignment. In: Rosen, K., Shier, D., & Goddard, W. (2nd Eds.), *Handbook of Discrete and Combinatorial Mathematics*. Boca Raton (FL): CRC Press/Taylor & Francis.
- Angélini, A., Amargier, A., Vandamme, P., & Duthoit, J.L. (1965). A granular virosis in the lepidopteran *Argyroplote leucotreta*. *Cotton and Tropical Fibers*, 20(2), 277–282.
- Asano, S. (2005). Ultraviolet protection of a granulovirus product using iron oxide. *Applied Entomology and Zoology*, 40(2), 359–364.
- Ballard, J., Ellis, D. J., & Payne, C. C. (2000). The Role of Formulation Additives in Increasing the Potency of *Cydia Pomonella* Granulovirus for Codling Moth Larvae, in Laboratory and Field Experiments. *Biocontrol Science and Technology*, 10, 627–640.
- Barnes, B.N., Hofmeyr, J.H., Groenewald, S., Conlong, D.E., & Wohlfarter, M. (2015). The sterile insect technique in agricultural crops in South Africa: a metamorphosis... but will it fly?. *African Entomology*, 23(1), 1–18.
- Batista, T.F.C. (1997). Fatores que limitam a eficiência de Baculovirus anticarsia sobre *Anticarsia gemmatalis* Hübner, 1818. *Tese de Mestrado, FAEM/UFPEL, Pelotas, 68p.*

- Beas-Catena, A., Sánchez-Mirón, A., García-Camacho, F., Contreras-Gómez, A., & Molina-Grima, E. (2014). Baculovirus biopesticides: An overview. *Journal of Animal and Plant Sciences*, 24(2), 362–373.
- Bedford, E.C.G., van den Berg, M.A., & de Villiers, E.A. (1998). *Citrus Pests in the Republic of South Africa* (2nd Ed.). Nelspruit, and Outspan, Hennopsmeer, South Africa: Institute for Tropical and Subtropical Crops.
- Behjati, S., & Tarpey, P.S. (2013). What is next generation sequencing? *Archives of Disease in Childhood: Education and Practice Edition*, 98(6), 236–238. <https://doi.org/10.1136/archdischild-2013-304340>.
- Behle, R., & Birthisel, T. (2014). Formulation of entomopathogens as bioinsecticides. In: Morales-Ramos, J. A., Guadalupe Rojas, M., & Shapro-Ilan, D.L. (Eds.), *Mass Production of Beneficial Organisms*. (pp. 483-517). Amsterdam: Elsevier.
- Benz, G.A. (1986). Introduction: historical perspective. In: Granados, R.R., & Federici, B.A. (Eds.), *The Biology of Baculoviruses*. (pp. 1-35). Boca Raton, Florida: CRC.
- Bergkessel, M., & Guthrie, C. (2013). Colony PCR. *Methods in Enzymology*, 529, 299–309. <https://doi.org/10.1016/B978-0-12-418687-3.00025-2>.
- Blissard, G.W. (1996). Baculovirus-insect cell interactions. *Cytotechnology*, 20, 73–93.
- Blissard, G.W., & Rohrmann, G.F. (1990). Baculovirus diversity and molecular biology. *Annual Review of Entomology*, 35(1), 127–155.
- Bloem, S., Carpenter, J.E., & Hofmeyr, J.H. (2003). Radiation Biology and Inherited Sterility in False Codling Moth (Lepidoptera: Tortricidae). *Journal of Economic Entomology*, 96(6), 1724–1731. <https://doi.org/10.1093/jee/96.6.1724>.
- Bloem, S., Carpenter, J., & Hofmeyer, H. (2007). Area-Wide Control Tactics for the False Codling Moth *Thaumatotibia leucotreta* in South Africa: a Potential Invasive Species. In: Vreysen, M.J.B., Robinson, A.S., & J. Hendrichs (Eds.), *Area-Wide Control of Insect Pests*. Dordrecht: Springer.
- Blomefield, T.L. (1989). Economic importance of false codling moth, *Cryptophlebia leucotreta*, and codling moth, *Cydia pomonella*, on peaches, nectarines and plums. *Phytophylactica*, 21(4), 435–436.

- Boardman, L., Grout, T.G., & Terblanche, J.S. (2012). False codling moth *Thaumatotibia leucotreta* (Lepidoptera, Tortricidae) larvae are chill-susceptible. *Insect Science*, *19*(3), 315–328. <https://doi.org/10.1111/j.1744-7917.2011.01464.x>.
- Bottrell, D.G., & Smith, R.F. (1982). Integrated pest management. *Environmental Science & Technology*, *16*(5), 282–288.
- Bozorgkhoo, Z., Pilehchian Langroudi, R., Khaki, P., Jabbari, A. R., Moradi Bidhendi, S., & Moosawi Shoshtari, M. (2014). Molecular cloning of Clostridium septicum vaccine strain alpha toxin gene in *E. coli*. *Archives of Razi Institute*, *69*(1), 15–20. <https://doi.org/10.7508/ari.2014.01.002>.
- Burges, H.D., & Jones, K.A. (1998). Formulation of bacteria, viruses and protozoa to control insects. In: Burges, H.D. (Eds.), *Formulation of Microbial Biopesticides*. (pp. 33–127). Dordrecht: Kluwer Academic Publishers.
- Burges, H. D., & Thompson, E. M. (1971). Standardization and assay of microbial insecticides. In: Burges, H.D. & Hussey, N. W. (Eds.), *Microbial Control of Insects and Mites*. (pp. 591–622). London: Academic Press.
- Carballo, A., Murillo, R., Jakubowska, A., Herrero, S., Williams, T., & Caballero, P. (2017). Co-infection with iflaviruses influences the insecticidal properties of Spodoptera exigua multiple nucleopolyhedrovirus occlusion bodies: Implications for the production and biosecurity of baculovirus insecticides. *PLOS ONE*, *12*(5), e0177301. <https://doi.org/Doi:10.1371/journal.pone.0177301>.
- Carruthers, W.R., Cory, J.S., & Entwistle, P.F. (1988). Recovery of pine beauty moth (*Panolis flammea*) nuclear polyhedrosis virus from pine foliage. *Journal of Invertebrate Pathology*, *52*(1), 27–32.
- Casali, N., & Preston, A. (2003). *E. coli plasmid vectors: methods and applications* (Eds.). USA: Humana Press.
- Catling, H.D., & Aschenborn, H. (1974). Population studies of the false codling moth, *Cryptophlebia lellcolrela* Meyr., on citrus in the Transvaal. *Phytophylactica*, *6*(1), 31–38.
- CGA (2013). *Key Industry Statistics; Citrus Growers' Association: Durban, South Africa*. Available at: <https://www.citrusresourcewarehouse.org.za/home/document-home/information/cga-key-industry-statistics/23-cga-key-industry-statistics-2013/file>.

- CGA (2017). *Key Industry Statistics*. CGA, Hillcrest, South Africa. Available at: <http://www.citrusresourcewarehouse.org.za/home/document-home/information/cga-key-industry-statistics>.
- CGA (2019). *Citrus Growers Association Annual Report 2019 v6 FINAL*.
- CGA (2020). *2020 Key Industry Statistics for citrus growers, 2019 Export Season*.
- Chandler, D., Bailey, A.S., Tatchell, M., Davidson, G., Greaves, J., & Grant, W.P. (2011). The development, regulation and use of biopesticides for integrated pest management. *Philosophical Transactions of the Royal Society*, 366, 1987–1998.
- Chateigner, A., Bézier, A., Labrousse, C., Jiolle, D., Barbe, V., & Herniou, E.A. (2015). Ultra deep sequencing of a baculovirus population reveals widespread genomic variations. *Viruses*, 7(7), 3625–3646. <https://doi.org/10.3390/v7072788>.
- Cho, M.H., Ciulla, D., Klanderman, B.J., Raby, B.A., & Silverman, E.K. (2008). High-resolution melting curve analysis of genomic and whole-genome amplified DNA. *Clinical Chemistry*, 54(12), 2055–2058.
- Claus, J.D., Gioria, V.V., Micheloud, G.A., & Visnovsky, G. (2012). Production of insecticidal baculoviruses in insect cell cultures: potential and limitations. In: Soloneski, S. & Larramendy M. (Eds.), *Insecticides-basic and other applications*. (pp. 127–152). Rijeka: InTech.
- Clavijo, G., Williams, T., Mun, D., Caballero, P., & Lo, M. (2010). Mixed genotype transmission bodies and virions contribute to the maintenance of diversity in an insect virus. *Proceedings of the Royal Society B*, 277(1683), 943–951. <https://doi.org/10.1098/rspb.2009.1838>.
- Coombes, C.A., Hill, M.P., Moore, S. D., & Dames, J. F. (2016). Entomopathogenic fungi as control agents of *Thaumatotibia leucotreta* in citrus orchards: field efficacy and persistence. *BioControl*, 61, 729–739.
- Cory, J.S., & Evans, H.F. (2007). Viruses. In: Lacey, L. A., & Kaya, H.K. (Eds.), *Field Manual of Techniques in Invertebrate Pathology*. (pp.149-174). Dordrecht: Springer.
- Cory, J.S., & Myers, J.H. (2003). The Ecology and Evolution of Insect Baculoviruses. *Annual Review of Ecology, Evolution, and Systematics*, 34(1), 239–272. <https://doi.org/10.1146/annurev.ecolsys.34.011802.132402>.

- Cox, C.S. (1989). Airborne bacteria and viruses. *Science Progress*, 73(4), 469–500.
- Crossley, B.M., Bai, J., Glaser, A., Maes, R., Porter, E., Killian, M.L., Clement, T., & Toohey-Kurth, K. (2020). Guidelines for Sanger sequencing and molecular assay monitoring. *Journal of Veterinary Diagnostic Investigation*, 32(6), 767–775. <https://doi.org/10.1177/1040638720905833>.
- Cunningham, J.C. (1995). Baculoviruses as microbial insecticides. In: Reuveni, R. (Eds.), *Novel Approaches to Integrated Pest Management*. (pp. 261-292). Boca Raton, Florida: Lewis.
- Daiber, C.C. (1978). Insecticidal control of false codling moth (*Cryptophlebia leucotreta* Meyr.) in peaches. *Phytophylactica*, 8, 109–110.
- Daiber, C.C. (1979a). A study of the biology of the False Codling Moth [*Cryptophlebia leucotreta* (Meyr.)]: The egg. *Phytophylactica*, 11, 129–132.
- Daiber, C.C. (1979b). A study of the biology of the false codling moth [*Cryptophlebia leucotreta* (Meyr.)]: the larva. *Phytophylactica*, 11, 141–144.
- Daiber, C.C. (1979c). A study of the biology of the false codling moth [*Cryptophlebia leucotreta* (Meyr.)]: the cocoon. *Phytophylactica*, 11, 151–157.
- Daiber, C.C. (1980). A study of the biology of the false codling moth *Cryptophlebia leucotreta* (Meyr.): the adult and generations during the year. *Phytophylactica*, 12(4), 187–193.
- Daryaei, F.A., Langroudi, R.P., & Eimani, B.G. (2017). Production and Evaluation of a New Recombinant Cloning Vector for the Clostridium novyi Type B Vaccine Strain Alpha Toxin Gene. *EC Microbiology* <https://www.Ecronicon.Com/Microbiology-Articles.Php>, (April). Retrieved from: <https://www.ecronicon.com/ecmi/pdf/ECMI-07-00214.pdf>.
- David, W.A.L., Gardiner, B.O.C., & Woolner, N. (1968). The effects of sunlight on a purified granulovirus of *P. brassicae*. *Journal of Invertebrate Pathology*, 14, 336–342.
- Day, W.H.E., & McMorris, F.R. (1992). Consensus sequences based on plurality rule. *Bulletin of Mathematical Biology*, 54, 1057–1068.
- de Jager, Z.M. (2013). Biology and ecology of the false codling moth, *Thaumatotibia leucotreta* (Meyrick), 1–98. <http://scholar.sun.ac.za/handle/10019.1/95453>.

- de Villiers, M., Heunis, J.M., & Pringle, K.L. (2015). Phytosanitary host status of apples as a host for false codling moth, *Thaumatotibia leucotreta* (Meyrick)(Lepidoptera: Tortricidae). *African Entomology*, 23(1), 234–238.
- de Villiers, M., & Pringle, K.L. (2007). Seasonal occurrence of vine pests in commercially treated vineyards in the Hex River Valley in the Western Cape Province, South Africa. *African Entomology*, 15(2), 241–260.
- Department of Agriculture, L.R. and R.D. (DALRRD). (2020). *Abstract of Agricultural Statistics*. [https://www.dalrrd.gov.za/Portals/0/Statistics and Economic Analysis/Statistical Information/Abstract 2020_organized.pdf](https://www.dalrrd.gov.za/Portals/0/Statistics%20and%20Economic%20Analysis/Statistical%20Information/Abstract%202020_organized.pdf).
- du Toit, W.J. (1998). Fruit flies. In: Bedford, E.C.G., & van den Berg, M.A. (Eds.), *Citrus pests in the Republic of South Africa*. (pp. 229-233). Nelspruit, South Africa: Dynamic Ad.
- Dyck, V.A., Hendrichs, J., & Robinson, A.S. (2021). *Sterile Insect Technique Principles and Practice in Area-Wide Integrated Pest Management*. Taylor & Francis. <https://library.oapen.org/handle/20.500.12657/43144>.
- EFSA PLH Panel (EFSA Panel on Plant Health) Bragard, C., Di Serio, F., Gonthier, P., Jaques Miret, J.A., Fejer Justesen, A., MacLeod, A., Sven Magnusson, C., Navas-Cortes, J.A., Parnell, S., Potting, R., Reignault, P.L., Thulke, H-H., Van der Werf, W., Vicent Civera, A., Yuen, J., Zappalà, L., Lucchi, A., Tena, A., Mosbach-Schulz, O., de la Peña, E., & Milonas, P. (2021). Scientific Opinion on the commodity risk assessment of *Citrus* L. fruits from South Africa for *Thaumatotibia leucotreta* under a systems approach. *EFSA Journal*, 19(8), 6799. <https://doi.org/10.2903/j.efsa.2021.6799>.
- El-Salamouny, S., Ranwala, D., Shapiro, M., Shepard, B.M., & Farrar Jr, R.R. (2009). Tea, coffee, and cocoa as ultraviolet radiation protectants for the beet armyworm nucleopolyhedrovirus. *Journal of Economic Entomology*, 102(5), 1767–1773.
- Erichsen, C., & Schoeman, A.S. (1992). Economic losses due to insect pests on avocado fruit in the Nelspruit/Hazyview region of South Africa during 1991. *South African Avocado Growers' Association Yearbook*, 15, 49–54.
- Erichsen, C., & Schoeman, A.S. (1994). Moth pests of avocados. *South African Avocado Growers' Association Yearbook*, 17, 109–112.

- Erjavec, M.S. (2020). Synthetic Biology - New Interdisciplinary Science. In: Nagpal, M.L., Boldura, O.M., Baltă, C., & S. Enany, S. (Eds.), 998. IntechOpen. <https://doi.org/DOI:10.5772/intechopen.85164>.
- Erlandson, M.A. (2009). Genetic variation in field populations of baculoviruses: Mechanisms for generating variation and its potential role in baculovirus epizootiology. *Virologica Sinica*, 24(5), 458–469. <https://doi.org/10.1007/s12250-009-3052-1>.
- Escribano, A., Williams, T., Goulson, D., Cave, R.D., Chapman, J.W., & Caballero, P. (1999). Selection of a nucleopolyhedrovirus for control of *Spodoptera frugiperda* (Lepidoptera: Noctuidae): Structural, genetic, and biological comparison of four isolates from the Americas. *Journal of Economic Entomology*, 92(5), 1079–1085. <https://doi.org/10.1093/jee/92.5.1079>.
- Evans, H. (1999). Principles of dose acquisition for bioinsecticides. In: Hall, F. & Menn, J. (Eds.), *Biopesticides: use and delivery*. (pp. 553-557). Totowa: Humana Press.
- Evans, H. F. (1994). Laboratory and field results with viruses for the control of insects. In: Hewitt, H.G., Casely J., Copping, L. G., Grayson, B.T. & Tyson, D. (Eds.), *BCPC Monograph No 59: Comparing Glasshouse and Field Pesticide Performance II*. (pp. 285-296). Farnham, UK: British Crop Protection Council.
- Fan, J., Wennmann, J.T., Wang, D., & Jehle, J.A. (2020). Single nucleotide polymorphism (SNP) frequencies and distribution reveal complex genetic composition of seven novel natural isolates of *Cydia pomonella* granulovirus. *Virology*, 541(November 2019), 32–40. <https://doi.org/10.1016/j.virol.2019.11.016>.
- Foster, S.P., & Harris, M.O. (1997). Behavioural manipulation methods for insect pest-management. *Annual Review of Entomology*, 42(1), 123–146. <https://doi.org/doi:10.1146/annurev.ento.42.1.123>.
- Fullard, T., & Hill, M.P. (2013). Impact of insecticides on the reproductive potential of false codling moth, *Thaumatotibia leucotreta* (Meyrick, 1913) (Lepidoptera: Tortricidae). *African Entomology*, 21(2), 310–315. <https://doi.org/10.4001/003.021.0221>.
- Fuller, E., Elderd, B.D., & Dwyer, G. (2012). Pathogen persistence in the environment and insect-baculovirus interactions: Disease-density thresholds, epidemic burnout, and insect outbreaks. *The American Naturalist*, 179(3), E70–E96. <https://doi.org/10.1086/664488>.

- Fuxa, J.R. (1987). Ecological considerations for the use of entomopathogens in IPM. *Annual Review of Entomology*, 32(1), 225–251.
- Fuxa, J.R. (1991). Insect control with baculoviruses. *Biotechnology Advances*, 9(3), 425–442.
- Gendall, K. (2005). Effect of ultra-violet (UV) radiation and formulation of the *Cryptophlebia leucotreta* granulovirus (CrleGV) on *Cryptophlebia leucotreta* Meyrick (Lepidoptera: Tortricidae). Honours Thesis, Rhodes University.
- Girard, P.M., Francesconi, S., Pozzebon, M., Graindorge, D., Rochette, P., Drouin, R., & Sage, E. (2011). UVA-induced damage to DNA and proteins: direct versus indirect photochemical processes. *Journal of Physics Conference Series*, 261, 012002.
- Gotoh, T., Ando, N., & Kikuchi, K.I. (2008). Analysis of inactivation of AcMNPV under various conditions by the ELVA method. *Bioscience, Biotechnology and Biochemistry*, 72(7), 1973–1976. <https://doi.org/10.1271/bbb.80105>.
- Green, M.R., & Sambrook, J. (2019). Polymerase chain reaction. *Cold Spring Harbor Protocols*, 2019(6), 436–456. <https://doi.org/10.1101/pdb.top095109>.
- Greenfield, P.F., Reid, S., Weiss, S., & Scholz, B. (1999). Baculoviruses as biological control agents: research, production and commercial issues. In: *The 5th Asia-Pacific Biochemical Engineering Conference Preceedings*. Pucket, Thailand.
- Grout, T.G., & Moore, S.D. (2015). Citrus. In: Prinsloo, G.L., & Uys, V.M. (Eds.), *Insects of cultivated plants and natural pastures in southern Africa*. (pp. 448-499). Cape Town: Entomological Society of Southern Africa.
- Grzywacz, D. (2017). Basic and Applied Research: Baculoviruses. In: Lacey, L.A. (Eds.), *Microbial control of insect and mite pests: from theory to practice*. (pp. 27-46). London: Academic Press.
- Grzywacz, D., & Moore, S.D. (2017). Production, formulation, and bioassay of baculoviruses for pest control. In: Lacey, L.A. (Eds.), *Microbial Control of Insects and Mite Pests: From Theory to Practice*. (pp. 109-124). London: Academic Press.
- Grzywacz, D., Rabindra, R.J., Brown, M., Jones, K.A., & Parnell, M. (2003). The *Helicoverpa Armigera* NPV Production Manual. *Production*, 1–113.

- Guedes, R.N.C., Smagghe, G., Stark, J.D., & Desneux, N. (2016). Pesticide-induced stress in arthropod pests for optimized integrated pest management programs. *Annual Review of Entomology*, *61*, 43–62.
- Gueli, A.G., Sauer, A., Weihrauch, B., Fritsch, E., Undorf-Spahn, K., Wennmann, J., & Jehle, J. (2017). Using Next Generation Sequencing to Identify and Quantify the Genetic Composition of Resistance-Breaking Commercial Isolates of *Cydia pomonella* Granulovirus. *Viruses*, *9*, 250.
- Gunn, D. (1921). The false codling moth (*Argyroplote leucotreta* Meyre.). *Science Bulletin, Department of Forestry, Union of South Africa*, *21*, 1–28.
- Haase, S., Sciocco-Cap, A., & Romanowski, V. (2015). Baculovirus Insecticides in Latin America: Historical Overview, Current Status and Future Perspectives. *Viruses*, *7*, 2230–2267.
- Harrison, R., & Hoover, K. (2012). Baculoviruses and other occluded insect viruses. In: Vega, F.E., & Kaya, H.K. (2nd Eds.), *Insect pathology*. (pp. 73-132). UK: Academic press.
- Harrison, R.L., & Bonning, B.C. (1999). The nucleopolyhedroviruses of *Rachiplusia ou* and *Anagrapha falcifera* are isolates of the same virus. *Journal of General Virology*, *80*(10), 2793–2798.
- Harrison, R.L., Herniou, E.A., Jehle, J.A., Theilmann, D.A., Burand, J.P., Becnel, J.J., Krell, P.J., van Oers, M.M., Mowery, J.D., & Bauchan, G.R. (2018). ICTV Virus Taxonomy Profile: Baculoviridae. *Journal of General Virology*. *Virol*, *99*, 1185–1186.
- Harrison, R., Rowley, D., Mowery, J., Bauchan, G., & Burand, J. (2017). The Operophtera brumata Nucleopolyhedrovirus (OpbuNPV) Represents an Early, Divergent Lineage within Genus Alphabaculovirus. *Viruses*, *9*, 307.
- Hatting, J.L., Moore, S.D., & Malan, A.P. (2019). Microbial control of phytophagous invertebrate pests in South Africa: Current status and future prospects. *Journal of Invertebrate Pathology*, *165*, 54–66. <https://doi.org/10.1016/j.jip.2018.02.004>.
- Hattingh, V., Moore, S., Kirkman, W., Goddard, M., Thackeray, S., Peyper, M., Sharp, G., Cronjé, P., Pringle, K., & Cha, D.H. (2020). An Improved Systems Approach as a Phytosanitary Measure for *Thaumatotibia leucotreta* (Lepidoptera: Tortricidae) in Export

- Citrus Fruit from South Africa. *Journal of Economic Entomology*, 113(2), 700–711. <https://doi.org/10.1093/jee/toz336>.
- Hefferon, K.L., Oomens, A.G.P., Monsma, S.A., Finnerty, C.M., & Blissard, G.W. (1999). Host cell receptor binding by baculovirus GP64 and kinetics of virion entry. *Virology*, 258(2), 455–468.
- Herniou, E.A., Arif, B.M., Bonning, B.C., Theilmann, D.A., Blissard, G.W., Becnel, J.J., Jehle, J.A., & Harrison, H. (2011). Baculoviridae. In: King, A.M.Q., Adams, M.J., Carstens, E.B., & Lefkowitz, E.B. (Eds.), *Virus taxonomy: Ninth report of the international committee on taxonomy of virus*. (pp. 163-174). Oxford: Elsevier.
- Herniou, E.A., Olszewski, J.A., Cory, J.S., & O'Reilly, D.R. (2003). The Genome Sequence and Evolution of Baculoviruses. *Annual Review of Entomology*, 48, 211–234. <https://doi.org/10.1146/annurev.ento.48.091801.112756>.
- Herniou, E., & Jehle, J. (2007). Baculovirus Phylogeny and Evolution. *Current Drug Targets*, 8(10), 1043–1050. <https://doi.org/10.2174/138945007782151306>.
- Hill, M.P., & Fullard, T. (2013). Impact of insecticides on the reproductive potential of false codling moth, *Thaumatotibia leucotreta* (Meyrick, 1913)(Lepidoptera: Tortricidae). *African Entomology*, 21(2), 310–315.
- Hitchman, R.B., Hodgson, D.J., King, L.A., Hails, R.S., Cory, J.S., & Possee, R.D. (2007). Host mediated selection of pathogen genotypes as a mechanism for the maintenance of baculovirus diversity in the field. *Journal of Invertebrate Pathology*, 94, 153–162.
- Hofmeyr, J.H. (2003). Integrated pest and disease management. In: *Integrated Production Guidelines for Export Citrus* (Vol. 3). (pp. 95-101). Nelspruit: Citrus Research International.
- Hofmeyr, J.H., Burger, B.V., & Calitz, F.J. (1991). Disruption of male orientation to female false codling moth, *Cryptophlebia leucotreta* (Lepidoptera: Tortricidae), using synthetic sex pheromone. *Phytophylactica*, 23(2), 153–156.
- Hofmeyr, J.H., Hofmeyr, M., Hattingh, V., & Slabbert, J.P. (2016). Postharvest Phytosanitary Disinfestation of *Thaumatotibia leucotreta* (Lepidoptera: Tortricidae) in Citrus Fruit: Determination of Ionising Radiation and Cold Treatment Conditions for Inclusion in a

- Combination Treatment. *African Entomology*, 24(1), 208–216.
<https://doi.org/10.4001/003.024.0208>.
- Hofmeyr, J.H., & Pringle, K.L. (1998). Resistance of false codling moth, *Cryptophlebia leucotreta* (Meyrick) (Lepidoptera: Tortricidae), to the chitin synthesis inhibitor, triflumuron: short communication. *African Entomology*, 6(2), 373–375. Available at: <http://content.ajarchive.org/cgi-bin/showfile.exe?CISOROOT=/10213589&CISOPTR=240%5Cnhttp://hdl.handle.net/10499/AJ12936>.
- Hunter-Fujita, F.R., Entwistle, P.F., & Evans, H.E. (1998). *Insect viruses and pest management*. John Wiley & Sons Ltd.
- Ignoffo, C.M. (1985). Manipulating enzootic-epizootic diseases of arthropods. In: Hoy, M.A., & Herzog, D.C. (Eds.), *Biological control in agricultural IPM systems*. (pp. 243-261). Orlando: Academic Press.
- Ignoffo, C.M. (1992). Environmental factors affecting persistence of entomopathogens. *Florida Entomologist*, 75(4), 516–525.
- Ignoffo, C.M., & Garcia, C. (1994). Antioxidant and oxidative enzyme effects on the inactivation of inclusion bodies of the *Heliothis* baculovirus by simulated sunlight-UV. *Environmental Entomology*, 23(4), 1025–1029.
- Ignoffo, C.M., Hostetter, D.L., Sikorowski, P.P., Sutter, G., & Brooks, W.M. (1977). Inactivation of representative species of entomopathogenic viruses, a bacterium, fungus, and protozoan by an ultraviolet light source. *Environmental Entomology*, 6(3), 411–415.
- IJkel, W.F., Westenberg, M., Goldbach, R.W., Blissard, G.W., Vlak, J.M., & Zuidema, D. (2000). A novel baculovirus envelope fusion protein with a proprotein convertase cleavage site. *Virology*, 275(1), 30–41.
- Jacques, R.P. (1972). The inactivation of foliar deposits of viruses of *Trichoplusia ni* (Lepidoptera: Noctuidae) and *Pieris rapae* (Lepidoptera: Pieridae) and tests on protectant additives. *The Canadian Entomologist*, 104, 1985–1994.
- Jacques, R.P. (1985). Stability of entomopathogenic viruses. *Miscellaneous Publications of the Entomological Society of America*, 10, 99–116.

- Jaques, R.P. (1977). Stability of entomopathogenic viruses. *Miscellaneous Publications of the Entomological Society of America*, 10, 99–116.
- Jehle, J.A., Backhaus, H., Fritsch, E., & Huber, J. (1992). Physical map of the *Cryptophlebia leucotreta* granulosis virus genome and its relationship to the genome of *Cydia pomonella* granulosis virus. *Journal of General Virology*, 73(7), 1621–1626. <https://doi.org/10.1099/0022-1317-73-7-1621>.
- Jehle, J.A., Blissard, G.W., Bonning, B.C., Cory, J.S., Herniou, E.A., Rohrmann, G.F., Theilmann, D.A., Thiem, S. M., & Vlak, J.M. (2006). On the classification and nomenclature of baculoviruses: A proposal for revision. *Archives of Virology*, 151(7), 1257–1266. <https://doi.org/10.1007/s00705-006-0763-6>.
- Jeyarani, S., Sathiah, N., & Karuppuchamy, P. (2013). An in vitro method for increasing UV-tolerance in a strain of *Helicoverpa armigera* (Lepidoptera: Noctuidae) nucleopolyhedrovirus. *Biocontrol Science and Technology*, 23(3), 305–316. <https://doi.org/10.1080/09583157.2012.757296>.
- Jones, K.A. (1988). *Studies on the persistence of Spodoptera littoralis nuclear polyhedrosis virus on cotton in Egypt*. University of Reading.
- Jones, K.A. (2000). Bioassays of entomopathogenic viruses. In: Navon, A., & Ascher, K.R.S. (Eds.), *Bioassay of entomopathogenic microbes and nematodes*. (pp. 95-140). Wallingford: CAB Publishing.
- Jones, K.A., Moawad, G., McKinley, D.J., & Grzywacz, D. (1993). The effect of natural sunlight on *Spodoptera littoralis* nuclear polyhedrosis virus. *Journal of Biocontrol Science and Technology*, 3, 189–194. <https://doi.org/10.1080/09583159309355275>.
- Jukes, M.D. (2017). *Baculovirus Synergism: Investigating Mixed Alphabaculovirus and Betabaculovirus Infections in the False Codling Moth, Thaumatotibia leucotreta, for Improved Pest Control*. PhD Thesis, Rhodes University.
- Jukes, M.D., Rabalski, L., Knox, C.M., Moore, S.D., Hill, M.P., & Szewczyk, B. (2017). *Baculovirus synergy: mixed Alphabaculovirus and Betabaculovirus infections for the control of Thaumatotibia leucotreta in South Africa*. 129, 170–174.

- Kingsley, D.H., Behbahani, A., Rashtian, A., Blissard, G.W., & Zimmerberg, J. (1999). A discrete stage of baculovirus GP64-mediated membrane fusion. *Molecular Biology of the Cell*, *10*(12), 4191–4200.
- Kirkman, W. (2007). Understanding and improving the residual efficacy of the *Cryptophlebia leucotreta* granulovirus (Cryptogran). Master's Thesis, Rhodes University. Available at: http://vital.seals.ac.za:8080/vital/access/manager/Repository/vital:5794?site_name=GlobalView.
- Kirkman, W., & Moore, S. (2007). A study of alternative hosts for the false codling moth, *Thaumatotibia* (= *Cryptophlebia*) *leucotreta* in the Eastern Cape. *SA Fruit Journal*, *6*(2), 33–38.
- Komai, F.A. (1999). A taxonomic review of the genus *Grapholita* and allied genera (Lepidoptera, Tortricidae) in the Palearctic region. *Entomologica Scand*, *55*, 1–226.
- Krejmer-Rabalska, M., Rabalski, L., Jukes, M.D., de Souza, M.L., Moore, S.D., & Szewczyk, B. (2019). New method for differentiation of granuloviruses (Betabaculoviruses) based on real-time polymerase chain reaction (real-time PCR). *Viruses*, *11*(2), 1–16. <https://doi.org/10.3390/v11020115>.
- La Croix, E.A.S., & Thindwa, H.Z. (1986). Macadamia pests in Malawi. III. The major pests. The biology of bugs and borers. *International Journal of Pest Management*, *32*(1), 11–20.
- Lacey, L.A., Grzywacz, D., Shapiro-Ilan, D.I., Frutos, R., Brownbridge, M., & Goettel, M.S. (2015). Insect pathogens as biological control agents: back to the future. *Journal of Invertebrate Pathology*, *132*, 1–41.
- Lange, M., & Jehle, J.A. (2003). The genome of the *Cryptophlebia leucotreta* granulovirus. *Virology*, *317*(2), 220–236. [https://doi.org/10.1016/S0042-6822\(03\)00515-4](https://doi.org/10.1016/S0042-6822(03)00515-4).
- Larem, A., BenTiba, S., Wennmann, J.T., G., G.Al., & Jehle, J.A. (2019). Elucidating the genetic diversity of *Phthorimaea operculella* granulovirus (PhopGV). *Journal of General Virology*, *100*, 679–690.
- LeBlanc, B.D., & Overstreet, R.M. (1991). Effect of desiccation, pH, heat, and ultraviolet irradiation on viability of *Baculovirus penaei*. *Journal of Invertebrate Pathology*, *57*(2), 277–286. [https://doi.org/10.1016/0022-2011\(91\)90128-D](https://doi.org/10.1016/0022-2011(91)90128-D).

- Lloyd, M., Knox, C.M., Thackeray, S.R., Hill, M.P., & Moore, S.D. (2017). Isolation, Identification and Genetic Characterisation of a Microsporidium Isolated from Carob Moth, *Ectomyelois ceratoniae* (Zeller) (Lepidoptera: Pyralidae). *African Entomology*, 25(2), 529–533. <https://doi.org/10.4001/003.025.0529>.
- Lodish, H., Berk, A., Zipursky, S.L., Matsudaira, P., Baltimore, D., & Darnell, J. (2000). *Molecular Cell Biology* (4th Ed.). New York: WH Freeman & Company. Retrieved from: <https://www.ncbi.nlm.gov/books/NBK21498>.
- López-Ferber, M., Simón, O., Williams, T., & Caballero, P. (2003). Defective or effective? Mutualistic interactions between virus genotypes. *Proceedings of the Royal Society B: Biological Sciences*, 270(1530), 2249–2255. <https://doi.org/10.1098/rspb.2003.2498>.
- Lorenz, T.C. (2012). Polymerase chain reaction: Basic protocol plus troubleshooting and optimization strategies. *Journal of Visualized Experiments*, 63, 1–14. <https://doi.org/10.3791/3998>.
- Love, C.N., Hill, M.P., & Moore, S.D. (2014). *Thaumatotibia leucotreta* and the Navel orange: Ovipositional preferences and host susceptibility. *Journal of Applied Entomology*, 138(8), 600–611. <https://doi.org/10.1111/jen.12126>.
- Love, C.N., Moore, S.D., & Hill, M.P. (2019). The role of abiotic factors in the pupation of *Thaumatotibia leucotreta* Meyrick (Lepidoptera: Tortricidae) in the soil. *Agricultural and Forest Entomology*, 21, 38–49.
- Lua, L., & Reid, S. (2005). Method of producing baculovirus. PCT publication number: WO/2005/045014.
- Madigan, M., Martinko, J., Stahl, D., & Clark, D. (2012). *Biology of Microorganisms* (13th Ed.). San Francisco: Pearson Education, Inc.
- Maeda, S. (1989). Increased insecticidal effect by a recombinant baculovirus carrying a synthetic diuretic hormone gene. *Biochemical and Biophysical Research Communications*, 165(3), 1177–1183.
- Malan, A.P., Diest, J.I.V., Moore, S.D., & Addison, P. (2018). Control Options for False Codling Moth, *Thaumatotibia leucotreta* (Lepidoptera: Tortricidae), in South Africa, with Emphasis on the Potential Use of Entomopathogenic Nematodes and Fungi. *African Entomology*, 26(1), 14–29. <https://doi.org/10.4001/003.026.0014>.

- Malan, A.P., Knoetze, R., & Moore, S.D. (2011). Isolation and identification of entomopathogenic nematodes from citrus orchards in South Africa and their biocontrol potential against false codling moth. *Journal of Invertebrate Pathology*, *108*, 115–125.
- Malan, A.P., Nguyen, K.B., & Addison, M.F. (2006). Entomopathogenic nematodes (Steinernematidae and Heterorhabditidae) from the south-western parts of South Africa. *African Plant Protection*, *12*, 65–69.
- Maniania, N.K., Ekesi, S., & Dolinski, C. (2017). Entomopathogens Routinely Used in Pest Control Strategies: Orchards in Tropical Climate. In: Lacey, L.A. (Eds.), *Microbial Control of Insect and Mite Pests: From Theory to Practice*. (pp. 269-282). Yakima: Elsevier.
- Masel, J. (2011). Genetic drift. *Current Biology*, *21*(20), R837–R838.
- McInerney, P., Adams, P., & Hadi, M.Z. (2014). Error Rate Comparison during Polymerase Chain Reaction by DNA Polymerase. *Molecular Biology International*, *2014*, 1–8. <https://doi.org/10.1155/2014/287430>.
- Miller, J.R., Koren, S., & Sutton, G. (2010). Assembly algorithms for next-generation sequencing data. *Genomics*, *95*(6), 315–327. <https://doi.org/10.1016/j.ygeno.2010.03.001>.
- Miller, L.K. (1996). Insect viruses. In: Fields, B.N., Knipe, D.M., & Howley, P.M. (Eds.), *Fields Virology*. (pp. 533-556). Philadelphia: Lippincott-Raven.
- Mishra, S. (1998). Baculoviruses as biopesticides. *Current Science*, *75*, 1015–1022.
- Moore, G.A. (2001). Oranges and lemons: clues to the taxonomy of Citrus from molecular markers. *TRENDS in Genetics*, *17*(9), 536–540.
- Moore, S., Coombes, C., Manrakhan, A., Kirkman, W., Hill, M., Ehlers, R.-U., Daneel, J.-H., Dewaal, J., Dames, J., & Malan, A. (2013). Subterranean control of an arboreal pest: EPNs and EPFs for FCM. *Insect Pathogens and Entomoparasitic Nematodes, IOBC-WPRS Bulletin*, *90*, 247–250.
- Moore, S.D. (2002). The development and evaluation of cryptophlebia leucotreta granulovirus (CrleGV) as a biological control agent for the management of false codling moth, *Cryptophlebia leucotreta*, on citrus. PhD Thesis, Rhodes University.

- Moore, S.D. (2012). Moths and butterflies: false codling moth. In: Grout, T.G. (Eds.), *Citrus Research International IPM production guidelines, Vol. 3, Part 9.4.* (pp. 1-9). Nelspruit, South Africa: Citrus Research International.
- Moore, S.D. (2019). *Moths and Butterflies: False Codling Moth. Integrated Production Guidelines Vol III, Chapter 3: Specific Pests Part 9.4.*
- Moore, S.D. (2021). Biological control of a phytosanitary pest (*Thaumatotibia leucotreta*): A case study. *International Journal of Environmental Research and Public Health*, 18(3), 1–19. <https://doi.org/10.3390/ijerph18031198>.
- Moore, S.D., & Hattingh, V. (2012). A review of current pre-harvest control options for false codling moth in citrus in southern Africa. *SA Fruit Journal*, 11(4), 82–85.
- Moore, S.D., Hendry, D.A., & Richards, G.I. (2011). Virulence of a South African isolate of the Cryptophlebia leucotreta granulovirus to *Thaumatotibia leucotreta* neonate larvae. *BioControl*, 56(3), 341–352. <https://doi.org/10.1007/s10526-010-9339-1>.
- Moore, S.D., Kirkman, W., & Hattingh, V. (2015a). The host status of lemons for the false codling moth, *Thaumatotibia leucotreta* (Meyrick)(Lepidoptera: Tortricidae) with particular reference to export protocols. *African Entomology*, 23(2), 519–525.
- Moore, S.D., Kirkman, W., Richards, G.I., & Stephen, P.R. (2015b). The Cryptophlebia leucotreta granulovirus—10 years of commercial field use. *Viruses*, 7(3), 1284–1312.
- Moore, S.D., Kirkman, W., & Stephen, P. (2004). Cryptogran: A virus for the biological control of false codling moth. *SA Fruit Journal (South Africa)*, 3, 35–39.
- Moore, S.D., Richards, G.I., Chambers, C., & Hendry, D. (2014). Improved Larval Diet for Commercial Mass Rearing of the False Codling Moth, *Thaumatotibia leucotreta* (Meyrick) (Lepidoptera: Tortricidae). *African Entomology*, 22, 216–219.
- Moore, S.D., Richards, G.I., Stephen, P.R., Singh, S., & Hendry, D. (2001). *The evaluation of the efficacy of a granulovirus (GV) for the control of false codling moth.*
- Moore, S., & Jukes, M. (2020). Advances in microbial control in IPM: entomopathogenic viruses. In: Kogan, M., & Heinrichs, E. (Eds.), *Integrated management of insect pests: Current and future developments.* (pp. 593-648). Burleigh Dodds Science Publishing Limited.

- Moore, S., & Kirkman, W. (2009). Citrus orchard sanitation with emphasis on false codling moth control. *South African Fruit Journal*, Dec/Jan, 57–60.
- Moore, S., Kirkman, W., & Stephen, P. (2004). Cryptogran. A virus for the biological control of false codling moth. *SA Fruit Journal (South Africa)*, January 2003, 56–60.
- Moscardi, F. (1999). Assessment of the application of baculoviruses for control of lepidoptera. *Annual Review of Entomology*, 44, 257–289. <https://doi.org/10.1146/annurev.ento.44.1.257>.
- Moscardi, F., De Souza, M.L., De Castro, M.E.B., Moscardi, M.L., & Szewczyk, B. (2011). Baculovirus pesticides: Present state and future perspectives. In: Ahmad, I., Ahmad, F., & Pichtel, J. (Eds.), *Microbes and microbial technology: Agricultural and environmental applications*. (pp. 415-445). New York, USA: Springer.
- Moscardi, F., & Sosa-Gómez, D.R. (1992). Use of viruses against soybean caterpillars in Brazil. In: Copping, L.G., Green, M.B., & Rees, R.T. (Eds.), *Pest Management in Soybean*. (pp. 98-109). London: Elsevier.
- Moscardi, F., & Sosa-Gómez, D.R. (1996). Soybean in Brazil. In: Persley, G.J. (Eds.), *Biotechnology and Integrated Pest Management*. (pp. 98-112). Wallingford, CT: CAB Int.
- Motsoeneng, B., Jukes, M.D., Knox, C.M., Hill, M.P., & Moore, S.D. (2019). Genome analysis of a novel south african cydia pomonella granulovirus (CpGV-SA) with resistance-breaking potential. *Viruses*, 11(7). <https://doi.org/10.3390/v11070658>.
- Mwanza, P. (2015). Determination of the effects of sunlight and UV irradiation on the structure, viability and reapplication frequency of the biopesticide *Cryptophlebia leucotreta* granulovirus in the protection against false codling moth infestation of citrus crops. Master's Thesis, Nelson Mandela University.
- Mwanza, P. (2019). Development of a UV-tolerant strain of the South African isolate of *Cryptophlebia leucotreta* granulovirus for use as an enhanced biopesticide for *Thaumatococcus leucocarpa* control on citrus. PhD Thesis, Nelson Mandela University.
- Mwanza, P., Jukes, M., Dealtry, G., Lee, M., & Moore, S. (2022). Selection for and Analysis of UV-Resistant *Cryptophlebia leucotreta* Granulovirus-SA as a Biopesticide for *Thaumatococcus leucocarpa*. *Viruses*, 14(1). <https://doi.org/10.3390/v14010028>.

- Mück, O. (1985). Biologie, verhalten und wirtschaftliche bedeutung von parasiten schädlicher Lepidopteren auf den Kapverden. *Neue Entomol Nachr*, 18, 168.
- Nakai, M., Harrison, R.L., Uchida, H., Ukuda, R., Hikiyama, S., Ishii, K., & Kunimi, Y. (2015). Isolation of an Adoxophyes orana granulovirus (AdorGV) occlusion body morphology mutant: biological activity, genome sequence and relationship to other isolates of AdorGV. *Journal of General Virology*, 96(4), 904-914.
- Newton, P.J. (1998). False codling moth *Cryptophlebia leucotreta* (Meyrick). In: Bedford, E.C.G., van den Berg, M.A., & de Villiers, E.A. (Eds.), *Citrus pests in the Republic of South Africa*. (pp. 192-200). Nelspruit, South Africa: Institute for Tropical and Subtropical Crops.
- Nguyen, Q., Qi, Y.M., Wu, Y., Chan, L.C., Nielsen, L.K., & Reid, S. (2011). In vitro production of Helicoverpa baculovirus biopesticides—automated selection of insect cell clones for manufacturing and systems biology studies. *Journal of Virological Methods*, 175(2), 197–205.
- Nishi, Y., & Nonaka, T. (1996). Biological control of the tea tortrix-using granulosis virus in the tea field. *Agrochemicals Journal*, 69, 7–10.
- Opoku-Debrah, J.K., Hill, M.P., Knox, C., & Moore, S.D. (2013). Overcrowding of false codling moth, *Thaumatotibia leucotreta* (Meyrick) leads to the isolation of five new *Cryptophlebia leucotreta* granulovirus (CrleGV-SA) isolates. *Journal of Invertebrate Pathology*, 112(3), 219–228. <https://doi.org/10.1016/j.jip.2012.12.008>.
- Opoku-Debrah, J.K., Hill, M.P., Knox, C., & Moore, S.D. (2014). Comparison of the biology of geographically distinct populations of the citrus pest, *Thaumatotibia leucotreta* (Meyrick)(Lepidoptera: Tortricidae), in South Africa. *African Entomology*, 22(3), 530–537.
- O'Reilly, D.R., & Miller, L.K. (1991). Improvement of a baculovirus pesticide by deletion of the *egt* gene. *Biotechnology*, 9(11), 1086–1089.
- Pearson, M.N., Groten, C., & Rohrmann, G.F. (2000). Identification of the Lymantria dispar Nucleopolyhedrovirus Envelope Fusion Protein Provides Evidence for a Phylogenetic Division of the Baculoviridae. *Journal of Virology*, 74(13), 6126–6131.

- Pijlman, G.P., Pruijssers, A.J.P., & Vlak, J.M. (2003). Identification of *pif-2*, a third conserved baculovirus gene required for per os infection of insects. *Journal of General Virology*, 84(8), 2041–2049. <https://doi.org/10.1099/vir.0.19133-0>.
- Popham, H.J., Bischoff, D.S., & Slavicek, J.M. (2001). Both *Lymantria dispar* Nucleopolyhedrovirus Enhancin Genes Contribute to Viral Potency. *Journal of Virology*, 75(18), 8639–8648.
- Potapov, V., & Ong, J.L. (2017). Examining sources of error in PCR by single-molecule sequencing. *PLoS ONE*, 12(1), 1–19. <https://doi.org/10.1371/journal.pone.0169774>.
- Prinsloo, G.L., & Uys, V.M. (2015). *Insects of cultivated plants and natural pastures in Southern Africa*. Pretoria, South Africa: Entomological Society of Southern Africa.
- Reed, G.H., & Wittwer, C.T. (2004). Sensitivity and specificity of single-nucleotide polymorphism scanning by high-resolution melting analysis. *Clinical Chemistry*, 50(10).
- Reed, W. (1974). The false codling moth, *Cryptophlebia leucotreta* Meyr. (Lepidoptera: Olethreutidae) as a pest of cotton in Uganda. *Cotton Growing Review*, 51(3), 213–225.
- Ridley, A.J., Whiteside, J.R., Mcmillan, T.J., & Allinson, S.L. (2009). Cellular and sub-cellular responses to UVA in relation to carcinogenesis. *International Journal of Radiation Biology*, 85(3), 177–195.
- Robberecht, R. (1989). Environmental photobiology. In: Smith, K.C. (Eds.), *The Science of photobiology*. (pp. 135-154). New York, USA: Plenum Press.
- Rohrmann, G.F. (2013). *Baculovirus Molecular Biology [Internet]* (3rd Ed.). Bethesda (MD): National Center for Biotechnology Information.
- Rohrmann, G.F. (2019). *Baculovirus Molecular Biology* (4th Ed.). Bethesda (MD): National Center for Biotechnology Information (US). <https://www.ncbi.nlm.nih.gov/books/NBK543458/>.
- Rothman, L.D., & Myers, J.H. (1996). Debilitating effects of viral diseases on host Lepidoptera. *Journal of Invertebrate Pathology*, 67, 1–10.
- Saiki, R., Scharf, S., Faloona, F., Mullis, K., Horn, G., Erlich, H., & Arnheim, N. (1985). Enzymatic amplification of β -globin genomic sequences and restriction site analysis for diagnosis of sickle cell anemia. *Science*, 230, 1350–1354.

- Seipp, M.T., Durtschi, J.D., Liew, M.A., Williams, J., Damjanovich, K., Pont-Kingdon, G., Lyon, E., Voelkerding, K.V., & Wittwer, C.T. (2007). Unlabeled oligonucleotides as internal temperature controls for genotyping by amplicon melting. *Journal of Molecular Diagnostics*, 9(3), 284–289. <https://doi.org/10.2353/jmoldx.2007.060136>.
- Serrano, A., Pijlman, G.P., Vlak, J.M., Muñoz, D., Williams, T., & Caballero, P. (2015). Identification of *Spodoptera exigua* nucleopolyhedrovirus genes involved in pathogenicity and virulence. *Journal of Invertebrate Pathology*, 126, 43–50. <https://doi.org/10.1016/j.jip.2015.01.008>.
- Shapiro, M. (1995). Radiation protection and activity enhancement of viruses. In: Hall, F.R., & Barry, J.W. (Eds.), *Biorational Pest Control Agents: Formulation and Delivery*, Am. Chem. Soc. Symp. 595. (pp. 153-164). Washington, DC: American Chemical Society.
- Shapiro, M., & Bell, R.A. (1984). Selection of a UV-tolerant Strain of the Gypsy Moth, *Lymantria dispar* (L.)(Lepidoptera: Lymantriidae) Nucleopolyhedrosis Virus. *Environmental Entomology*, 13(6), 1522–1526.
- Shapiro, M., El Salamouny, S., & Shepard, B.M. (2008). Green tea extracts as ultraviolet protectants for the beet armyworm, *Spodoptera exigua*, nucleopolyhedrovirus. *Biocontrol Science and Technology*, 18(6), 591–603.
- Shapiro, M., El Salamouny, S., & Shepard, B.M. (2009). Plant extracts as ultraviolet radiation protectants for the beet armyworm (Lepidoptera: Noctuidae) nucleopolyhedrovirus: screening of extracts. *Journal of Agricultural and Urban Entomology*, 26(2), 47–61.
- Shapiro, M., Farrar Jr., R.R., Domek, J., & Javaid, I. (2002). Effects of virus concentration and ultraviolet irradiation on the activity of corn earworm and beet armyworm (Lepidoptera: Noctuidae) nucleopolyhedroviruses. *Journal of Economic Entomology*, 95(2), 243–249. <https://doi.org/10.1603/0022-0493-95.2.243>.
- Shibai, A., Takahashi, Y., Ishizawa, Y., Motooka, D., Nakamura, S., Ying, B.W., & Tsuru, S. (2017). Mutation accumulation under UV radiation in *Escherichia coli*. *Scientific Reports*, 7(1), 1–12. <https://doi.org/10.1038/s41598-017-15008-1>.
- Silva, M.D. da. (1986). Estudo comparativo sobre o uso de Baculovirus anticarsia por diversos equipamentos de aplicação. *Trigo e Soja*, 87, 22–29.

- Silva, M.T.B., & Moscardi, F. (2002). Field efficacy of the nucleopolyhedrovirus of *Anticarsia gemmatalis* Hübner (Lepidoptera: Noctuidae): Effect of formulations, water pH, volume and time of application, and type of spray nozzle. *Neotropical Entomology*, 31(1), 75–83. <https://doi.org/10.1590/s1519-566x2002000100011>.
- Silva, M.T. da. (1987). Baculovirus anticarsia: época de aplicação e efeito residual sobre plantas de soja. *Revista Do Centro de Ciências Rurais*, 17(4).
- Singh, S., Moore, S., Spillings, B., & Hendry, D. (2003). South African isolate of *Cryptophlebia leucotreta* granulovirus. *Journal of Invertebrate Pathology*, 83(3), 249–252. [https://doi.org/10.1016/S0022-2011\(03\)00081-8](https://doi.org/10.1016/S0022-2011(03)00081-8).
- Sinngu, T., & Antwi, M. (2014). Competitiveness of the South African Citrus Fruit Industry Relative to Its Southern Hemisphere Competitors. *Journal of Agricultural Science*, 6(12), 1–15. <https://doi.org/10.5539/jas.v6n12pxx>.
- Smith, G.D., Chadwick, B.E., Willmore-Payne, C., & Bentz, J.S. (2008). Detection of epidermal growth factor receptor gene mutations in cytology specimens from patients with non-small cell lung cancer utilising high-resolution melting amplicon analysis. *Journal of Clinical Pathology*, 61(4), 487–493.
- Smits, P.H. (1987). *Nuclear polyhedrosis virus as a biological control agent of Spodoptera exigua*. PhD Thesis, Wageningen Agricultural University.
- Sohn, J.II, & Nam, J.W. (2018). The present and future of de novo whole-genome assembly. *Briefings in Bioinformatics*, 19(1), 23–40. <https://doi.org/10.1093/bib/bbw096>.
- Steyn, V.M. (2019). Integrated management of false codling moth, *Thaumatotibia leucotreta*, on stone fruit and table grapes. PhD Thesis, University of Stellenbosch.
- Stofberg, F.J. (1954). False codling moth of citrus. *Farming in South Africa*, 29(339), 273–276.
- Stotter, R.L. (2009). Spatial and temporal distribution of false codling moth across landscapes in the Citrusdal area (Western Cape Province, South Africa). March, 101. PhD Thesis, University of Stellenbosch.
- Szewczyk, B., de Souza, M.L., de Castro, M.E.B., Lara, M., & Moscardi, F. (2011). Baculovirus Biopesticides. *Pesticides - Formulations, Effects, Fate*, January. <https://doi.org/10.5772/13219>.

- Szewczyk, B., Hoyos-Carvajal, L., Paluszek, M., Skrzecz, I., & Lobo De Souza, M. (2006). Baculoviruses - Re-emerging biopesticides. *Biotechnology Advances*, 24(2), 143–160. <https://doi.org/10.1016/j.biotechadv.2005.09.001>.
- Thermo Fisher Scientific. (2015). *Product Information: CloneJET PCR Cloning Kit, #K1232*. https://assets.thermofisher.com/TFS-Assets/LSG/manuals/MAN0012966_CloneJET_PCR_Cloning_40rxn_UG.pdf.
- Thézé, J., Lopez-Vaamonde, C., Cory, J.S., & Herniou, E.A. (2018). Biodiversity, evolution and ecological specialization of baculoviruses: A treasure trove for future applied research. *Viruses*, 10(7), 366.
- Thomas, S.R., & Elkinton, J.S. (2004). Pathogenicity and virulence. *Journal of Invertebrate Pathology*, 85(3), 146–151. <https://doi.org/10.1016/j.jip.2004.01.006>.
- Thompson, C.G., Scott, D.W., & Wickman, B.E. (1981). Long-term persistence of the nuclear polyhedrosis virus of the Douglas-fir tussock moth, *Orgyia pseudotsugata* (Lepidoptera: Lymantriidae), in forest soil. *Environmental Entomology*, 10(2), 254–255.
- Timm, A.E., Geertsema, H., & Warnich, L. (2010). Population genetic structure of economically important Tortricidae (Lepidoptera) in South Africa: a comparative analysis. *Bulletin of Entomological Research*, 100(4), 421.
- Tyrrell, R.M., Ley, R.D., & Webb, R.B. (1974). Induction of single-strand breaks (alkali-labile bonds) in bacterial and phage DNA by near UV (365 nm) radiation. *Photochemistry and Photobiology*, 20(5), 395–398.
- Untergasser, A., Cutcutache, I., Koressaar, T., Ye, J., Faircloth, B.C., Remm, M., & Rozen, S.G. (2012). Primer3-new capabilities and interfaces. *Nucleic Acids Research*, 40(15), 1–12. <https://doi.org/10.1093/nar/gks596>.
- van der Merwe, M. (2021). An investigation into yeast-baculovirus synergism for the improved control of *Thaumatotibia leucotreta*, an economically important pest of citrus. PhD Thesis, Rhodes University.
- van der Merwe, M., Jukes, M.D., Knox, C., Moore, S.D., & Hill, M.P. (2022). Mutualism between Gut-Borne Yeasts and Their Host, *Thaumatotibia leucotreta*, and Potential Usefulness in Pest Management. *Insects*, 13, x. <https://doi.org/10.3390/> (in press).

- van der Merwe, M., Jukes, M.D., Rabalski, L., Knox, C., Opoku-Debrah, J.K., Moore, S.D., Krejmer-Rabalska, M., Szewczyk, B., & Hill, M.P. (2017). Genome analysis and genetic stability of the *Cryptophlebia leucotreta* granulovirus (CrleGV-SA) after 15 years of commercial use as a biopesticide. *International Journal of Molecular Sciences*, *18*(11). <https://doi.org/10.3390/ijms18112327>.
- Vernet, G. (2017). Genomics of Infectious Diseases and Private Industry. In: Tibayrenc, M. (2nd Ed.), *Genetics and Evolution of Infectious Diseases*. (pp. 421-434). Netherlands: Elsevier Inc.
- Vincent, J., Gurling, H., & Melmer, G. (1994). Oligonucleotides as Short as 7-Mers Can Be Used for PCR Amplification. *DNA and Cell Biology*, *13*(1), 75–82. <https://doi.org/10.1089/dna.1994.13.75>.
- Wadapurkar, R.M., & Vyas, R. (2018). Computational analysis of next generation sequencing data and its applications in clinical oncology. *Informatics in Medicine Unlocked*, *11*(May), 75–82. <https://doi.org/10.1016/j.imu.2018.05.003>.
- Wennmann, J., Radtke, P., Eberle, K., Gueli Alletti, G., & Jehle, J. (2017). Deciphering Single Nucleotide Polymorphisms and Evolutionary Trends in Isolates of the *Cydia pomonella* granulovirus. *Viruses*, *9*, 227.
- Wennmann, J.T., Fan, J., & Jehle, J.A. (2020). Bacsnp: Using single nucleotide polymorphism (SNP) specificities and frequencies to identify genotype composition in baculoviruses. *Viruses*, *12*(6). <https://doi.org/10.3390/v12060625>.
- Wennmann, J.T., & Jehle, J.A. (2014). Detection and quantitation of *Agrotis* baculoviruses in mixed infections. *Journal of Virology Methods*, *197*, 39–46. <https://doi.org/10.1016/j.jviromet.2013.11.010>.
- Wilson, K., Grzywacz, D., Curcic, I., Scoates, F., Harper, K., Rice, A., Paul, N., & Dillon, A. (2020). A novel formulation technology for baculoviruses protects biopesticide from degradation by ultraviolet radiation. *Scientific Reports*, *10*(1), 1–10. <https://doi.org/10.1038/s41598-020-70293-7>.
- Witt, D.J., & Hink, W.F. (1979). Selection of *Autographa californica* nuclear polyhedrosis virus for resistance to inactivation by near ultraviolet, far ultraviolet, and thermal radiation. *Journal of Invertebrate Pathology*, *33*(2), 222–232.

- Witt, D.J., & Stairs, G.R. (1975). The effects of ultraviolet irradiation on a baculovirus infecting *Galleria mellonella*. *Journal of Invertebrate Pathology*, 26(3), 321–327.
- Wysoki, M. (1986). New records of lepidopterous pests of macadamia in Israel. *Phytoparasitica*, 14(2).
- Yoon, J.H., Lee, C.S., O'Connor, T.R., Yasui, A., & Pfeifer, G.P. (2000). The DNA damage spectrum produced by simulated sunlight. *Journal of Molecular Biology*, 299, 681–693. <https://doi.org/https://doi.org/10.1006/jmbi.2000.3771>.
- Young, S.Y., & Kring, T.J. (1991). Selection of healthy and nuclear polyhedrosis virus infected *Anticarsia gemmatalis* [Lep.: Noctuidae] as prey by nymphal *Nabis roseipennis* [Hemiptera: Nabidae] in laboratory and on soybean. *Entomophaga*, 36(2), 265–273.
- Zhou, L., Myers, A.N., Vandersteen, J.G., Wang, L., & Wittwer, C.T. (2004). Closed-tube genotyping with unlabeled oligonucleotide probes and a saturating DNA dye. *Clinical Chemistry*, 50(8), 1328–1335. <https://doi.org/10.1373/clinchem.2004.034322>.
- Zipper, H., Brunner, H., Bernhagen, J., & Vitzthum, F. (2004). Investigations on DNA intercalation and surface binding by SYBR Green I, its structure determination and methodological implications. *Nucleic Acids Research*, 32(12). <https://doi.org/10.1093/nar/gnh101>.